Kemper, Annika; Schmeck, Maren Diane

Working Paper

Pricing of electricity swaps with geometric averaging

Center for Mathematical Economics Working Papers, No. 676

Provided in Cooperation with:
Center for Mathematical Economics (IMW), Bielefeld University

Suggested Citation: Kemper, Annika; Schmeck, Maren Diane (2023) : Pricing of electricity swaps with geometric averaging, Center for Mathematical Economics Working Papers, No. 676, Bielefeld University, Center for Mathematical Economics (IMW), Bielefeld, https://nbn-resolving.de/urn:nbn:de:0070-pub-29781549

This Version is available at:
https://hdl.handle.net/10419/278466

Center for Mathematical Economics
Working Papers

676

March 2023

Pricing of Electricity Swaps with Geometric Averaging

Annika Kemper and Maren Diane Schmeck

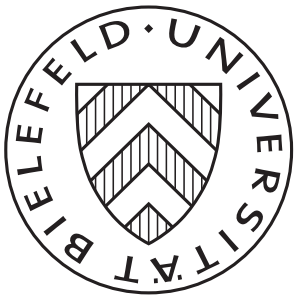

Center for Mathematical Economics (IMW)
Bielefeld University
Universitätsstraße 25
D-33615 Bielefeld · Germany

e-mail: imw@uni-bielefeld.de
uni-bielefeld.de/zwe/imw/research/working-papers
ISSN: 0931-6558

Pricing of Electricity Swaps with Geometric Averaging*

Annika Kemper† Maren Diane Schmeck‡

March 26, 2023

Abstract

In this paper, we provide empirical evidence on the market price of risk for delivery periods (MPDP) of electricity swap contracts. As introduced by Kemper et al. (2022), the MPDP arises through the use of geometric averaging while pricing electricity swaps in a geometric framework. In preparation for empirical investigations, we adjust the work by Kemper et al. (2022) in two directions: First, we examine a Merton type model taking jumps into account. Second, we transfer the model to the physical measure by implementing mean-reverting behavior. We compare swap prices resulting from the classical arithmetic (approximated) average to the geometric weighted average. Under the physical measure, we discover a decomposition of the swap's market price of risk into the classical one and the MPDP. In our empirical study, we analyze two types of models, characterized either by seasonality in the delivery period or by a term-structure effect, and identify the resulting MPDP in both cases.

JEL classification: G130, Q400.
Keywords: Electricity Swaps, Delivery Period, MPDP for Diffusion and Jump Risk, Mean-Reversion, Jumps, Samuelson Effect, Seasonality.

1 Introduction

With the turn of the millennium, pricing derivatives on electricity has become important through the liberalization of the energy markets. Nowadays, new challenges appear due to the transition to a climate neutral energy system: Electricity generated from renewable energy sources, like wind and solar energy, clearly depends on the weather conditions of the season. Consequently, a rising share of renewable energy induces stronger intermittency and seasonality effects influencing especially delivery-dependent pricing effects. In electricity markets, futures contracts are the most important derivatives. They deliver the underlying over a period of time since electricity is not storable on a large scale. We therefore call them electricity *swaps*. The dependence on the delivery time affects the price dynamics, the pricing measure, and the swap's market price of risk for delivery periods (MPDP) introduced by Kemper et al. (2022). One might expect, that the rising share of electricity strengthen these effects due to the involved delivery *period*. In this paper, we provide empirical evidence for the MPDP. To do so, we extend their pricing approach to the physical measure allowing for mean-reversion and jumps. In addition, under the physical measure, we identify a decomposition of the market price of risk into the classical one and the MPDP.

The delivery period is a unique feature of electricity markets that differs from other commodities such as oil, gas, or corn. In fact, it plays a crucial role in the pricing of electricity swaps. Following the market model

*We would like to thank Viviana Fanelli, Carme Frau, and Christa Cuchiero for their fruitful comments and suggestions. Financial support from the Deutsche Forschungsgemeinschaft (DFG, German Research Foundation) – SFB 1283/2 2021 – 317210226 is gratefully acknowledged.

†Center for Mathematical Economics (IMW) at Bielefeld University, annika.kemper@uni-bielefeld.de.
‡Center for Mathematical Economics (IMW) at Bielefeld University, maren.schmeck@uni-bielefeld.de.

approach, the electricity swap price results from averaging an instantaneous stream of futures with respect to the delivery time. This goes back to the famous model by Heath et al. (1990). This approach was firstly connected to energy-related derivatives by Clewlow and Strickland (1999) and to electricity derivatives by Bjerksund et al. (2010) followed by a row of works (see, e.g., Table 1 for geometric settings, Hinderks et al. (2020) for a structural model and Cuchiero et al. (2022) for measure-valued processes).

Averaging with respect to the delivery period can be conducted in different ways. We distinguish between three types of averaging: Arithmetic, approximated, and geometric averaging. *Arithmetic averaging* is the classical way to implement the swap's delivery period and is convenient for arithmetic price dynamics. In particular, continuous arithmetic averaging is applied by Benth et al. (2007), Benth et al. (2008a), Benth et al. (2014), Latini et al. (2019), Benth et al. (2019), and Kleisinger-Yu et al. (2020), among others (see also Table 1). For discrete arithmetic averaging, we refer to Lucia and Schwartz (2002) and Burger et al. (2004). Instead, arithmetic averaging of geometric price dynamics is poorly suited since the resulting swap price dynamics are neither geometric nor Markovian. It requires, e.g., an approximation of the swap price volatility introduced by Bjerksund et al. (2010) whenever we want to consider tractable swap price dynamics (see also Benth et al. (2008a), Benth and Koekebakker (2008)). We call this procedure *approximated averaging*. *Geometric averaging*, instead, does not require any approximations whenever the price dynamics are of geometric type and lead to suitable geometric dynamics (see Kemper et al. (2022)). Hence, the geometric average is tailor-made for relative growth rate models. Nevertheless, the geometric average does not preserve the martingale property. This issue is tackled by Kemper et al. (2022) using a measure change with their MPDP. Usually, negative prices are not observable in the data of the futures prices, such that we stick to a geometric setting and compare the ladder averaging procedures adjusting the MPDP to a Merton type model.

	Geometric Price Dynamics
Arithmetic Average	Koekebakker and Ollmar (2005) Benth and Koekebakker (2008)
Approximated Average	Bjerksund et al. (2010) Benth et al. (2008a)
Geometric Average	Kemper et al. (2022)

Table 1: Classification of selected electricity swap price models.

Both papers, Kemper et al. (2022) and Bjerksund et al. (2010), investigate the modeling of the delivery period explicitly through a continuous weighted averaging approach for geometric futures prices. Both approaches lead to Markovian and geometric swap price dynamics. We discuss similarities and differences between these approaches and introduce a numéraire caused by the different averaging techniques in Section 2. In line with the market model approach, we base the averaging procedure on a continuous stream of futures contracts that is a martingale under the futures risk-neutral measure $\mathbb{Q}$. We consider electricity futures with instantaneous delivery as artificial contracts and we therefore refer to $\mathbb{Q}$ as the *artificial measure*. The resulting swap price dynamics based on geometric averaging are not a martingale under $\mathbb{Q}$. We then define the MPDP of diffusion and jump risk and a new pricing measure $\widetilde{\mathbb{Q}}$, which can thus be used to price derivatives on the swap. We may refer to $\widetilde{\mathbb{Q}}$ as the "correct" or "true" risk-neutral measure since the swap price is a $\widetilde{\mathbb{Q}}$-martingale without any approximations. Under the artificial measure, the swap based on the approximated version is directly a martingale. Therefore, we call $\mathbb{Q}$ also the "classical" risk-neutral measure. It is a clear advantage that the approximated average preserves the martingale property of the swap under the measure $\mathbb{Q}$. A decomposition

of the market price of risk for electricity swaps arises when turning to the physical measure $\mathbb{P}$. Figure 1 gives an overview over the connections between the different measures $\mathbb{P}$, $\mathbb{Q}$, and $\widetilde{\mathbb{Q}}$ and the true market price of risk $\Pi^{\mathbb{P}\mathbb{Q}}$, the classical market price of risk $\Pi^{\mathbb{P}\widetilde{\mathbb{Q}}}$, and the MPDP denoted by $\Pi^{\mathbb{Q}\widetilde{\mathbb{Q}}}$.

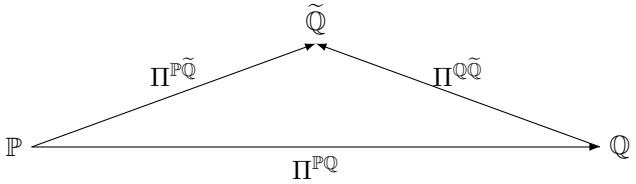

Figure 1: Considered measure changes between the physical measure $\mathbb{P}$, the artificial risk-neutral measure $\mathbb{Q}$, and the swap's pricing measure $\widetilde{\mathbb{Q}}$ as well as their connections with the true market prices of risk $\Pi^{\mathbb{P}\mathbb{Q}}$, the classical market price of risk $\Pi^{\mathbb{P}\widetilde{\mathbb{Q}}}$, and the MPDP $\Pi^{\mathbb{Q}\widetilde{\mathbb{Q}}}$.

Indeed, the MPDP is triggered by typical features of the electricity market entering the swap's volatility. In particular, delivery-dependent effects like seasonalities and term-structure effects play a crucial role. Fanelli and Schmeck (2019) empirically identify seasonalities in the swap's delivery period by considering implied volatilities of electricity options. Renewable energy, like wind and solar energy, intensify especially the seasonal effects mentioned before. Hence, the higher the market share of renewables, the more pronounced the MPDP will be. This applies especially for Germany, having ambitious plans for future investments in renewable energy. An additional property of electricity and commodity markets is the Samuelson effect (see Samuelson (1965)): The closer we reach the end of the maturity, the more effect the volatility has. Benth and Paraschiv (2016) and Jaeck and Lautier (2016) provide empirical evidence for the Samuelson effect in the volatility term-structure of electricity swaps. It can also be observed in the implied volatilities of electricity options, especially far out and in the money (see Kiesel et al. (2009)). Kemper et al. (2022) characterize the MPDP for such seasonalities and term-structure effects within a stochastic volatility model through the variance per unit of expectation of the delivery-dependent effects. We contribute to the literature by investigating the MPDP empirically, affected by seasonalities and the Samuelson effect.

Further characteristics of the electricity swap market are mean-reversion and jump behavior. As mentioned by Latini et al. (2019) and Kleisinger-Yu et al. (2020) among others, mean-reversion is an important property of the electricity swap prices. Koekebakker and Ollmar (2005) empirically validate that the short-term price varies around the long-term price, which confirms mean-reverting behavior. As Benth et al. (2019), we face the problem of changing a mean-reverting process to the risk-neutral measure. We extend their measure change to the geometric setting. We even provide a proof for stochastic volatility settings in order to address models such as Kemper et al. (2022) and Schneider and Tavin (2018). Besides mean-reversion, Benth et al. (2019) include jumps as an outstanding characteristic of electricity prices. In particular, they consider compound Poisson processes under the physical measure in a mean-reverting, arithmetic setting. While extending the paper by Kemper et al. (2022) to jumps, we establish the MPDP of jump risk whenever the jump coefficient relies on delivery-dependent effects.

In our empirical analysis, we investigate twelve swap contracts with monthly delivery from January to December 2019. Each swap is treated as a separate contract assuming that it is driven by an independent Brownian motion. To this data, we fit a model indicating seasonality effects in the volatility coefficient. On the other hand, we estimate the parameters of a Samuelson type model. In order to avoid overfitting, we restrict ourselves to separate effects and do not consider joint effects. The estimation procedure is split in two steps: In a first step, we identify jumps for each contract using a thresholding technique. In a second step, we give

the model's jump free likelihood to fit the remaining parameters by Maximum-Likelihood-Estimation (MLE). Note that we do not perform a term-structure fit by estimating all swap prices occurring at a fixed day since the presence of parallel contracts is limited. The objective of our analysis is not to perform an exhaustive empirical study of swap price modeling but to provide evidence for the MPDP.

The contribution to the literature is threefold: First, we extend the paper by Kemper et al. (2022) to the jump case under the artificial risk-neutral measure leading to an extended characterization of the MPDP regarding diffusion *and* jump risk. Second, we transfer the model to the physical measure and compare the swap prices resulting from geometric and approximated averaging as well as their risk-neutral measures revealing the decomposition of the market price of risk into the classical one and the MPDP. Third, we investigate the model empirically and provide empirical evidence for the MPDP in the case of two separate delivery-dependent volatility effects.

The paper is organized as follows: Section 2 presents the geometric averaging approach under the artificial risk-neutral measure applied to the jump-type futures curve. In addition, it presents the MPDP of diffusion and jump risk. Section 3 introduces the model under the physical measure and identifies the decomposition of the market price of risk. The estimation procedure and the empirical findings are presented in Section 4. Finally, Section 5 concludes our main findings.

2 On the MPDP of Diffusion and Jump Risk

We focus on an electricity swap contract delivering 1 MWh of electricity during the agreed delivery period $(\tau_1, \tau_2]$. At a trading day $t \leq \tau_1$ before the contract expires, we denote the swap price by $F(t, \tau_1, \tau_2)$ settled such that the contract is entered at no cost. It can be interpreted as an average price of instantaneous delivery. Motivated by this interpretation, we consider an artificial futures contract with price $f(t, \tau)$ that stands for instantaneous delivery at time $\tau \in (\tau_1, \tau_2]$. Note that such a contract does not exist on the market but it turns out to be useful for modeling purposes when considering delivery periods (see, e.g., Benth et al. (2019) and Kemper et al. (2022)).

Consider a filtered probability space $(\Omega, \mathcal{F}, (\mathcal{F}_t)_{t\in[0,\tau]}, \mathbb{Q})$, where the filtration satisfies the usual conditions. We first model the solution of a futures contract and then derive the corresponding dynamics to avoid lacks of existence in the presence of jumps (see Papapantoleon (2008)). At time $t \leq \tau$, let the logarithmic price process of the futures contract be defined as

$$\ln f(t,\tau) = \ln f(0,\tau) + Y(t,\tau) \,, \tag{2.1}$$

$$Y(t,\tau) = \int_0^t \sigma(s,\tau) dW_s^{\mathbb{Q}} + \int_0^t \eta(s,\tau) d\widetilde{J}_s^{\mathbb{Q}} - \int_0^t c^{\mathbb{Q}}(s,\tau) ds \,, \tag{2.2}$$

where $W^{\mathbb{Q}}$ is a standard Brownian motion under $\mathbb{Q}$ independent of the jump process $\widetilde{J}^{\mathbb{Q}}$. In particular, $\widetilde{J}^{\mathbb{Q}}$ is a compound compensated jump process defined through the compensated Poisson random measure $\widetilde{N}^{\mathbb{Q}}(dt, dz) = N(dt, dz) - \ell^{\mathbb{Q}}(dz)dt$:

$$\widetilde{J}_t^{\mathbb{Q}} = \int_0^t \int_{\mathbb{R}} z \widetilde{N}^{\mathbb{Q}}(ds, dz) \,, \tag{2.3}$$

with Lévy measure $\ell^{\mathbb{Q}}(dz) = \lambda^{\mathbb{Q}} G(dz)$, which is independent of the delivery time, and where $\lambda^{\mathbb{Q}} > 0$ indicates the jump intensity and $G(dz)$ the jump size distribution. The last term of the logarithmic rate Y in Equation (2.2)

defines its compensator under the current measure $\mathbb{Q}$:

$$c^{\mathbb{Q}}(t,\tau) = \frac{1}{2}\sigma^2(t,\tau) + \psi^{\mathbb{Q}}(i\eta(t,\tau)) \,, \tag{2.4}$$

with initial non-random conditions $f(0,\tau) > 0$. In addition, $\psi^{\mathbb{Q}}(ir)$ is the integrand of the Lévy-Khintchine exponential and the moment generating function is defined by

$$\psi^{\mathbb{Q}}(r) := \int_{\mathbb{R}} (e^{rz} - 1 - rz)\, \ell^{\mathbb{Q}}(dz) \,. \tag{2.5}$$

We assume that the futures price volatility and jump coefficients, $\sigma(t,\tau)$ and $\eta(t,\tau)$, are deterministic and that the futures price $f(t,\tau)$ is $\mathcal{F}_t$-adapted for $t \in [0,\tau]$. We further assume that they satisfy suitable integrability and measurability conditions (see Assumption 1 in Appendix A for details) to ensure that the process in Equation (2.1) is a $\mathbb{Q}$-martingale, and that Equation (2.1) gives the unique solution to the process evolving as

$$\frac{df(t,\tau)}{f(t-,\tau)} = \sigma(t,\tau)dW_t^{\mathbb{Q}} + \int_{\mathbb{R}} \left(e^{\eta(t,\tau)z} - 1\right) \widetilde{N}^{\mathbb{Q}}(dt,dz) \,. \tag{2.6}$$

As $\sigma(t,\tau)$ depends on both, trading time t and delivery time τ, we allow for volatility structures as the Samuelson effect or seasonalities in the delivery time, which are addressed in Section 4.2.

Following the Heath-Jarrow-Morton approach to price futures and swaps in electricity markets, the swap price is usually defined as the *arithmetic weighted average* of futures prices (see, e.g., Benth et al. (2008a), Bjerksund et al. (2010), and Benth et al. (2019)):

$$F^A(t,\tau_1,\tau_2) := \int_{\tau_1}^{\tau_2} w(u,\tau_1,\tau_2) f(t,u) du \,, \tag{2.7}$$

for a general weight function

$$w(u,\tau_1,\tau_2) := \frac{\hat{w}(u)}{\int_{\tau_1}^{\tau_2} \hat{w}(v)dv} \,, \quad \text{for } u \in (\tau_1,\tau_2] \,, \tag{2.8}$$

where $\hat{w}(u) > 0$ is the corresponding settlement function. Note that w defines a probability density function with support on $(\tau_1,\tau_2]$ since it is positive and integrates to one, that is $\int_{\tau_1}^{\tau_2} w(u,\tau_1,\tau_2)du = 1$. Hence, we denote U as a random delivery variable with density $w(u,\tau_1,\tau_2)$ (see also Kemper et al. (2022)). The most popular example is given by a constant settlement type $\hat{w}(u) = 1$, such that the density becomes $w(u,\tau_1,\tau_2) = \frac{1}{\tau_2-\tau_1}$ and $U \sim \mathcal{U}((\tau_1,\tau_2])$ is uniformly distributed over the delivery period. This corresponds to a one-time settlement. A continuous settlement over the time interval $(\tau_1,\tau_2]$ is covered by a continuous discount function $\hat{w}(u) = e^{-ru}$, where r is the constant interest rate (see, e.g., Benth et al. (2008a)).

The arithmetic average of the futures price as in Equation (2.7) leads to tractable dynamics for the swap as long as one assumes an arithmetic structure of the futures prices as well. This is based on the fact that arithmetic averaging is tailor-made for absolute growth rate models. Nevertheless, if one defines the futures price as a geometric process as in Equation (2.6), one can show that the dynamics of the swap price F^A defined through Equation (2.7) are given by

$$\begin{aligned}\frac{dF^A(t,\tau_1,\tau_2)}{F^A(t-,\tau_1,\tau_2)} = &\left[\sigma(t,\tau_2) - \int_{\tau_1}^{\tau_2} \frac{\partial\sigma}{\partial u}(t,u)\frac{w(\tau,\tau_1,\tau_2)}{w(\tau,\tau_1,u)}\frac{F^A(t,\tau_1,u)}{F^A(t,\tau_1,\tau_2)}du\right] dW_t^{\mathbb{Q}} \\ &+ \int_{\mathbb{R}} \left(e^{\eta(t,\tau_2)z} - 1 - \int_{\tau_1}^{\tau_2} \frac{\partial e^{\eta(s,u)z}}{\partial u}\frac{w(\tau,\tau_1,\tau_2)}{w(\tau,\tau_1,u)}\frac{F^A(t,\tau_1,u)}{F^A(t,\tau_1,\tau_2)}du\right) \widetilde{N}^{\mathbb{Q}}(dz,dt) \,,\end{aligned} \tag{2.9}$$

for any $\tau \in (\tau_1,\tau_2]$ (see Benth et al. (2008a), cf. Chapter 6.3.1). Thus, the dynamics of the swap price is

neither a geometric process nor Markovian, which makes it unhandy for further analysis. To overcome this issue, Bjerksund et al. (2010) suggest an approximation in the continuous setting, which we call *approximated averaging* since it is the arithmetic average of approximated logarithmic returns. Approximated averaging maintains the martingale property meaning that the swap is a martingale whenever f is a martingale. If we transfer the approximated averaging procedure to our jump setting, we can define the swap price process based on approximated averaging by

$$\frac{dF^a(t,\tau_1,\tau_2)}{F^a(t-,\tau_1,\tau_2)} := \int_{\tau_1}^{\tau_2} w(u,\tau_1,\tau_2)\frac{df(t,u)}{f(t-,u)}du \,. \tag{2.10}$$

In contrast, *geometric averaging* originates from the arithmetic average of logarithmic returns without any need for approximations. Hence, in line with Kemper et al. (2022), we define the swap price originating from geometric averaging by

$$F(t,\tau_1,\tau_2) := e^{\int_{\tau_1}^{\tau_2} w(u,\tau_1,\tau_2)\ln f(t,u)du} \,, \tag{2.11}$$

(see also Kemna and Vorst (1990)). Assume that the volatility and jump coefficients satisfy further integrability conditions (see Assumption 2 in Appendix A). It turns out, that the resulting swap price dynamics is a geometric process with a non-zero drift term:

Lemma 2.1. *Let Assumption 2 in Appendix A be satisfied. Under the artificial pricing measure $\mathbb{Q}$, the dynamics of the swap price, defined in Equation (2.11), are given by*

$$\begin{aligned}\frac{dF(t,\tau_1,\tau_2)}{F(t-,\tau_1,\tau_2)} &= \mathbb{E}[\sigma(t,U)]\; dW_t^{\mathbb{Q}} + \int_{\mathbb{R}} \left(e^{\mathbb{E}[\eta(t,U)]z} - 1\right)\widetilde{N}^{\mathbb{Q}}(dt,dz) \\ &\quad - \left(\frac{1}{2}\mathbb{V}\left[\sigma(t,U)\right] + \mathbb{E}[\psi^{\mathbb{Q}}(\eta(t,U))] - \psi^{\mathbb{Q}}(\mathbb{E}[\eta(t,U)])\right)dt \,,\end{aligned} \tag{2.12}$$

where U denotes the random delivery variable with density $w(u,\tau_1,\tau_2)$.

Proof. Plugging Equation (2.1) into Equation (2.11) gives us

$$F(t,\tau_1,\tau_2) = F(0,\tau_1,\tau_2)e^{\bar{X}(t,\tau_1,\tau_2)} \,,$$

where $\bar{X}(t,\tau_1,\tau_2) := \int_{\tau_1}^{\tau_2} w(u,\tau_1,\tau_2)\ln f(t,u)du$ is the swap price rate. Using the integral representation of the futures rate process from Equation (2.1) and applying stochastic Fubini Theorem (see Protter (2005), cf. Theorem 65, Chapter IV.6) leads to

$$\bar{X}(t,\tau_1,\tau_2) = \int_0^t \mathbb{E}\Big[\sigma(s,U)\Big]dW_s^{\mathbb{Q}} + \int_0^t \mathbb{E}[\eta(s,U)]d\widetilde{J}_s^{\mathbb{Q}} - \frac{1}{2}\int_0^t \mathbb{E}\Big[\sigma^2(s,U)\Big]ds - \int_0^t \mathbb{E}[\psi^{\mathbb{Q}}(\eta(s,U))]ds \,.$$

Then, Equation (2.12) follows using Itô's formula (see, e.g., Øksendal and Sulem (2007)). □

Having presented the three procedures of continuous time averaging that are used to derive the swap from an underlying artificial futures curve, we would like to compare them. Arithmetic averaging, defined by Equation (2.7), is tractable for arithmetic futures curves, whereas approximated averaging, defined by Equation (2.10), and geometric averaging, defined by Equation (2.11), are well suited for geometric futures curves. In line with a series of literature (see Table 1), we follow the geometric approach. Our goal throughout this paper is to investigate the pricing spread between geometric and approximated averaging theoretically and empirically.

Although the futures price f and the approximated F^a are martingales under the pricing measure $\mathbb{Q}$, the swap price F is not a $\mathbb{Q}$-martingale: Indeed, the swap price process under $\mathbb{Q}$ has a negative drift term consisting

of two parts given by the swap's variance and the difference between the averaged Lévy-Khintchine integrand and the Lévy-Khintchine integrand of the averaged jump coefficient. Hence, using geometric averaging leads to a new interpretation of risk related to the delivery period as we will analyze in the following.

Analogous to Kemper et al. (2022), we derive the corresponding risk-neutral measure $\widetilde{\mathbb{Q}}$ under which the electricity swap price F is a martingale. For deriving the swap's risk-neutral measure, we thus define the MPDP extended to jumps in the following.

Definition 2.1. *At time $t \in [0, \tau_1]$, the market price of jump and diffusion risk for delivery periods associated to the delivery period $(\tau_1, \tau_2]$ is defined by $\Pi^{\mathbb{Q}\widetilde{\mathbb{Q}}} := (\Pi_1^{\mathbb{Q}\widetilde{\mathbb{Q}}}, \Pi_2^{\mathbb{Q}\widetilde{\mathbb{Q}}})$, where*

$$\Pi_1^{\mathbb{Q}\widetilde{\mathbb{Q}}}(t, \tau_1, \tau_2) := -\frac{1}{2} \frac{\mathbb{V}\left[\sigma(t,U)\right]}{\mathbb{E}\left[\sigma(t,U)\right]} , \tag{2.13}$$

$$\Pi_2^{\mathbb{Q}\widetilde{\mathbb{Q}}}(t, \tau_1, \tau_2) := -\frac{\mathbb{E}[\psi^{\mathbb{Q}}(\eta(t,U))] - \psi^{\mathbb{Q}}(\mathbb{E}[\eta(t,U)])}{\int_{\mathbb{R}} \left(e^{\mathbb{E}[\eta(t,U)]z} - 1\right) \ell^{\mathbb{Q}}(dz)} = -\frac{\int_{\mathbb{R}} \mathbb{E}[e^{\eta(t,U)z}] - e^{\mathbb{E}[\eta(t,U)]z} \ell^{\mathbb{Q}}(dz)}{\int_{\mathbb{R}} \left(e^{\mathbb{E}[\eta(t,U)]z} - 1\right) \ell^{\mathbb{Q}}(dz)} . \tag{2.14}$$

In particular, Π_1 refers to the additional diffusion risk, which is measurable and $\mathcal{F}_t$-adapted as $\sigma(t,u)$ is. It can be interpreted as the trade-off between the weighted average variance of a stream of futures, on the one hand, and the variance of the swap, on the other hand (see also Kemper et al. (2022) for an elaboration of the MPDP $\Pi_1^{\mathbb{Q}\widetilde{\mathbb{Q}}}$ and a detailed interpretation). $\Pi_2^{\mathbb{Q}\widetilde{\mathbb{Q}}}$ is the additional jump risk, which is the difference between the Lévy-Khintchine integrands standardized by the swap's jump coefficient.

Remark 2.1. (*i*) *Note that $\Pi^{\mathbb{Q}\widetilde{\mathbb{Q}}}$ would be zero, whenever the volatility and jump coefficients are independent of delivery time. For this reason, we call $\Pi^{\mathbb{Q}\widetilde{\mathbb{Q}}}$ the market price of risk for delivery periods (MPDP).*

(*ii*) *The MPDP of diffusion and jump risk is strengthened by delivery-dependent effects within the volatility and jump coefficients. For example, pronounced term-structure effects or seasonalities in the delivery period within these coefficients capture a distinct dependence on the delivery period and, consequently, lead to a high MPDP.*

(*iii*) *$\Pi_1^{\mathbb{Q}\widetilde{\mathbb{Q}}}$ is in line with the MPDP for diffusion risk found in Kemper et al. (2022), where a stochastic volatility scenario is considered.*

We define a new pricing measure $\widetilde{\mathbb{Q}}$, such that the swap price process $F(\cdot, \tau_1, \tau_2)$ is a martingale. Following Øksendal and Sulem (2007), define the Radon-Nikodym density through

$$Z^{\mathbb{Q}\widetilde{\mathbb{Q}}}(t, \tau_1, \tau_2) = \prod_{j=1}^{2} Z_j^{\mathbb{Q}\widetilde{\mathbb{Q}}}(t, \tau_1, \tau_2) , \tag{2.15}$$

where

$$Z_1^{\mathbb{Q}\widetilde{\mathbb{Q}}}(t, \tau_1, \tau_2) := e^{-\int_0^t \Pi_1^{\mathbb{Q}\widetilde{\mathbb{Q}}}(s,\tau_1,\tau_2) d\widetilde{W}^{\mathbb{Q}}(s) - \frac{1}{2}\int_0^t \Pi_1^{\mathbb{Q}\widetilde{\mathbb{Q}}}(s,\tau_1,\tau_2)^2 ds} , \tag{2.16}$$

$$Z_2^{\mathbb{Q}\widetilde{\mathbb{Q}}}(t, \tau_1, \tau_2) := e^{\int_0^t \int_{\mathbb{R}} \ln(1-\Pi_2^{\mathbb{Q}\widetilde{\mathbb{Q}}}(s,\tau_1,\tau_2)) \tilde{N}^{\mathbb{Q}}(ds,dz) + \int_0^t \int_{\mathbb{R}} \left(\ln(1-\Pi_2^{\mathbb{Q}\widetilde{\mathbb{Q}}}(s,\tau_1,\tau_2)) + \Pi_2^{\mathbb{Q}\widetilde{\mathbb{Q}}}(s,\tau_1,\tau_2)\right) \ell^{\mathbb{Q}}(dz) ds} . \tag{2.17}$$

Assume that

$$\mathbb{E}_{\mathbb{Q}}[Z^{\mathbb{Q}\widetilde{\mathbb{Q}}}(\tau_1, \tau_1, \tau_2)] = 1 , \tag{2.18}$$

which means that $Z^{\mathbb{Q}\widetilde{\mathbb{Q}}}(\cdot, \tau_1, \tau_2)$ is indeed a martingale for the entire trading time. We will show later that the martingale property is satisfied for suitable models such that Equation (2.18) holds true. We then define the

new measure $\widetilde{\mathbb{Q}}$ through the Radon-Nikodym density

$$\frac{d\widetilde{\mathbb{Q}}}{d\mathbb{Q}} = Z^{\mathbb{Q}\widetilde{\mathbb{Q}}}(\tau_1, \tau_1, \tau_2) \,, \tag{2.19}$$

which clearly depends on the delivery period $(\tau_1, \tau_2]$. Girsanov's theorem states that if we define the process $W^{\widetilde{\mathbb{Q}}}$ and the random measure $\widetilde{N}^{\widetilde{\mathbb{Q}}}(dt, dz)$ by

$$dW_t^{\widetilde{\mathbb{Q}}} = dW_t^{\mathbb{Q}} + \Pi_1^{\mathbb{Q}\widetilde{\mathbb{Q}}}(t, \tau_1, \tau_2)dt \,, \tag{2.20}$$

$$\widetilde{N}^{\widetilde{\mathbb{Q}}}(dt, dz) = \widetilde{N}^{\mathbb{Q}}(dt, dz) + \Pi_2^{\mathbb{Q}\widetilde{\mathbb{Q}}}(t, \tau_1, \tau_2)\ell^{\mathbb{Q}}(dz)dt \,, \tag{2.21}$$

then $W^{\widetilde{\mathbb{Q}}}$ is a Brownian motion under $\widetilde{\mathbb{Q}}$ and $\widetilde{N}^{\widetilde{\mathbb{Q}}}(\cdot,\cdot)$ is the $\widetilde{\mathbb{Q}}$-compensated Poisson random measure of $N(\cdot,\cdot)$ with compensator $\left(1 - \Pi_2^{\mathbb{Q}\widetilde{\mathbb{Q}}}(s, \tau_1, \tau_2)\right)\ell^{\mathbb{Q}}(dz)$. Under some further assumptions, ensuring that $Z_2^{\mathbb{Q}\widetilde{\mathbb{Q}}}$ stays positive and that $Z^{\mathbb{Q}\widetilde{\mathbb{Q}}}$ is a true martingale (see Assumption 3 in Appendix A), a straightforward valuation leads to the following result:

Proposition 2.1. *Let Assumption 3 in Appendix A be satisfied. The swap price process $F(\cdot, \tau_1, \tau_2)$, defined in (2.11), is a martingale under $\widetilde{\mathbb{Q}}$. The swap price dynamics are given by*

$$\frac{dF(t, \tau_1, \tau_2)}{F(t-, \tau_1, \tau_2)} = \mathbb{E}[\sigma(t, U)]dW_t^{\widetilde{\mathbb{Q}}} + \int_{\mathbb{R}} \left(e^{\mathbb{E}[\eta(t,U)]z} - 1\right)\widetilde{N}^{\widetilde{\mathbb{Q}}}(dt, dz) \,, \tag{2.22}$$

where $W^{\widetilde{\mathbb{Q}}}$ is a Brownian motion under $\widetilde{\mathbb{Q}}$ and $\widetilde{N}^{\widetilde{\mathbb{Q}}}(\cdot,\cdot)$ is the compound compensated Poisson random measure under $\widetilde{Q}$ with Lévy measure $\left(1 - \Pi_2^{\mathbb{Q}\widetilde{\mathbb{Q}}}(t, \tau_1, \tau_2)\right)\ell^{\mathbb{Q}}(dz)$ for $t \in [0, \tau_1]$.

Proof. We know by definition that $\Pi_1^{\mathbb{Q}\widetilde{\mathbb{Q}}}$ is a continuous adapted process that is square-integrable and $\Pi_2^{\mathbb{Q}\widetilde{\mathbb{Q}}}$ is deterministic and càdlàg in time. Hence, all processes are predictable. Following Øksendal and Sulem (2007) (cf. Theorem 1.35), we need to show that Equation (2.18) is satisfied, so that $Z^{\mathbb{Q}\widetilde{\mathbb{Q}}}$ is a true martingale. Considering the dynamics of $Z^{\mathbb{Q}\widetilde{\mathbb{Q}}}$ using Itô's formula, we have

$$dZ^{\mathbb{Q}\widetilde{\mathbb{Q}}}(t, \tau_1, \tau_2) = Z^{\mathbb{Q}\widetilde{\mathbb{Q}}}(t-, \tau_1, \tau_2)\left[-\Pi_1^{\mathbb{Q}\widetilde{\mathbb{Q}}}(t, \tau_1, \tau_2)dW_t^{\mathbb{Q}} - \int_{\mathbb{R}} \Pi_2^{\mathbb{Q}\widetilde{\mathbb{Q}}}(t, \tau_1, \tau_2)z\widetilde{N}^{\mathbb{Q}}(dt, dz)\right] \,,$$

so that $Z^{\mathbb{Q}\widetilde{\mathbb{Q}}}$ is a local $\mathbb{Q}$-martingale, where $W^{\mathbb{Q}}$ and $\widetilde{N}^{\mathbb{Q}}(\cdot,\cdot)$ are independent of each other. Hence, it is enough to show, that $Z_1^{\mathbb{Q}\widetilde{\mathbb{Q}}}$ and $Z_2^{\mathbb{Q}\widetilde{\mathbb{Q}}}$ are true martingales. We can prove Novikov's condition regarding the continuous part (see, e.g., Protter (2005), cf. Theorem 41, Chapter III.8) as $\Pi_1^{\mathbb{Q}\widetilde{\mathbb{Q}}}$:

$$\mathbb{E}_{\mathbb{Q}}\left[e^{\frac{1}{2}\int_0^{\tau_1} \Pi_1^{\mathbb{Q}\widetilde{\mathbb{Q}}}(s,\tau_1,\tau_2)dW_s^{\mathbb{Q}}}\right] = e^{\frac{1}{2}\int_0^{\tau_1} \Pi_1^{\mathbb{Q}\widetilde{\mathbb{Q}}}(s,\tau_1,\tau_2)^2 ds} < \infty \,.$$

Hence, $Z_1^{\mathbb{Q}\widetilde{\mathbb{Q}}}$ is a true martingale. Moreover, $Z_2^{\mathbb{Q}\widetilde{\mathbb{Q}}}$ is a true martingale under $\mathbb{Q}$ since

$$\mathbb{E}_{\mathbb{Q}}[Z_2^{\mathbb{Q}\widetilde{\mathbb{Q}}}(\tau_1, \tau_1, \tau_2)] = \mathbb{E}_{\mathbb{Q}}\left[e^{\lambda^{\mathbb{Q}}\int_0^{\tau_1}\int \ln(1-\Pi_2^{\mathbb{Q}\widetilde{\mathbb{Q}}}(s,\tau_1,\tau_2))\widetilde{N}^{\mathbb{Q}}(ds,dz)}\right] e^{\int_0^{\tau_1}\int_{\mathbb{R}}\left(\ln(1-\Pi_2^{\mathbb{Q}\widetilde{\mathbb{Q}}}(s,\tau_1,\tau_2))+\Pi_2^{\mathbb{Q}\widetilde{\mathbb{Q}}}(s,\tau_1,\tau_2)\right)ds} = 1 \,,$$

where the last equality follows from the Lévy-Khintchine representation and Assumption 3 in Appendix A. Hence, we can apply Girsanov's Theorem (see, e.g., Øksendal and Sulem (2007), cf. Theorem 1.35) and the assertion follows. □

Note that the MPDP of diffusion and jump risk, $\Pi_1^{\mathbb{Q}\widetilde{\mathbb{Q}}}$ and $\Pi_2^{\mathbb{Q}\widetilde{\mathbb{Q}}}$, are negative following from Jensen's inequality. Hence, the geometric averaging technique induces less risk than the application of the approximated arithmetic average for which we need to pay a cost of approximation risk.

We would like to compare the approximated swap price F^a under $\mathbb{Q}$ with the swap price F under $\widetilde{\mathbb{Q}}$. The continuous parts of the swap price dynamics coincide since we consider a deterministic volatility structure. The only differences are located in the compensator of the compound compensated Poisson process and the jump coefficient. If the jump coefficient is independent of delivery time, the distribution of F^a under $\mathbb{Q}$ and the distribution of F under $\widetilde{\mathbb{Q}}$ are the same. For differences in a stochastic volatility setting, we refer to Kemper et al. (2022). For the swap prices F and F^a, both under the artificial measure $\mathbb{Q}$, we have the following result:

Corollary 2.1. *(i) The swap price F is always smaller or equal than F^A.*

(ii) The swap price F is smaller or equal than F^a. The pricing spread is attained by

$$F^a(t,\tau_1,\tau_2) - F(t,\tau_1,\tau_2) = F^a(t,\tau_1,\tau_2)\Big[1 - D(t,\tau_1,\tau_2)\Big] \,, \tag{2.23}$$

$$D(t,\tau_1,\tau_2) = e^{-\frac{1}{2}\int_0^t \mathbb{V}[\sigma(s,U)]ds - \int_0^t \int_{\mathbb{R}} \left(\ln \mathbb{E}[e^{\eta(s,U)z}] - \mathbb{E}[\eta(s,U)]z\right) N(ds,dz)} \,. \tag{2.24}$$

Proof.

(i) The continuous arithmetic weighted average is greater than the geometric one, which directly follows from Jensen's inequality.

(ii) Using Equation (2.10), we find that $F^a(t,\tau_1,\tau_2) = e^{\bar{X}^a(t,\tau_1,\tau_2)}$, where $\bar{X}^a(t,\tau_1,\tau_2)$ is the solution of the following arithmetic Brownian motion:

$$\begin{aligned} d\bar{X}^a(t,\tau_1,\tau_2) = \mathbb{E}[\sigma(t,U)]dW_t^{\mathbb{Q}} + \int_{\mathbb{R}} \ln \mathbb{E}[e^{\eta(t,U)z}]\widetilde{N}^{\mathbb{Q}}(dt,dz) \\ - \left(\frac{1}{2}\mathbb{E}[\sigma(t,U)]^2 + \int_{\mathbb{R}} \mathbb{E}[e^{\eta(t,U)z}] - 1 - \ln \mathbb{E}[e^{\eta(t,U)z}]\right) dt \,. \end{aligned}$$

Hence, the difference between the approximated and exact solution is given by

$$F^a(t,\tau_1,\tau_2) - F(t,\tau_1,\tau_2) = F^a(t,\tau_1,\tau_2)\left(1 - D(t,\tau_1,\tau_2)\right) \,,$$

such that $F(t,\tau_1,\tau_2) = F^a(t,\tau_1,\tau_2)D(t,\tau_1,\tau_2)$, where

$$D(t,\tau_1,\tau_2) = e^{\bar{X}(t,\tau_1,\tau_2) - \bar{X}^a(t,\tau_1,\tau_2)} = e^{-\frac{1}{2}\int_0^t \mathbb{V}[\sigma(s,U)]ds - \int_0^t \int_{\mathbb{R}} \ln \mathbb{E}[e^{\eta(s,U)z}] - \mathbb{E}[\eta(s,U)]z N(ds,dz)} \,.$$

Since $\mathbb{V}[\sigma(\cdot,U)] \geq 0$ and $\ln \mathbb{E}[e^{\eta(\cdot,U)z}] \geq \mathbb{E}[\eta(\cdot,U)]z$ by Jensen, it follows that $D(t,\tau_1,\tau_2) \in (0,1]$ and thus $F \leq F^a$. □

We conclude that arithmetic and approximated averaging lead to higher swap prices than the geometric average. We would like to stress that D in Equation (2.24) is not affected by measure changes since it is characterized by a drift component and a pure jump component exclusively (see also Equation (2.26)). Moreover, note that D can be seen as stochastic discount factor, which can be used to derive the swap price F given F^a. Vice versa, consider

$$F^a(t,\tau_1,\tau_2) = F(t,\tau_1,\tau_2)D^{-1}(t,\tau_1,\tau_2) \,. \tag{2.25}$$

The exponential part of D^{-1} can be interpreted as a price (premium) per share, which we pay for an imprecise averaged swap. Moreover, we can see D as the price process of a non-dividend paying asset evolving as

$$\frac{dD(t,\tau_1,\tau_2)}{D(t-,\tau_1,\tau_2)} = -\frac{1}{2}\mathbb{V}[\sigma(t,U)]dt + \int_{\mathbb{R}} \left(\frac{e^{\mathbb{E}[\eta(t,U)]z}}{\mathbb{E}[e^{\eta(t,U)z}]} - 1\right) N(dt,dz) \,, \tag{2.26}$$

such that we can interpret D as a numéraire. If F^a is a martingale, then $\frac{F}{D}$ is also a martingale. If F is a martingale, then $F^a D$ is a martingale (see, e.g., Shreve (2004), cf. Theorem 9.2.2). We can thus use it to price options and other derivatives on the swap. In order to investigate the model empirically, we introduce the model under its physical measure $\mathbb{P}$ in the subsequent section.

3 The Real-World Model

A typical feature of electricity prices beyond seasonalities and the Samuelson effect is the mean-reverting behavior (see, e.g., Benth et al. (2008a) and Benth et al. (2019)). In order to implement the drift feature and to investigate the model empirically, we derive the futures under the physical measure $\mathbb{P}$. Note that we will include mean-reversion at the futures and thus the swap's *rate* level. We then consider the resulting market prices of risk transferring to the artificial and the swap's risk-neutral measure.

3.1 The Swap Price under the Physical Measure

We now derive the price of a swap contract that delivers one unit of electricity during the fixed delivery period $(\tau_1, \tau_2]$, similar to Section 2 but now under the physical measure $\mathbb{P}$. Hence, starting from the physical measure $\mathbb{P}$, the logarithmic futures price process from Equation (2.1), given by

$$\ln f(t,\tau) = \ln f(0,\tau) + Y(t,\tau) \,, \tag{3.1}$$

is now characterized by the futures logarithmic rate component Y under the physical measure given by

$$dY(t,\tau) = \left(\mu(t,\tau) - \kappa(t) Y(t,\tau)\right) dt + \sigma(t,\tau) dW_t^{\mathbb{P}} + \eta(t,\tau) d\widetilde{J}_t^{\mathbb{P}} \,, \tag{3.2}$$

for $Y(0,\tau) = 0$, where $W^{\mathbb{P}}$ is a Brownian motion under the physical measure $\mathbb{P}$ independent of the compound compensated jump process $\widetilde{J}^{\mathbb{P}}$. In particular, $\widetilde{J}^{\mathbb{P}}$ is defined through the $\mathbb{P}$-compensated Poisson random measure $\widetilde{N}^{\mathbb{P}}(dt,dz) = N(dt,dz) - \ell^{\mathbb{P}}(dz)dt$ with Lévy measure $\ell^{\mathbb{P}}(dz) = \lambda^{\mathbb{P}} G(dz)$ that is independent of delivery time. Note that $\lambda^{\mathbb{P}} > 0$ indicates the jump intensity under the physical measure and $G(dz)$ is the jump size distribution.

In order to characterize the futures logarithmic rate in more detail, we introduce the following lemma.

Lemma 3.1. *We assume that the coefficients satisfy suitable integrability and measurability conditions (see Assumption 4 in Appendix A) such that the dynamics of the futures logarithmic rate are given by*

$$d \ln f(t,\tau) = dY(t,\tau) \,. \tag{3.3}$$

The unique strong solution is given by

$$Y(t,\tau) = \int_0^t e^{-\int_v^t \kappa(q)dq} \mu(v,\tau) dv + \int_0^t e^{-\int_v^t \kappa(q)dq} \sigma(v,\tau) dW_v^{\mathbb{P}} + \int_0^t e^{-\int_v^t \kappa(q)dq} \eta(v,\tau) d\widetilde{J}_v^{\mathbb{P}} \,. \tag{3.4}$$

Proof. The unique strong solution follows from Benth et al. (2008a) (cf. Proposition 3.1). □

Hence, the futures logarithmic return is again an Ornstein-Uhlenbeck process.

Lemma 3.2. *Under the Assumptions 4 and 5 in Appendix A, Equation (3.1) is the unique strong solution to the dynamics*

$$\frac{df(t,\tau)}{f(t-,\tau)} = \sigma(t,\tau) dW_t^{\mathbb{P}} + \int_{\mathbb{R}} \left(e^{\eta(t,\tau)z} - 1\right) \widetilde{N}^{\mathbb{P}}(dt,dz) + c^{\mathbb{P}}(t,\tau,Y(t,\tau)) dt \,, \tag{3.5}$$

where the drift-term is characterized by

$$c^{\mathbb{P}}(t,\tau,Y) = \mu(t,\tau) - \kappa(t)Y + \frac{1}{2}s^2(t,\tau)\sigma^2(t,\tau) + \psi^{\mathbb{P}}(\eta(t,\tau)) \; . \tag{3.6}$$

Proof. Applying Ito's formula to $e^{Y(t,\tau)}$ leads to the desired dynamics (see Øksendal and Sulem (2007), cf. Theorem 1.16). □

Note that the assumptions behind the model induce a finite second moment as well as a finite moment generating function of the jump size distribution. We will consider later some suitable distributions for these jump sizes.

As in the previous section, we now derive the swap prices resulting from geometric and approximated averaging.

Lemma 3.3. *Let Assumptions 4 to 6 in Appendix A be satisfied. Then, the swap price resulting from geometric averaging is defined by*

$$F(t,\tau_1,\tau_2) := F(0,\tau_1,\tau_2)e^{\bar{Y}(t,\tau_1,\tau_2)} \; , \tag{3.7}$$

where the swap's logarithmic rate $\bar{Y}(t,\tau_1,\tau_2) := \int_{\tau_1}^{\tau_2} w(u,\tau_1,\tau_2)Y(t,u)du$ *evolves as*

$$d\bar{Y}(t,\tau_1,\tau_2) = \left(\mathbb{E}[\mu(t,U)] - \kappa(t)\bar{Y}(t,\tau_1,\tau_2)\right)dt + \mathbb{E}[\sigma(t,U)]dW_t^{\mathbb{P}} + \mathbb{E}[\eta(t,U)]d\widetilde{J}_t^{\mathbb{P}} \; . \tag{3.8}$$

Moreover, the swap price based on geometric averaging evolves as

$$\frac{dF(t,\tau_1,\tau_2)}{F(t-,\tau_1,\tau_2)} = \mathbb{E}[\sigma(t,U)]dW_t^{\mathbb{P}} + \int_{\mathbb{R}} \left(e^{\mathbb{E}[\eta(t,U)]z} - 1\right)\widetilde{N}^{\mathbb{P}}(dt,dz) + \widetilde{c}^{\mathbb{P}}(t,\tau_1,\tau_2,\bar{Y}(t,\tau_1,\tau_2))dt \; , \tag{3.9}$$

where the drift term is given by

$$\widetilde{c}^{\mathbb{P}}(t,\tau_1,\tau_2,\bar{Y}) = \mathbb{E}[\mu(t,U)] - \kappa(t)\bar{Y} + \frac{1}{2}\mathbb{E}[\sigma(t,U)]^2 + \psi^{\mathbb{P}}(\mathbb{E}[\eta(t,U)]) \; . \tag{3.10}$$

Proof. Following the considerations in the previous section, the swap price is defined by the geometric average in Equation (2.11). Using the notation from Lemma 2.1, Equation (3.7) follows. Using the stochastic Fubini theorem (see Protter (2005), cf. Theorem 65), we can introduce the dynamics of $\bar{Y}$. An application of Ito's formula (see Øksendal and Sulem (2007), cf. Theorem 1.16) yields the desired swap dynamics. □

Lemma 3.4. *Let Assumptions 4 to 6 in Appendix A be satisfied. Then, the swap price dynamics based on approximated averaging evolve as*

$$\frac{dF^a(t,\tau_1,\tau_2)}{F^a(t-,\tau_1,\tau_2)} = \mathbb{E}[\sigma(t,U)]dW_t^{\mathbb{P}} + \int_{\mathbb{R}} \left(\mathbb{E}[e^{\eta(t,U)z}] - 1\right)\widetilde{N}^{\mathbb{P}}(dt,dz) + \mathbb{E}_U[c^{\mathbb{P}}(t,U,Y(t,U))]dt \; , \tag{3.11}$$

where $\mathbb{E}_U[c^{\mathbb{P}}(t,U,Y)] = \mathbb{E}[\mu(t,U)] - \kappa(t)\mathbb{E}_U[Y] + \frac{1}{2}\mathbb{E}[\sigma^2(t,U)] + \mathbb{E}[\psi^{\mathbb{P}}(\eta(t,U))]$, *with* $\mathbb{E}_U$ *denoting the expectation with respect to the random delivery variable* U *having density* $w(u,\tau_1,\tau_2)$. *The dynamics are solved by*

$$F^a(t,\tau_1,\tau_2) = F^a(0,\tau_1,\tau_2)e^{\bar{Y}(t,\tau_1,\tau_2) + \frac{1}{2}\int_0^t \mathbb{V}[\sigma(t,U)]dv + \int_0^t \int_{\mathbb{R}} \left(\ln \mathbb{E}[e^{\eta(v,U)z}] - \mathbb{E}[\eta(v,U)]z\right)N(dv,dz)} \; , \tag{3.12}$$

where $\bar{Y}(t,\tau_1,\tau_2)$ *is defined in the previous lemma.*

Proof. We use the approximated averaging methodology (see Equation (2.10)) in order to derive the

swap price evolution and apply the stochastic Fubini theorem (see Protter (2005), cf. Theorem 65) leading to Equation (3.11). By Ito's formula (see Øksendal and Sulem (2007), cf. Theorem 1.16), we find that Equation (3.12) solves the dynamics. □

Note that the speed of mean-reversion $\kappa(t)$ has to be independent of the delivery time. This assumption ensures that $\bar{Y}$, in Equation (3.8), is again an Ornstein-Uhlenbeck process and that the swaps' logarithmic rates in Equations (3.7) and (3.12) stay tractable. This is also in line with the findings in Benth et al. (2019) (cf. Proposition 2.2) and Latini et al. (2019).

Similar to Corollary 2.1, we now evaluate the error between the exact geometric averaged swap and the approximated version under the physical measure in the next corollary.

Corollary 3.1. *The spread between the swap prices F and F^a under $\mathbb{P}$ resulting from Lemma 3.3 and Lemma 3.4 coincides with the pricing spread from Corollary 2.1.*

As the numéraire in Equation (2.26) is not affected by a change of measure, the error between the exact and approximated swap price stays the same independent of the measure.

3.2 The Swap Price F under its Risk-Neutral Measure $\widetilde{\mathbb{Q}}$

In order to derive the swap's martingale measure $\widetilde{\mathbb{Q}}$, we introduce the *true* market price of risk for the swap price resulting from geometric averaging in the next definition:

Definition 3.1. *We define the true market price of risk for the swap by $\Pi^{\mathbb{P}\widetilde{\mathbb{Q}}} := (\Pi_1^{\mathbb{P}\widetilde{\mathbb{Q}}}, \Pi_2^{\mathbb{P}\widetilde{\mathbb{Q}}})$, where*

$$\Pi_1^{\mathbb{P}\widetilde{\mathbb{Q}}}(t,\tau_1,\tau_2) := \frac{\mathbb{E}[\mu(t,U)] - \kappa(t)\bar{Y}(t,\tau_1,\tau_2) + \frac{1}{2}\mathbb{E}[\sigma(t,U)]^2}{\mathbb{E}[\sigma(t,U)]}\,, \tag{3.13}$$

$$\Pi_2^{\mathbb{P}\widetilde{\mathbb{Q}}}(t,\tau_1,\tau_2) := 1 - \int_{\mathbb{R}} z\ell^{\mathbb{P}}(dz)\frac{\mathbb{E}[\eta(t,U)]}{\int_{\mathbb{R}}\left(e^{\mathbb{E}[\eta(t,U)]z}-1\right)\ell^{\mathbb{P}}(dz)}\,. \tag{3.14}$$

Note that the market price of risk does not enter the jump size distribution since we restrict $\Pi_2^{\mathbb{P}\widetilde{\mathbb{Q}}}$ to depend on trading time and delivery period. Hence, the market price of jump risk affects the jump intensity only.

We follow the methodology of Benth et al. (2019) to change the measure from the physical measure $\mathbb{P}$ to the swap's risk-neutral measure $\widetilde{\mathbb{Q}}$. Therefore, let $\pi = (\pi_1, \pi_2)$ be a predictable process satisfying

$$\mathbb{E}\left[\int_0^{\tau_1} \|\pi(s,\tau_1,\tau_2)\|^2\, ds\right] < \infty\,. \tag{3.15}$$

We define a new process $Z^{\mathbb{P}\widetilde{\mathbb{Q}}}$ being the unique strong solution of

$$dZ^{\mathbb{P}\widetilde{\mathbb{Q}}}(t,\tau_1,\tau_2) = Z^{\mathbb{P}\widetilde{\mathbb{Q}}}(t-,\tau_1,\tau_2)dH(t,\tau_1,\tau_2)\,, \tag{3.16}$$

such that $Z^{\mathbb{P}\widetilde{\mathbb{Q}}}(0,\tau_1,\tau_2) = 1$, where

$$dH(t,\tau_1,\tau_2) = \pi_1(t,\tau_1,\tau_2)dW_t^{\mathbb{P}} + \pi_2(t,\tau_1,\tau_2)d\widetilde{J}_t^{\mathbb{P}}\,. \tag{3.17}$$

If π_j satisfies Equation (3.15), then H is a well-defined square integrable martingale. Note that the process $Z^{\mathbb{P}\widetilde{\mathbb{Q}}}$ is known as the Doléans-Dade exponential of H that is explicitly given by

$$Z^{\mathbb{P}\widetilde{\mathbb{Q}}}(t,\tau_1,\tau_2) = e^{H(t,\tau_1,\tau_2) - \frac{1}{2}\int_0^t \pi_1(s,\tau_1,\tau_2)^2 ds} \prod_{0<s\le t} (1+\Delta H(s,\tau_1,\tau_2))\, e^{-\Delta H(s,\tau_1,\tau_2)}\,. \tag{3.18}$$

If $Z^{\mathbb{P}\widetilde{\mathbb{Q}}}$ is a strictly positive martingale, then we can define the equivalent probability measure $\widetilde{\mathbb{Q}}$ by

$$\frac{d\widetilde{\mathbb{Q}}}{d\mathbb{P}} = Z^{\mathbb{P}\widetilde{\mathbb{Q}}}(\tau_1, \tau_1, \tau_2) \,, \tag{3.19}$$

where $Z^{\mathbb{P}\widetilde{\mathbb{Q}}}$ functions as the Radon-Nikodym derivative. If we further assume that $\mathbb{E}_{\mathbb{P}}[Z^{\mathbb{P}\widetilde{\mathbb{Q}}}(\tau_1, \tau_1, \tau_2)] = 1$, then Girsanov's theorem (see Øksendal and Sulem (2007), cf. Theorem 1.35) states for $\pi := -\Pi^{\mathbb{P}\widetilde{\mathbb{Q}}}$ that

$$W_t^{\widetilde{\mathbb{Q}}} = W_t^{\mathbb{P}} + \int_0^t \Pi_1^{\mathbb{P}\widetilde{\mathbb{Q}}}(s, \tau_1, \tau_2) ds \,, \tag{3.20}$$

is a Brownian motion with respect to $\widetilde{\mathbb{Q}}$ and

$$\widetilde{N}^{\widetilde{\mathbb{Q}}}(dt, dz) = \widetilde{N}^{\mathbb{P}}(dt, dz) + \Pi_2^{\mathbb{P}\widetilde{\mathbb{Q}}}(t, \tau_1, \tau_2)\ell^{\mathbb{P}}(dz)dt \,, \tag{3.21}$$

is a $\widetilde{\mathbb{Q}}$-compensated Poisson random measure of $N(\cdot, \cdot)$.

Under the above assumptions specified later a straightforward valuation leads to the following result:

Proposition 3.1. *The swap price process F defined in Equation (2.11) is a martingale under $\widetilde{\mathbb{Q}}$ given by*

$$\frac{dF(t, \tau_1, \tau_2)}{F(t-, \tau_1, \tau_2)} = \mathbb{E}[\sigma(t, U)]dW_t^{\widetilde{\mathbb{Q}}} + \int_{\mathbb{R}} \left(e^{\mathbb{E}[\eta(t,U)]z} - 1\right) \widetilde{N}^{\widetilde{\mathbb{Q}}}(dt, dz) \,. \tag{3.22}$$

We would like to investigate the consequences of our previous assumptions.

Remark 3.1. (*i*) *The Doléans-Dade exponential in Equation (3.18) is positive if $\pi_2(s-)\Delta J > -1$, i.e., if $\Pi_2^{\mathbb{P}\widetilde{\mathbb{Q}}}\Delta J < 1$. Hence, similar to Benth et al. (2019), we need to assume that the market price of jump risk is bounded and deterministic over the entire time period such that $\Pi_2^{\mathbb{P}\widetilde{\mathbb{Q}}}(t, \tau_1, \tau_2)z < 1$ for $\ell^{\mathbb{P}}$-a.e. $z \in \mathbb{R}$ and for each $t \in [0, \tau_1]$.*

(*ii*) *If Y is driven by a compensated Poisson process only, then the swap's market price of risk is attained by $\Pi^{\mathbb{P}\widetilde{\mathbb{Q}}} := (0, \Pi_2^{\mathbb{P}\widetilde{\mathbb{Q}}})$, where*

$$\Pi_2^{\mathbb{P}\widetilde{\mathbb{Q}}}(t, \tau_1, \tau_2) := 1 - \frac{\mathbb{E}[\eta(t, U)] \int_{\mathbb{R}} z\ell^{\mathbb{P}}(dz)}{\int_{\mathbb{R}} \left(e^{\mathbb{E}[\eta(t,U)]z} - 1\right) \ell^{\mathbb{P}}(dz)} + \frac{\mathbb{E}[\mu(t, U)] - \kappa(t)\bar{Y}(t, \tau_1, \tau_2)}{\int_{\mathbb{R}} \left(e^{\mathbb{E}[\eta(t,U)]z} - 1\right) \ell^{\mathbb{P}}(dz)} \,. \tag{3.23}$$

In this setting, we need to require that $\kappa(t) \equiv 0$.

Note that a positive local martingale is a supermartingale. Hence, in order to prove that the Radon-Nikodym density $Z^{\mathbb{P}\widetilde{\mathbb{Q}}}$ is a true martingale, it is sufficient to verify that $\mathbb{E}_{\mathbb{P}}[Z^{\mathbb{P}\widetilde{\mathbb{Q}}}(\tau_1, \tau_1, \tau_2)] = 1$ is satisfied, which is proven in the next proposition.

Proposition 3.2. *Under Assumption 7 in Appendix A, the process $Z^{\mathbb{P}\widetilde{\mathbb{Q}}}$ defined by Equation (3.16) is a strictly positive true martingale.*

Proof. In Appendix B, we prove this proposition even in a stochastic volatility framework. □

3.3 The Approximated Swap Price F^a under the Artificial Risk-Neutral Measure

We introduce the *classical* market price of risk for the approximated swap price in the next definition.

Definition 3.2. *We define the classical market price of risk for the approximated swap by* $\Pi^{\mathbb{PQ}} := (\Pi_1^{\mathbb{PQ}}, \Pi_2^{\mathbb{PQ}})$, *where*

$$\Pi_1^{\mathbb{PQ}}(t,\tau_1,\tau_2) := \frac{\mathbb{E}[\mu(t,U)] - \kappa(t)\bar{Y}(t,\tau_1,\tau_2) + \frac{1}{2}\mathbb{E}[\sigma^2(t,U)]}{\mathbb{E}[\sigma(t,U)]} , \tag{3.24}$$

$$\Pi_2^{\mathbb{PQ}}(t,\tau_1,\tau_2) := 1 - \int_{\mathbb{R}} z\ell^{\mathbb{P}}(dz) \frac{\mathbb{E}[\eta(t,U)]}{\int_{\mathbb{R}} \left(\mathbb{E}[e^{\eta(t,U)z}] - 1\right) \ell^{\mathbb{P}}(dz)} . \tag{3.25}$$

Note that we assume that the market price of jump risk affects the jump intensity only. The market price of risk does not enter the jump size distribution since we restrict $\Pi_2^{\mathbb{PQ}}$ to depend on trading and delivery period.

Similar to the last subsection, we can define the equivalent (artificial) probability measure $\mathbb{Q}$ by

$$\frac{d\mathbb{Q}}{d\mathbb{P}} = Z^{\mathbb{PQ}}(\tau_1,\tau_1,\tau_2) , \tag{3.26}$$

where $Z^{\mathbb{PQ}}$ functions as the Radon-Nikodym derivative characterized by $\pi_j := -\Pi_j^{\mathbb{PQ}}$. If we further assume that $\mathbb{E}_{\mathbb{P}}[Z^{\mathbb{PQ}}(\tau_1,\tau_1,\tau_2)] = 1$, then Girsanov's theorem (see Øksendal and Sulem (2007), cf. Theorem 1.35) states that

$$W_t^{\mathbb{Q}} = W_t^{\mathbb{P}} + \int_0^t \Pi_1^{\mathbb{PQ}}(s,\tau_1,\tau_2)ds , \tag{3.27}$$

is a Brownian motion with respect to $\mathbb{Q}$ and

$$\widetilde{N}^{\mathbb{Q}}(dt,dz) = \widetilde{N}^{\mathbb{P}}(dt,dz) + \Pi_2^{\mathbb{PQ}}(t,\tau_1,\tau_2)\ell^{\mathbb{P}}(dz)dt , \tag{3.28}$$

is a $\mathbb{Q}$-compensated Poisson random measure of $N(\cdot,\cdot)$.

Under the above assumptions a straightforward valuation leads to the following result:

Proposition 3.3. *The approximated swap price process* F^a *defined in Equation (2.10) is a martingale under* $\mathbb{Q}$ *given by*

$$\frac{dF^a(t,\tau_1,\tau_2)}{F^a(t-,\tau_1,\tau_2)} = \mathbb{E}[\sigma(t,U)]dW_t^{\mathbb{Q}} + \int_{\mathbb{R}} \left(\mathbb{E}[e^{\eta(t,U)z}] - 1\right) \widetilde{N}^{\mathbb{Q}}(dt,dz) . \tag{3.29}$$

We refer to Section 3.2 for the consequences of the assumptions made above.

3.4 The Decomposition of the Market Price of Risk

We now introduce the *decomposition* of the true market price of risk, from Definition 3.1, which finally connects the classical market price of risk, specified in Definition 3.2, and the MPDP, defined in Definition 2.1. The decomposition result is stated in the next proposition.

Proposition 3.4. *The swap's true market price of risk,* $\Pi^{\mathbb{P}\widetilde{\mathbb{Q}}}$, *resulting from geometric averaging (see Definition 3.1), decomposes into*

$$\Pi_j^{\mathbb{P}\widetilde{\mathbb{Q}}}(t,\tau_1,\tau_2) = \Pi_j^{\mathbb{PQ}}(t,\tau_1,\tau_2) + \bar{\Pi}_j^{\mathbb{Q}\widetilde{\mathbb{Q}}}(t,\tau_1,\tau_2) , \quad \text{for } j = 1,2 , \tag{3.30}$$

where $\Pi_j^{\mathbb{P}\mathbb{Q}}$ *is specified in Definition 3.2 and* $\bar{\Pi}_j^{\mathbb{Q}\widetilde{\mathbb{Q}}}$ *defines the spread of diffusion and jump risk. More precisely,*

$$\bar{\Pi}_1^{\mathbb{Q}\widetilde{\mathbb{Q}}} = -\frac{1}{2}\frac{\mathbb{V}[\sigma(t,U)]}{\mathbb{E}[\sigma(t,U)]}\,, \tag{3.31}$$

$$\bar{\Pi}_2^{\mathbb{Q}\widetilde{\mathbb{Q}}} = -\mathbb{E}[\eta(t,U)]\int_{\mathbb{R}} zG(dz)\frac{\int_{\mathbb{R}}\mathbb{E}[e^{\eta(t,U)z}] - e^{\mathbb{E}[\eta(t,U)]z}G(dz)}{\int_{\mathbb{R}}\left(\mathbb{E}[e^{\eta(t,U)z}]-1\right)G(dz)\int_{\mathbb{R}}\left(e^{\mathbb{E}[\eta(t,U)]z}-1\right)G(dz)}\,, \tag{3.32}$$

where $\bar{\Pi}_2^{\mathbb{Q}\widetilde{\mathbb{Q}}}$ *is independent of the jump intensity.*

Proof. The result is attained by subtracting the true market price of risk defined in Definition 3.1 from the classical market price of risk defined in Definition 3.2. □

Hence, we found a representation of the true market price of risk of the swap price F, characterized by the classical market price of risk of the approximated swap F^a and the spread $\bar{\Pi}_j^{\mathbb{Q}\widetilde{\mathbb{Q}}}$. We further investigate the spread in the next lemma.

Lemma 3.5. (*i*) *The spread of diffusion risk,* $\bar{\Pi}_1^{\mathbb{Q}\widetilde{\mathbb{Q}}}(t,\tau_1,\tau_2)$*, is negative for all trading times* $t \in [0,\tau_1]$*.*

(*ii*) *If the average jump size is positive, i.e., if* $\mathbb{E}[Z] > 0$*, then the spread of jump risk,* $\bar{\Pi}_2^{\mathbb{Q}\widetilde{\mathbb{Q}}}$*, is always negative.*

(*iii*) *If the volatility is independent of the delivery, i.e., if* $\sigma(t,u) \perp\!\!\!\perp u$*, then the spread of diffusion risk is zero, i.e.,* $\bar{\Pi}_1^{\mathbb{Q}\widetilde{\mathbb{Q}}}(t,\tau_1,\tau_2) \equiv 0$*.*

(*iv*) *If the jump coefficient is independent of the delivery, i.e., if* $\eta(t,u) \perp\!\!\!\perp u$*, then the spread of jump risk is zero, i.e.,* $\bar{\Pi}_2^{\mathbb{Q}\widetilde{\mathbb{Q}}}(t,\tau_1,\tau_2) \equiv 0$*.*

Proof. The results in (*i*) and (*ii*) follow directly from Jensen's inequality. The results in (*iii*) and (*iv*) follow from the fact that the numerator becomes zero whenever the delivery period disappears. □

As a result, whenever the spread $\bar{\Pi}_j^{\mathbb{Q}\widetilde{\mathbb{Q}}}$ is negative for $j = 1, 2$, then the approximated swap induces more risk than the swap price based on geometric averaging. In particular, the considered spread has the same properties as the MPDP (see Kemper et al. (2022)). Indeed, a comparison with our previous considerations in Section 2 gives the following insights:

Remark 3.2. (*i*) *The spread of diffusion risk,* $\bar{\Pi}_1^{\mathbb{Q}\widetilde{\mathbb{Q}}}$*, coincides with the MPDP of diffusion risk,* $\Pi_1^{\mathbb{Q}\widetilde{\mathbb{Q}}}$*, in Equation (2.13) from Section 2.*

(*ii*) *The spread of jump risk,* $\bar{\Pi}_2^{\mathbb{Q}\widetilde{\mathbb{Q}}}$*, does not coincide with the MPDP of jump risk,* $\Pi_2^{\mathbb{Q}\widetilde{\mathbb{Q}}}$*, from Equation (2.14) but with* $\Pi_2^{\mathbb{Q}\widetilde{\mathbb{Q}}}(1-\Pi_2^{\mathbb{P}\mathbb{Q}})$*. This connection occurs naturally by the change of measure.*

In a next step, we would like to characterize the MPDP of diffusion risk $\Pi_1^{\mathbb{Q}\widetilde{\mathbb{Q}}}$, and thus the spread, more explicitly. The MPDP of diffusion risk arises through delivery-dependent volatility effects such as seasonality in delivery periods and the Samuelson effect (see Kemper et al. (2022)). We state the corresponding MPDP in the following two examples while assuming a one-time settlement such that $w(t,\tau_1,\tau_2) = \frac{1}{\tau_2-\tau_1}$.

Example 3.1. *Inspired by Fanelli and Schmeck (2019), we capture seasonality in the delivery period by the following trigonometric function*

$$S_1(u) := a + b\cos(2\pi(u+c))\,, \tag{3.33}$$

for $a > b > 0$ *and* $c \in [0,1)$*. Setting* $\sigma(t,u) = S_1(u)$ *in Equation (2.13) leads to the following MPDP of diffusion risk*

$$\Pi_1^{\mathbb{Q}\widetilde{\mathbb{Q}}}(t,\tau_1,\tau_2) = -\frac{1}{2}\frac{\mathbb{V}[S_1(U)]}{\mathbb{E}[S_1(U)]}\,, \tag{3.34}$$

where

$$\mathbb{E}[S_1(U)] = a + \frac{b}{2\pi(\tau_2 - \tau_1)}\Big[\sin(2\pi(u+c))\Big]_{u=\tau_1}^{u=\tau_2}, \tag{3.35}$$

$$\mathbb{E}[S_1(U)^2] = a^2 + \frac{b^2}{2} + \frac{ab}{\pi(\tau_2 - \tau_1)}\Big[\sin(2\pi(u+c))\Big]_{u=\tau_1}^{u=\tau_2} + \frac{b^2}{8\pi(\tau_2 - \tau_1)}\Big[\sin(4\pi(u+c))\Big]_{u=\tau_1}^{u=\tau_2}. \tag{3.36}$$

Example 3.2. *We implement the Samuelson effect as in Schneider and Tavin (2018) through an exponential function with exponential damping factor $\Lambda > 0$. We choose a constant volatility $\bar{\lambda} > 0$ such that the delivery-dependent function is attained by*

$$S_2(u-t) := \bar{\lambda} e^{-\Lambda(u-t)}. \tag{3.37}$$

Setting $\sigma(t,u) = S_2(u-t)$ in Equation (2.13) yields the following MPDP of diffusion risk

$$\Pi_1^{\mathbb{Q}\widetilde{\mathbb{Q}}}(t,\tau_1,\tau_2) = -\frac{1}{2}\frac{\bar{\bar{\Lambda}} - \bar{\Lambda}^2}{\bar{\Lambda}} e^{-\Lambda(\tau_1 - t)}, \tag{3.38}$$

for constant parameters $\bar{\Lambda} := \frac{\bar{\lambda}(1-e^{-\Lambda(\tau_2-\tau_1)})}{\Lambda(\tau_2-\tau_1)}$ and $\bar{\bar{\Lambda}} := \frac{\bar{\lambda}^2(1-e^{-2\Lambda(\tau_2-\tau_1)})}{2\Lambda(\tau_2-\tau_1)}$.

Hence, the MPDP of diffusion risk is constant for a fixed contract in Example 3.1, whereas the Samuelson effect remains still visible in Example 3.2.

The MPDP of jump risk and the spread of jump risk are triggered by delivery-dependent jump effects. For notational convenience, we choose $\eta(t,u)$ independent of trading time and again assume a one-time settlement. In the following examples, we characterize the MPDP of jump risk and the spread based on two suitable jump size distributions: Normal and exponential. We also state corresponding moments of the distributions following Gray and Pitts (2012) (cf. Chapter 2).

Example 3.3. *If the jump sizes are normally distributed with $Z \sim \mathcal{N}(\mu_J, \sigma_J^2)$, then the moment generating function is given by*

$$M_Z(\eta) = e^{\mu_J \eta + \frac{1}{2}\sigma_J^2 \eta^2}, \tag{3.39}$$

such that the MPDP and the spread in Equations (2.14) and (3.32) are given by

$$\Pi_2^{\mathbb{Q}\widetilde{\mathbb{Q}}}(\tau_1,\tau_2) = -\frac{\mathbb{E}[e^{\frac{1}{2}\eta^2(U)\sigma_J^2 + \eta(U)\mu_J}] - e^{\frac{1}{2}\mathbb{E}[\eta(U)]^2\sigma_J^2 + \mathbb{E}[\eta(U)]\mu_J}}{e^{\frac{1}{2}\mathbb{E}[\eta(U)]^2\sigma_J^2 + \mathbb{E}[\eta(U)]\mu_J} - 1}, \tag{3.40}$$

$$\bar{\Pi}_2^{\mathbb{Q}\widetilde{\mathbb{Q}}}(\tau_1,\tau_2) = -\mu_J \mathbb{E}[\eta(U)] \frac{\mathbb{E}[e^{\frac{1}{2}\eta^2(U)\sigma_J^2 + \eta(U)\mu_J}] - e^{\frac{1}{2}\mathbb{E}[\eta(U)]^2\sigma_J^2 + \mathbb{E}[\eta(U)]\mu_J}}{\left(\mathbb{E}[e^{\frac{1}{2}\eta^2(U)\sigma_J^2 + \eta(U)\mu_J}] - 1\right)\left(e^{\frac{1}{2}\mathbb{E}[\eta(U)]^2\sigma_J^2 + \mathbb{E}[\eta(U)]\mu_J} - 1\right)}. \tag{3.41}$$

The fourth moment is attained by $\int_{\mathbb{R}} z^4 G(dz) = \mu_J^4 + 6\mu_J^2\sigma_J^2 + 3\sigma_J^4$.

Example 3.4. *If the jump sizes are exponentially distributed with $Z \sim \mathcal{E}xp(\lambda_J)$, for $\lambda_J > 0$, then the moment generating function is given by*

$$M_Z(\eta) = \left(1 - \frac{\eta}{\lambda_J}\right)^{-1}, \tag{3.42}$$

for $\eta < \lambda_J$, such that the MPDP and the spread in Equations (2.14) and (3.32) are given by

$$\Pi_2^{\mathbb{Q}\widetilde{\mathbb{Q}}}(\tau_1,\tau_2) = -\frac{\lambda_J}{\mathbb{E}[\eta(U)]}\left(1-\mathbb{E}\left[\frac{\lambda_J-\mathbb{E}[\eta(U)]}{\lambda_J-\eta(U)}\right]\right), \tag{3.43}$$

$$\bar{\Pi}_2^{\mathbb{Q}\widetilde{\mathbb{Q}}}(\tau_1,\tau_2) = \frac{\mathbb{E}[\eta(U)]\mathbb{E}[\frac{1}{\lambda_J-\eta(U)}]}{\mathbb{E}[\frac{\eta(U)}{\lambda_J-\eta(U)}]} - 1\,, \tag{3.44}$$

defined for $\eta(U) < \lambda_J$ and $\mathbb{E}[\eta(U)] < \lambda_J$. The n-th moment is attained by $\int_{\mathbb{R}} z^n G(dz) = \frac{n!}{\lambda_J^n}$ for $n \in \mathbb{N}$. Note that the parameter in matlab is indicated by the mean $\mu_J = \lambda_J^{-1}$.

Remark 3.3. *In the literature, we sometimes find the application of lognormal distributed jump sizes (see, e.g., Borovkova and Permana (2006) and Borovkova and Schmeck (2017)). This distribution, however, is not suitable for our setting since its moment generating function $\mathbb{E}[e^{\eta Z}]$ is not finite at any positive value η (see, e.g., Gray and Pitts (2012), cf. Chapter 2.2.6). Hence, the lognormal distribution contradicts the integrability assumption 4 (i) under the physical measure in Appendix A.*

4 Empirical Analysis

In this section, we aim to provide empirical evidence for the MPDP of monthly electricity swap contracts. We therefore extend our model to a multi-dimensional framework and discretize the model under the physical measure. In particular, we consider two types of delivery-dependent functions covering seasonality and the term-structure effects. We then proceed estimating the model's parameter values. In a first step, jumps are filtered by a thresholding method. In a second step, we fit the remaining parameters by Maximum-Likelihood-Estimation (MLE).

4.1 The Multidimensional Model

In the previous sections, we considered a single tradable swap contract delivering electricity over the interval $(\tau_1,\tau_2]$. Typically, however, we observe more than one traded delivery period. We therefore extend our model under the physical measure $\mathbb{P}$ from Section 3 to a multi-dimensional setting covering subsequent monthly delivery periods. More precisely, we would like to handle M swaps simultaneously in this section comprising delivery periods $(\tau_m,\tau_{m+1}]$ for $m = 1,\dots,M$. For notational convenience, we always refer to all swap contracts $m = 1,\dots,M$, when using the index m. We follow the methodology presented by Kemper et al. (2022) who suggest a single artificial futures price (similar to Equation (3.1)) expanded by several factors in the logarithmic return component Y:

$$dY(t,\tau) = (\mu(t,\tau) - \kappa(t)Y(t,\tau))\,dt + \sum_{j=1}^{M} \mathbb{1}_{j\in\mathcal{T}}\sigma(t,\tau)dW_t^{\mathbb{P},j} + \sum_{j=1}^{M} \mathbb{1}_{j\in\mathcal{T}}\eta(t,\tau)d\widetilde{J}_t^{\mathbb{P},j}\,, \tag{4.1}$$

where $W^{\mathbb{P},1},\dots,W^{\mathbb{P},M}$ are independent Brownian motions under the physical measure $\mathbb{P}$ and $\widetilde{J}^{\mathbb{P},1},\dots,\widetilde{J}^{\mathbb{P},M}$ are independent compound compensated jump processes defined through $J_t^{\mathbb{P},j} = \int_{\mathbb{R}} z\widetilde{N}_j^{\mathbb{P}}(dt,dz)$ and the compensated Poisson random measures $\widetilde{N}_j^{\mathbb{P}}(dt,dz) = N_j(dt,dz) - \ell_j^{\mathbb{P}}(dz)dt$ with the same compensator $\ell_j^{\mathbb{P}}(dz) = \lambda^{\mathbb{P}}G(dz)$ for $j = 1,\dots,M$. In addition, we restrict the j-th component to a set $\mathcal{T}$ that might influence certain contracts exclusively.

As in Section 2, the swap price with delivery period $(\tau_m,\tau_{m+1}]$ results from geometric averaging of Equation (4.1) with respect to the delivery time. Hence, similar to our previous considerations in Lemma 3.3, we

state the dynamics of the logarithmic return of a swap contract with delivery time $(\tau_m, \tau_{m+1}]$ by

$$\begin{aligned} d\bar{Y}(t,\tau_m,\tau_{m+1}) = &\left(\mathbb{E}[\mu(t,U_m)] - \kappa(t)\bar{Y}(t,\tau_m,\tau_{m+1})\right)dt \\ &+ \sum_{j=1}^{M} \mathbb{1}_{j\in\mathcal{T}}\mathbb{E}[\sigma(t,U_m)]dW_t^{\mathbb{P},j} + \sum_{j=1}^{M} \mathbb{1}_{j\in\mathcal{T}}\mathbb{E}[\eta(t,U_m)]d\widetilde{J}_t^{\mathbb{P},j} \,, \end{aligned} \tag{4.2}$$

where $U_m \sim \mathcal{U}((\tau_m,\tau_{m+1}])$ is a random variable with density $w(\cdot,\tau_m,\tau_{m+1})$. To keep the model simple, we choose $\mathcal{T} := \{m\}$, $\eta \equiv 1$, and κ independent of time such that

$$d\bar{Y}(t,\tau_m,\tau_{m+1}) = \left(\mathbb{E}[\mu(t,U_m)] - \kappa\bar{Y}(t,\tau_m,\tau_{m+1})\right)dt + \mathbb{E}[\sigma(t,U_m)]dW_t^{\mathbb{P},m} + d\widetilde{J}_t^{\mathbb{P},m} \,. \tag{4.3}$$

Hence, we assign separate dynamics for each monthly swap contract.

Remark 4.1. *Note that we set $\eta \equiv 1$ in Equation (4.3), thus, excluding any delivery dependence in the jump component. Consequently, the MPDP of jump risk becomes zero by construction to turn the focus on the first dimension of the MPDP.*

4.2 The Discretized Model

In order to discretize the model of Section 3 under the physical measure $\mathbb{P}$, we follow the Euler-type discretization procedure with step size $\Delta t = \frac{1}{252}$. Furthermore, we implement the discretization of jumps as in Johannes and Polson (2010) (cf. Chapter 5.1.3). The discretized logarithmic returns of the swap from Equation (4.3) are denoted by $y_t \in \mathbb{R}^M$, with $y_{t,m} := \bar{Y}(t,\tau_m,\tau_{m+1})$, and are given by

$$y_{t+\Delta t} = \bar{\phi}\cdot y_t + \bar{\mu}_t\Delta t + \bar{\sigma}_t\sqrt{\Delta t}\epsilon_{t+\Delta t} + ZJ_{t+\Delta t} \,, \tag{4.4}$$

for $t = 1,\dots,T_m$, where we denote T_m as the length of the time series with delivery during $(\tau_m,\tau_{m+1}]$. Moreover, $\epsilon \sim \mathcal{N}(\mathbf{0},\mathbf{1})$ is a standard normal distributed random variable, where $\mathbf{0}$ is an M-dimensional vector of zeros and $\mathbf{1}$ is the $M\times M$-dimensional identity matrix. Further, Z is a random variable with distribution G characterizing the jump sizes. Moreover, J is an independent M-dimensional Bernoulli distributed random variable with parameter $\lambda^{\mathbb{P}}\Delta t\mathbf{1} \in \mathbb{R}^M$ determining a jump, where $\mathbf{1}$ is an M-dimensional vector of ones. Moreover, the coefficients to be estimated are $\bar{\mu}_t \in \mathbb{R}^M$, where $\bar{\mu}_{t,m} = \mathbb{E}[\mu(t,U_m)] - \mathbb{E}[\eta(t,U_m)]\lambda^{\mathbb{P}}\mathbb{E}[Z]$, $\bar{\phi} = \mathbf{1} - \boldsymbol{\kappa} \in \mathbb{R}^M$, and $\bar{\sigma}_t \in \mathcal{S}^M$, which is a diagonal volatility matrix with diagonal entries $\bar{\sigma}_{t,m} = \mathbb{E}[\sigma(t,U_m)]$.

Remark 4.2. *By stationarity of the underlying Poisson process, the probability of the absence of a jump during a time step Δt is given by $e^{-\lambda^{\mathbb{P}}\Delta t}$. Merton (1976) reformulates this in terms of short time asymptotic behavior using $1-\lambda^{\mathbb{P}}\Delta t + O(\Delta t)$. Therefore, Johannes and Polson (2010) assume the jumps to be Bernoulli distributed in the discretized setting, that is*

$$\mathbb{P}[J_{t+\Delta t}^m = 1] = \lambda^{\mathbb{P}}\Delta t \qquad \textit{and} \qquad \mathbb{P}[J_{t+\Delta t}^m = 0] = 1-\lambda^{\mathbb{P}}\Delta t \,, \tag{4.5}$$

where at most one jump can occur during a time interval Δt. We follow their approach assuming $J_{t+\Delta t}^m \sim \mathcal{B}er(\lambda^{\mathbb{P}}\Delta t)$ for $m = 1,\dots,M$.

Remark 4.3. *By construction, the contracts are independent of each other. We justify this assumption since the drivers of forthcoming contracts do not influence dynamics of the other contracts that deliver electricity further ahead due to their non-storability.*

We refer to Kemper et al. (2022) (cf. Section 4) for further insights on multiple and overlapping swap contracts. We make the following assumption in order to reduce the number of parameters and thus to avoid overfitting.

Assumption 4.1. *We assume that* $\mu(t,u) = \mu\sigma(t,u)$ *for* $t \in [0,\tau_m]$ *and* $u \in (\tau_m, \tau_{m+1}]$ *and all* $m = 1,\dots,M$.

Due to the low interest rate level, we make further assumptions on the settlement type.

Assumption 4.2. *We assume that* $U_m \sim \mathcal{U}((\tau_m,\tau_{m+1}])$, *which induces a one-time settlement for all contracts* $m = 1,\dots,M$.

Based on these assumptions, we consider two types of delivery-dependent functions, which will be investigated empirically. We consider the *seasonality type* from Example 3.1, which induces the seasonality function $S_1(u)$ that is independent of trading time and we refer to it as *Type 1*. Moreover, we investigate the *Samuelson type* model from Example 3.2 depending on time to maturity and refer to it as *Type 2*.

Type 1. *The model of "seasonality type" is based on Example 3.1. Under Assumptions 4.1 and 4.2, the coefficients of Equation (4.4) become*

$$\begin{aligned}
\bar{\phi} &= \mathbf{1} - \boldsymbol{\kappa}\boldsymbol{\Delta t}\,,\\
\bar{\mu} &= \mu\left(\mathbb{E}[S_1(U_1)],\dots,\mathbb{E}[S_1(U_M)]\right)^\top - \lambda^{\mathbb{P}}\mathbb{E}[Z]\mathbf{1}\,,\\
\bar{\sigma} &= diag\left(\mathbb{E}[S_1(U_1)],\dots,\mathbb{E}[S_1(U_M)]\right)^\top\,.
\end{aligned}$$

Type 2. *The model of "Samuelson type" follows Example 3.2. Under Assumptions 4.1 and 4.2, the coefficients of Equation (4.4) become*

$$\begin{aligned}
\bar{\phi} &= \mathbf{1} - (\boldsymbol{\kappa} - \boldsymbol{\Lambda})\boldsymbol{\Delta t}\,,\\
\bar{\mu}_t &= \mu\bar{\Lambda}\left(e^{-\Lambda(T_1-t)\Delta t},\dots,e^{-\Lambda(T_M-t)\Delta t}\right)^\top - \lambda^{\mathbb{P}}\mathbb{E}[Z]\mathbf{1}\,,\\
\bar{\sigma}_t &= \bar{\Lambda}\ diag\left(e^{-\Lambda(T_1-t)\Delta t},\dots,e^{-\Lambda(T_M-t)\Delta t}\right)^\top\,.
\end{aligned}$$

We fit both types to the data presented in Section 4.4 using the method described in the following section.

4.3 The Method

We use the dataset described later in Section 4.4 to estimate our discretized model of Types 1 and 2 within a two-step procedure.

In a first step, we filter jumps by the thresholding procedure as presented in Borovkova and Schmeck (2017). They define certain upper and lower boundaries in which all logarithmic returns are assumed to be normally distributed. If such a boundary is passed, the corresponding logarithmic return is identified as a jump. We use a time window of two weeks (10 data points) and a threshold 1.96 associated with 95% of standard-normal distribution. The annualized jump intensity is typically derived as the total number of identified jumps appearing in each contract divided by the annualized number of observations (see also Benth et al. (2012)). We define the annualized jump intensity $\lambda^{\mathbb{P}}$ as the mean intensity over all contracts so that the intensity is independent of the delivery time.

We fit the identified jump sizes of all twelve contracts jointly and assume that they follow the same jump size distribution G. Indeed, the number of identified positive and negative jumps per contract might be too small for separate estimations. In particular, we consider two different types of jump size distributions: Normal and exponential distribution. The normal distribution is embraces real-valued variables, whereas exponential distribution covers positive variables only. Consequently, we split the jump part into two independent jump components for the ladder distribution to take negative jumps into account as well. In particular,

$$ZJ_{t+\Delta t} = Z^+ J^+_{t+\Delta t} - Z^- J^-_{t+\Delta t}\,, \tag{4.6}$$

where $Z^+, Z^- > 0$ are the absolute values of positive and negative jump sizes and $J^+_{t+\Delta t}, J^-_{t+\Delta t}$ are M-dimensional Bernoulli distributed random variables with positive parameters $\lambda^{\mathbb{P}+}\Delta t\mathbf{1}$ and $\lambda^{\mathbb{P}-}\Delta t\mathbf{1}$, respectively, which are derived analogously as explained before. In addition, we determine the joint jump compensator and the moment generating function as an intensity weighted sum $\lambda^{\mathbb{P}}\mathbb{E}[Z] = \lambda^{\mathbb{P}+}\mathbb{E}[Z^+] - \lambda^{\mathbb{P}-}\mathbb{E}[Z^-]$ and $\lambda^{\mathbb{P}}\mathbb{E}[e^Z] = \lambda^{\mathbb{P}+}\mathbb{E}[e^{Z^+}] - \lambda^{\mathbb{P}-}\mathbb{E}[e^{Z^-}]$, whenever we split into positive and negative jumps. We employ the first window of the thresholding procedure as a training period, which should be excluded from the data used to estimate the parameters in the second step. Otherwise, the thresholding procedure might not exclude all jumps, especially within the first half of the considered training period.

In a second step, we fit the jump free logarithmic returns $\bar{y}_{t+\Delta t} := y_{t+\Delta t} - ZJ_{t+\Delta t}$ using the MLE technique to obtain the remaining parameter estimates. In particular, the likelihood is expressed in terms of the conditional probability density function

$$\mathcal{L}(\bar{y}_m; \Theta_m) = \prod_{j=1}^{T_m} p_{\Theta_m}(\bar{y}_{j,m} | \{\bar{y}_{1,m}, \dots, \bar{y}_{j-1,m}\}) \,, \tag{4.7}$$

where Θ is the set of parameters, and $p_{\Theta_m}(\bar{y}_{j,m} | \{\bar{y}_{1,m}, \dots, \bar{y}_{j-1,m}\})$ determines the conditional probability density function for contract m at data point j. For each type, we characterize the density more precisely.

Type 1. The jump free model of *seasonality type* is characterized by $\bar{y}_{j,m} | \{\bar{y}_{1,m}, \dots, \bar{y}_{j-1,m}\} \sim \mathcal{N}(\bar{\mu}_m \Delta t + \bar{\phi}_m \bar{y}_{j-1,m}, \bar{\sigma}^2_m \Delta t)$ having a conditional probability density function given by

$$p_{\Theta_m}(\bar{y}_{j,m} | \{\bar{y}_{1,m}, \dots, \bar{y}_{j-1,m}\}) = (2\pi\bar{\sigma}^2_m \Delta t)^{-\frac{1}{2}} \exp\left\{ -\frac{1}{2\bar{\sigma}^2_m \Delta t} \left(\bar{y}_{j,m} - \bar{\mu}_m \Delta t - \bar{\phi}_m \bar{y}_{j-1,m} \right)^2 \right\} \,,$$

where the set of parameters is defined by $\Theta_m := \{\bar{\mu}_m, \bar{\phi}_m, \bar{\sigma}^2_m\}$ subject to $\bar{\phi}_m < 1$, $\bar{\sigma}^2_m > 0$, and $\bar{\mu}_m \in \mathbb{R}$. We recalibrate the parameters to characterize κ, μ, and $\bar{\sigma}$ accordingly.

Type 2. The jump free model of *Samuelson type* induces $\bar{y}_{j,m} | \{\bar{y}_{1,m}, \dots, \bar{y}_{j-1,m}\} \sim \mathcal{N}(\bar{\mu}_{j,m} \Delta t + \bar{\phi}_m \bar{y}_{j-1,m}, \bar{\sigma}^2_{j,m} \Delta t)$ such that the conditional probability density function is given by

$$p_{\Theta_m}(\bar{y}_{j,m} | \{\bar{y}_{1,m}, \dots, \bar{y}_{j-1,m}\}, \lambda^{\mathbb{P}}\mathbb{E}[Z]) = (2\pi\bar{\sigma}^2_{j,m} \Delta t)^{-\frac{1}{2}} \exp\left\{ -\frac{1}{2\bar{\sigma}^2_{j,m} \Delta t} \left(\bar{y}_{j,m} - \bar{\mu}_{j,m} \Delta t - \bar{\phi}_m \bar{y}_{j-1,m} \right)^2 \right\} \,,$$

where the set of parameter values $\Theta_m := \{\mu_m, \bar{\phi}_m, \bar{\Lambda}^2_m, \Lambda_m\}$ is subject to $\bar{\phi}_m < 1$, $\bar{\Lambda}^2_m, \Lambda_m > 0$, and $\mu_m \in \mathbb{R}$. Note that $\bar{\mu}$ depends on $\lambda^{\mathbb{P}}\mathbb{E}[Z]$, as defined in Type 2, which we already know from the first step and is therefore used as an input. We recalibrate the parameters to characterize κ, μ, Λ, and $\bar{\lambda}$ accordingly.

The optimization procedure is implemented in Matlab using the `simulannealbnd` function based on simulated annealing (see Goffe et al. (1994), also used by Schneider and Tavin (2018)).

4.4 Description of the Dataset

We consider twelve electricity swap contracts with monthly delivery periods in 2019 traded at EEX. In particular, we work with time series of the *Phelix Base Monthly Energy Futures*[1] from May 2nd, 2018 to November 29th, 2019, spanning on average about 150 data points before the contract expires. We use weekday prices to exclude weekend effects.

[1] Note that the name *Futures* refers in our context to swap contracts.

We provide an overview over the general characteristics of each electricity swap contract in Table 2, including the start and maturity of the available time series, the range of available trading time, the amount of assessable data points, minimum, maximum, average prices, and the average standard deviation. For some contracts, we have data covering a longer trading horizon, especially October. On the contrary, for some contracts, we have a very short trading horizon available, like November and December. The average prices are highest in the first quarter of the year. The standard deviations computed over all monthly contracts range from 2.863 to 6.396, appearing highest for winter and summer months like January, February, and June.

Figure 2 depicts the time series of prices and logarithmic returns for each swap contract with respect to time to maturity. Note that the histograms and the logarithmic returns for each contract can be found in Appendix C. The plotted prices sometimes display a constant behavior at the beginning of the trading time. This might indicate an illiquid market. In Figure 2 (c), we clearly observe jump behavior not only close to delivery but over the whole trading horizon. For this reason, we formally test the swap's logarithmic returns on normality using Matlab's Lilliefors test `lillietest`. The test returns a decision for the null hypothesis that the data comes from a normal distribution. We summarize our test results in Table 3, where 0 indicates a failure to reject the null hypothesis of normal distributed logarithmic returns at significance level 0.05. It turns out that except from March, April, June, and December, all swap contracts reject the normal hypothesis. The histogram and the logarithmic returns for each contract in Appendix C give an intuition on the normal distribution fit. In addition, we tested the mean-reverting behavior using the Augmented Dickey-Fuller test `adftest` for autocorrelation, where 1 indicates mean-reverting effects whenever the p-value is below the significance level 0.05. Indeed, all swap contracts reject the null hypothesis so that mean-reverting behavior is clearly present.

Next, we move on to the results of the two-step estimation procedure. Given the parameter estimates, we will be able to calculate the MPDP.

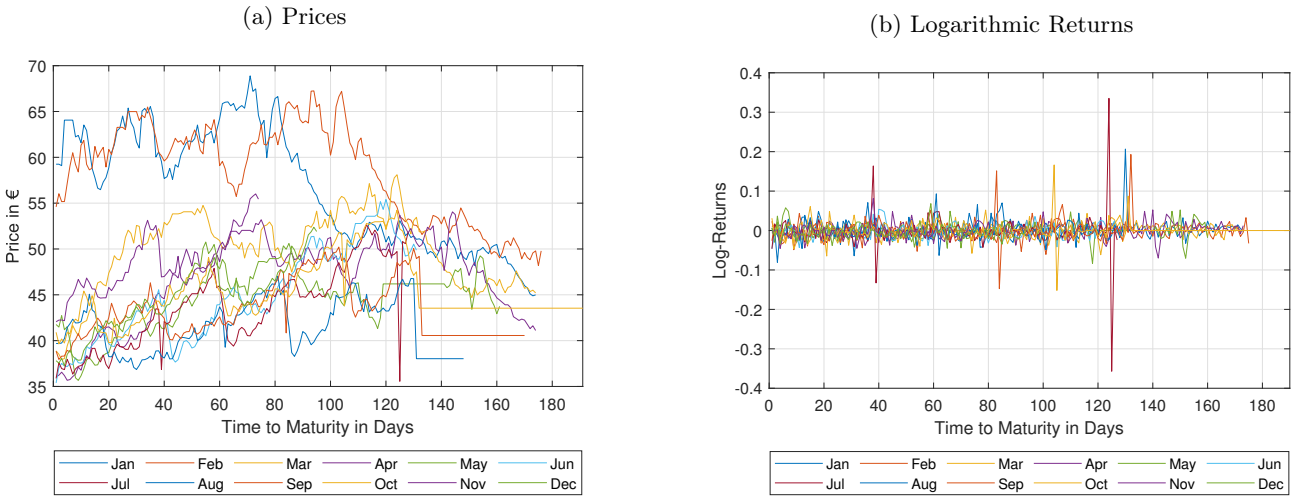

Figure 2: Time series for prices and logarithmic returns of all monthly electricity swap contracts maturing in 2019 plotted with respect to time to maturity.

Contracts	Starting Date	Maturity	Data Points	Minimum	Maximum	Average Price	Standard Deviation
January	02-05-2018	31-12-2018	174	44.89	68.89	56.75	6.396
February	31-05-2018	31-01-2019	176	48.19	67.25	58.43	5.210
March	02-07-2018	28-02-2019	174	37.95	58.10	49.86	4.205
April	31-07-2018	29-03-2019	174	35.67	54.05	46.80	4.758
May	31-08-2018	12-04-2019	161	35.66	50.60	44.58	3.240
June	30-11-2018	31-05-2019	131	35.38	55.40	44.93	5.148
July	02-01-2019	28-06-2019	128	35.56	52.63	43.59	4.462
August	07-01-2019	31-07-2019	148	36.85	47.03	41.43	2.863
September	07-01-2019	30-08-2019	170	37.95	50.21	43.32	3.150
October	07-01-2019	30-09-2019	191	39.65	54.24	45.21	3.430
November	22-07-2019	31-10-2019	74	42.06	56.01	48.37	3.379
December	22-07-2019	29-11-2019	95	37.24	52.37	44.65	3.817
Average	–	–	149.67	38.92	55.57	47.33	4.171

Table 2: General characteristics of the Phelix Base Monthly Energy Futures dataset.

Contracts	Normality Test		Mean-Reversion Test	
	Decision `lillietest`	p-value	Decision `adftest`	p-value
January	1	0.011	1	0.001
February	1	0.046	1	0.001
March	0	0.152	1	0.001
April	0	0.387	1	0.001
May	1	0.001	1	0.001
June	0	0.188	1	0.001
July	1	0.001	1	0.001
August	1	0.001	1	0.001
September	1	0.001	1	0.001
October	1	0.001	1	0.001
November	1	0.018	1	0.001
December	0	0.055	1	0.001

Table 3: Test results for normality and mean-reversion at significance level 0.05. (`lillietest` h=1 indicates rejection of normal distribution. `adftest` h=1 indicates an AR(1) model with drift coefficient.) Note that the `adftest` returns minimum (0.001) or maximum (0.999) p-values if the test statistics are outside the tabulated critical values.

4.5 Results

In this section, we present the results of the empirical analysis of the swap price data presented in Section 4.4 based on the two-step procedure outlined in Section 4.3.

Step I. We identify the jumps as described in Section 4.3. The procedure is visualized in Figure 3, exemplified for January and July. The dotted lines indicate the 95% band of normal distribution based on the moving mean depicted in dashed. Whenever the swap's logarithmic return, in solid line, exceeds the threshold, a jump is identified and highlighted with a red star. The total number of jumps is higher in January than in July. This does not only result from the longer trading time since the annualized jump intensity in January is also higher (see Figure 4 (a) and Table 4).

On average, we can identify 14 jumps per contract. This leads to an annualized average intensity $\lambda^{\mathbb{P}}$ of almost 25 jumps per year (see Table 4 and Figure 4 (a)). Note the seasonal pattern in the monthly jump intensities: From January, June, July, November, and December the annualized intensity is higher than the average intensity. Hence, we observe a higher intensity during winter and summer months. For the scope of this paper, however, we will assume a constant jump intensity $\lambda^{\mathbb{P}} = 24.811$, which is the mean of all annualized jump intensities (indicated in red in Figure 4 (a)).

We identify all jumps regarding time to maturity in Figure 4 (b). We observe many small jumps and 5–8 large jumps in each direction, so that jump size distributions with high tails might be useful. In Figure 4 (c), we plot the accumulated jump numbers with respect to time to maturity until 74 days before the contracts expire, i.e., when all contracts are available. Note that the linear behavior indicates a constant intensity so especially no term-structure effects. In blue, we observe the accumulated number of all jumps, in red of all positive jumps, and in yellow of all negative jumps. We observe in total 169 jumps from which 85 are positive and 84 are negative. There seems to be no indication for a Samuelson effect within the jump intensity since there is no higher amount of jumps the closer we reach the end of the maturity. In fact, the accumulated jump number seems rather linear. Further plots on the jump identification can be found in Appendix D.

Having identified all jumps, we are interested in finding the best jump size distribution. Borovkova and Permana (2006) find that the exponential distribution gives a good fit for jump sizes of electricity spot prices. Borovkova and Schmeck (2017) identify a lognormal or exponential distribution for negative jumps and an exponential distribution for positive jumps in their electricity spot price dataset, whereas Hinderks et al. (2020) suggest a gamma distribution. Normally distributed jumps are rarely considered in electricity markets due to their flat tails but used in stock markets (see, e.g., Merton (1976)) and in the setting of commodity markets (see, e.g., Crosby and Frau (2022)). For the sake of comparison, we consider two distributions: Normal and exponential. Note that we fit the jump sizes jointly for all contracts since for some contracts the number of identified jumps is too little. For example, the November contract has three positive jumps.

In Figure 5, we consider all identified jumps jointly for all contracts and estimate parameters for normal jump sizes. Both, histogram and QQ-plot, confirm that the normal distribution underestimates the fat-tail risk (both, positive and negative). This is also reflected in the p-value as the parameter of the mean is not significantly below 0.05. In Figure 6, we consider positive and negative jumps separately for exponentially distributed jump sizes. From the QQ-plot, we observe again outliers on the tails but not as extreme as in the normal distribution. We find that the exponential distribution fits well according to the p-values, which are significantly below 0.05. A gamma distribution would require two parameters to describe the data. We also checked the gamma fit empirically and received similar results. Since the exponential distribution can explain the jump size sufficiently well with one parameter, we base our analysis on the exponential distribution in Step II.

In Table 5, we summarize the estimated jump intensities and the average of each distribution. The annualized average intensity of all jumps is 25 consisting of a jump frequency around 11.991 for positive and around 12.820 for negative jumps. Hence, the intensity for positive jumps is sightly lower than for negative jumps. The average jump sizes range from 0.0005 to 0.0212. Moreover, we observe that negative jump sizes are smaller on average than the positive jumps. As outlined before, the exponential distribution fits better than the normal distribution. Thus, we set the jump compensator used in Step II, to be $\lambda^{\mathbb{P}}\mathbb{E}[Z] = -0.0086$ for all contracts.

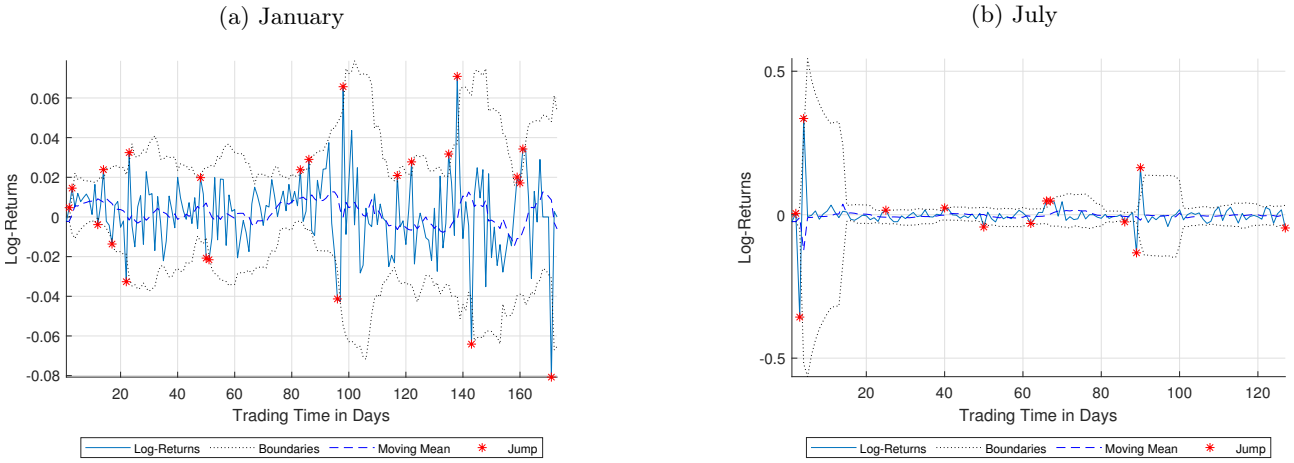

Figure 3: Identified jumps by thresholding using a time window of 10 days (exemplified for January and July).

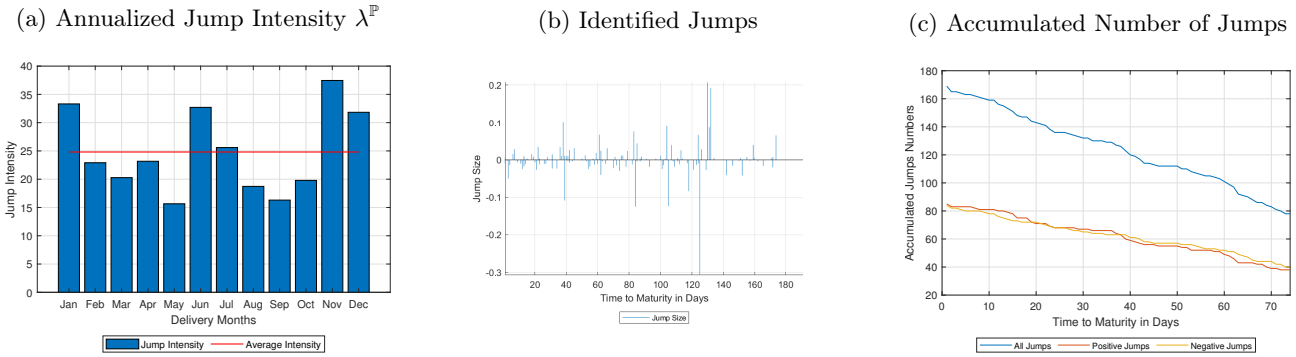

Figure 4: Subfigure (a): Annualized jump intensity per electricity swap contract. Subfigure (b): Identified jumps of all contracts with respect to time to maturity. Subfigure (c): Accumulated number of positive and negative jumps of all contracts with respect to time to maturity.

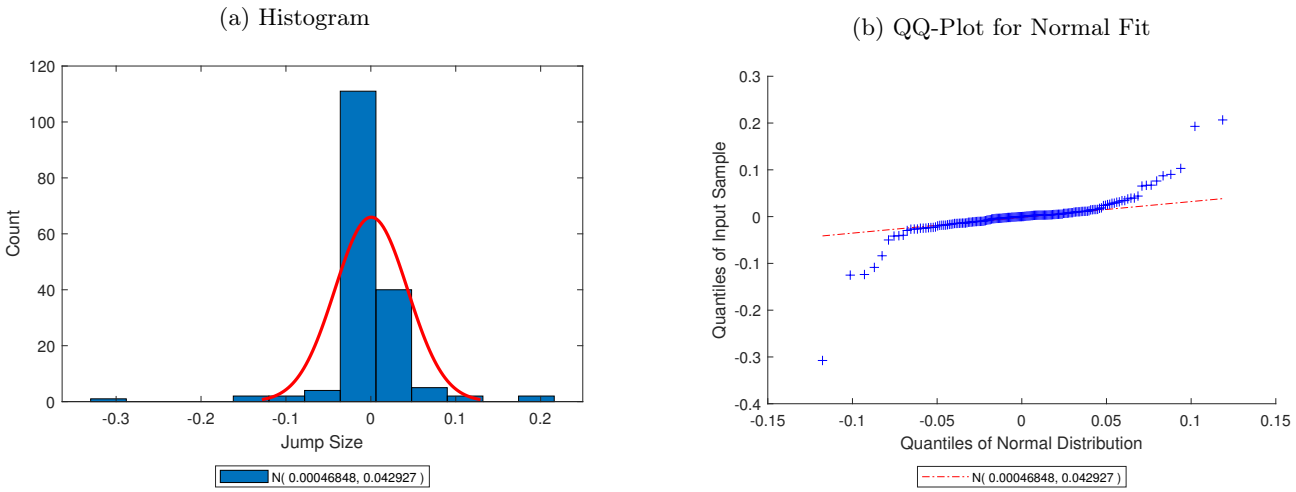

Figure 5: Histogram and QQ-Plot of all identified jumps for all contracts fitted with a normal distribution. (p-value of μ_J: 0.8965 and p-value of σ_J: 8.4341e-66.)

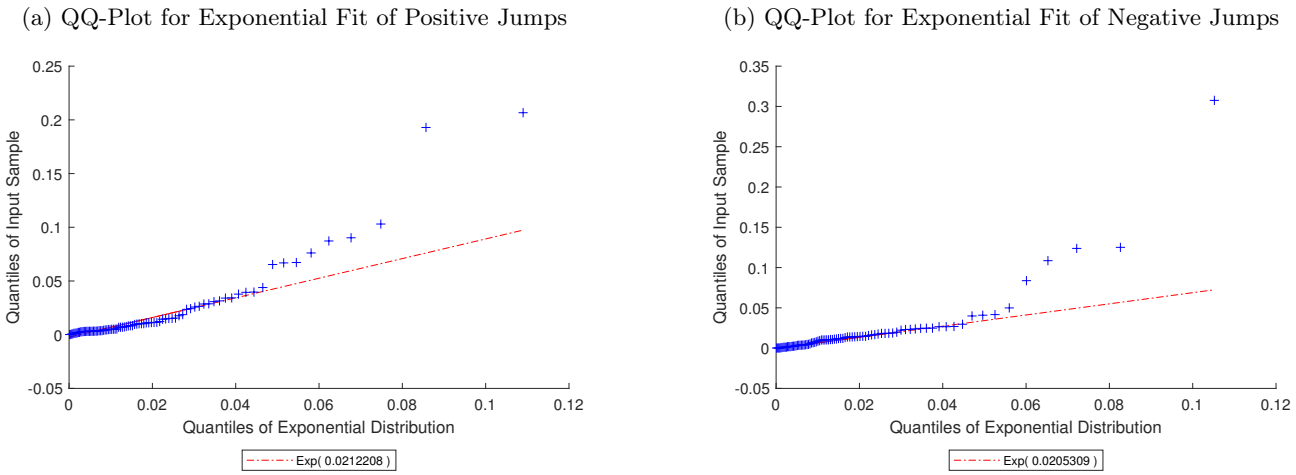

Figure 6: QQ-Plots of positive and negative jumps over all contracts. (Positive jumps – p-value of μ_J: 3.11536e-18. Negative jumps – p-value of μ_J: 4.91286e-18.)

Contracts	# Jumps	$\lambda^{\mathbb{P}}$	# Positive Jumps	$\lambda^{\mathbb{P}+}$	# Negative Jumps	$\lambda^{\mathbb{P}-}$
January	23	33.310	15	21.724	8	11.586
February	16	22.909	10	14.318	6	8.591
March	14	20.276	6	8.690	8	11.586
April	16	23.172	6	8.690	10	14.483
May	10	15.652	5	7.826	5	7.826
June	17	32.702	8	15.389	9	17.313
July	13	25.594	7	13.781	6	11.812
August	11	18.730	6	10.216	5	8.514
September	11	16.306	8	11.859	3	4.447
October	15	19.791	6	7.916	9	11.874
November	11	37.459	3	10.216	8	27.243
December	12	31.832	5	13.263	7	18.568
Average	14.083	24.811	7.083	11.991	7	12.820

Table 4: Identified total, positive, and negative number of jumps in the logarithmic returns of each contract and its annualized jump intensities $\lambda^{\mathbb{P}}$, $\lambda^{\mathbb{P}+}$, and $\lambda^{\mathbb{P}-}$.

	Intensity	Normal $\mathbb{E}[Z]$	Exponential $\mathbb{E}[Z]$
Positive	$\lambda^{\mathbb{P}+} = 11.991$	–	0.0212
Negative	$\lambda^{\mathbb{P}-} = 12.820$	–	0.0205
Total	$\lambda^{\mathbb{P}} = 24.811$	0.0005	–

Table 5: Estimated components of the jump compensator: Intensity and mean of jump sizes.

Step II. For each contract, we fit the jump free logarithmic returns by maximizing the likelihood in Equation (4.7). For both types of models (Type 1 and Type 2), the parameter estimates can be found in Table 6. The seasonality function $\mathbb{E}[S_1(U)]$ resulting from Equation (3.35) is characterized by the parameter values in Table 7 and depicted in Figure 7 (a). The Samuelson function $\mathbb{E}[S_2(U-t)]$ resulting from $\bar{\Lambda}e^{-\Lambda(\tau_1-t)}$ (see Example 3.2) is visualized in Figure 7 (b) for each contract. In particular, we fit the resulting $\bar{\sigma}$ to the seasonality curve (see Table 7).

In Table 6, we observe that the speed of mean-reversion κ is very high for both models so that the half life lies within one day. The level on mean-reversion μ is often around zero and in November and December negative for both models: It is the smallest in December in both cases. One possible explanation for this observation might be the uncertainty regarding the availability of electricity especially for heating intense seasons. The volatility $\bar{\sigma}$ ranges from 0.2303 in September to 0.2726 in February.

Remark 4.4. *In Figure 7 (a), we observe rather flat seasonal behavior. The seasonality might be covered by the identified jumps, which are already excluded from the data in this step.*

For the Samuelson type model, we observe that the average volatility $\bar{\lambda}$ is higher than the one of seasonality type $\bar{\sigma}$. This can be explained by the Samuelson effect, which dampens the volatility such that it has to be higher. Note that $\bar{\lambda}$ is smallest in June and highest in October connected with a relatively low or very high Samuelson parameter, respectively. Indeed, we observe the highest Samuelson parameter Λ in October in connection with the highest volatility. This combination leads to a very pronounced Samuelson effect visualized in Figure 7 (b), highlighted with a bold yellow. The closer we reach the end of the maturity, the more effect the volatility has. The contrary happens for the smallest Samuelson parameter in April for which the volatility appears to be a straight line in bold purple. The average Samuelson effect is highlighted by the blue dotted line starting 150 days before maturity at 0.2055 and reaching 0.3187 at the end of the maturity.

Contracts	Type 1			Type 2			
	κ	μ	$\bar{\sigma}$	κ	μ	Λ	$\bar{\lambda}$
January	244.92	1.7405	0.2623	248.59	2.8216	1.3157	0.4145
February	232.61	-0.1563	0.2726	233.05	2.8325	1.0185	0.3877
March	227.92	-0.5633	0.2626	234.79	-0.3857	0.1527	0.2776
April	230.46	0.6467	0.2715	231.61	-1.0383	0.0000	0.2705
May	218.10	0.7244	0.2645	219.04	-0.0517	0.0784	0.2703
June	216.75	-2.5650	0.2570	215.60	-2.4209	0.0639	0.2619
July	232.81	-2.4204	0.2690	223.40	-5.1624	1.5731	0.4073
August	222.69	-0.9235	0.2566	234.41	0.0055	0.0874	0.2648
September	245.81	-1.4060	0.2303	246.20	-0.8744	0.6958	0.2920
October	238.24	-0.3833	0.2380	242.77	0.0130	2.3314	0.5387
November	235.73	-4.6677	0.2380	221.90	-2.0064	0.4599	0.2624
December	277.94	-5.8982	0.2397	261.33	-5.8582	1.1832	0.3084
Average	235.33	-1.3227	0.2552	234.39	-1.0104	0.7467	0.3297

Table 6: Parameter estimates for seasonality type (Type 1) and Samuelson type (Type 2).

Type 1		
a	b	c
0.2550	0.0170	0.7017

Table 7: Parameters for seasonality function from Equation (3.35) with RMSE of 0.0097 for all contracts.

(a) Seasonality Type Function

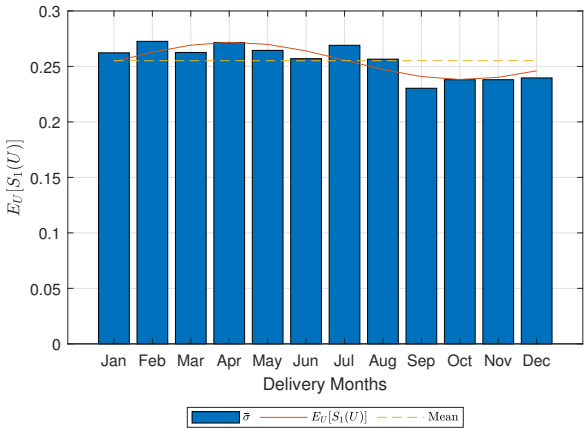

(b) Samuelson Type Function

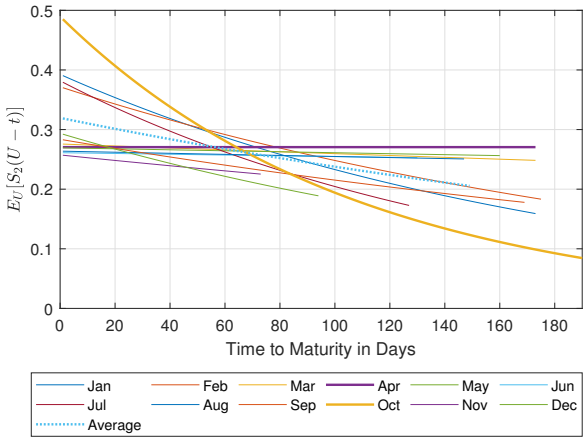

Figure 7: Volatility function for both types of models. Subfigure (a): Model of seasonality type (Type 1). Subfigure (b): Model of Samuelson type (Type 2).

	LLH	AIC	BIC
Type 1	389.14	-772.29	-763.50
Type 2	392.34	-776.68	-764.96

Table 8: Relative Goodness of Fit – Loglikelihood (LLH), Akaike Information Criterion (AIC), and Baysian Information Criterion (BIC) for seasonality type (Type 1) and Samuelson type (Type 2).

	Deviance	LRT	p-value of LRT
Type 1	6.392	0	0.094
Type 2	0	0	1

Table 9: Absolute Goodness of Fit – Deviance and Likelihood-Ratio-Test (LRT) and the p-value of the LRT for seasonality function (Type 1) and Samuelson effect (Type 2).

Model Ranking. In order to compare both models according to their relative and absolute goodness of fit, we rely on a procedure applied, e.g., by Zucchini et al. (2021) and Schneider and Tavin (2018).

For the *relative goodness of fit*, we consider the models' logarithmic likelihoods (LLH), their Akaike Information Criterion (AIC) and the Bayesian Information Criterion (BIC) described in Table 8. As we aim to maximize the likelihood, the higher the LLH, the better. Moreover, the best model ideally induces the smallest AIC and BIC. Hence, the Samuelson model fits better in all criteria.

For the *absolute goodness of fit*, we consider the deviance and the Likelihood-Ratio-Test (LRT). The deviance is zero for the model with the highest likelihood. The closer the deviance for the remaining models, the better the models are. As Type 2 is the better model, its deviance is zero. However, it is hard to verify whether 6.3917 is close or far away from zero. As it is known that the deviance follows a $\mathcal{X}^2$ distribution with three parameters in the seasonality type model, we apply the LRT. The LRT returns the rejection decision and p-value for the hypothesis test conducted at significance level 0.05. If the p-value is below this threshold, this indicates a strong evidence suggesting that the model with the higher likelihood fits the data better than the model restricted to three parameters only. Since the LRT does not reject the hypothesis, we can conclude that both models fit the data equally well. The simulations in Appendix E confirm that even the model with the lower likelihood fits the data comparably well. However, we observe for some contracts that fat tails are underestimated (see also Figure 6). We also observe that the lognormal distribution would fit the data well. However, we refer to Remark 3.3 that the distribution is not suitable for the model.

On the MPDP. We calculate the MPDP derived in Equation (2.13) from the estimated parameter values in Tables 6 and 7. The explicit characterizations can be found in Examples 3.1 and 3.2. In Figure 8, we depict the MPDP for both types. We observe a constant negative MPDP in the model of Type 1 for each contract, in Figure 8 (a). The MPDP varies in a seasonal fashion having its minimal extreme values in winter and summer – in particular in January, July, and December. In the April and October contracts, the MPDP is close to zero. Nevertheless, the average MPDP is rather small around -6.3891e-06 in dashed. In fact, the MPDP of diffusion risk is high, whenever the variance of the seasonality function S_1 is high and, thus, whenever the changes in S_1 are the largest (see also Remark 2.1 (ii) and Kemper et al. (2022)). We expect a growing MPDP with a rising share of renewable energy since they strongly depend on the weather conditions of the season. Hence, they induce a more pronounced seasonality with respect to the delivery time. The seasonal behavior of the MPDP under Type 1 of delivery-dependent function has been observed firstly by Kemper et al. (2022) numerically using $a = [1.2; 2], b = [0.2; 1]$, and $c = 0$. We here provide the empirical evidence for the shape of MPDP, which is less pronounced and shifted horizontally since we estimate $a = 0.2550$ and $c = 0.7017$. Figure 8 (b) depicts the MPDP of Type 2 for each contract over time to maturity. The MPDP is negative and decreases further the closer we reach the expiration date. Especially for July and October, the MPDP is highest in absolute values. For the sake of comparison, we include a barplot of the terminal MPDP under Type 2 in Figure 8 (c). According to Figure 8 (c), a delivery dependence in terms of the Samuelson effect is especially visible in January, July, and October. At terminal time, the average MPDP is found at -1.2643e-04 in dashed.

(a) Seasonality (Type 1)

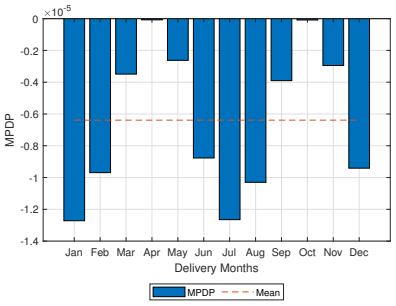

(b) Samuelson (Type 2)

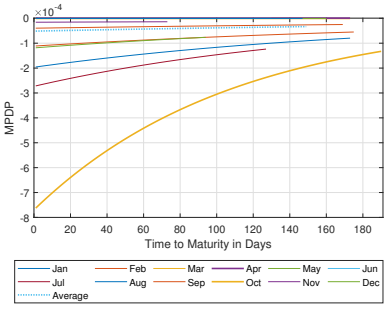

(c) Terminal Samuelson (Type 2)

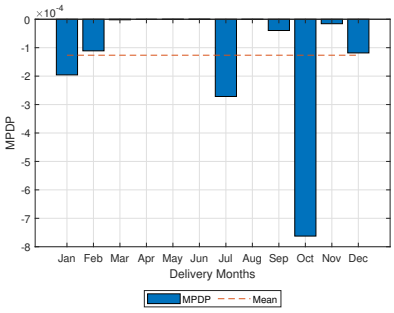

Figure 8: MPDP of diffusion risk Π_1 for all contracts. Subfigure (a): MPDP in the model of seasonality type (Type 1). Subfigure (b): MPDP in the model of Samuelson type (Type 2). Subfigure (c): Terminal MPDP in the model of Type 2.

5 Conclusion

In this paper, we provide empirical evidence as well as analytical characteristics of the MPDP for electricity swaps embedded in a Merton type model.

We adjust the Heston type setting of Kemper et al. (2022) to a jump framework of Merton type leading to the MPDP for diffusion *and* jump risk. We thus identify the MPDP for the jump component, which turns out to be negative as it is the case for the diffusion component. In addition, we transfer the model to the physical measure under which we allow for mean-reversion, seasonalities, and term-structure effects. A comparison of the risk-neutral measures of the swap resulting from geometric and approximated averaging, $\mathbb{Q}$ and $\widetilde{\mathbb{Q}}$, offers the decomposition of the "true" market price of risk comprising the "classical" market price of risk and the MPDP for jump and diffusion risk. We may refer $\widetilde{\mathbb{Q}}$ to the "correct" or "true" risk-neutral measure since the swap price is a $\widetilde{\mathbb{Q}}$-martingale without any approximations. In contrast, the "classical" or artificial risk-neutral measure, $\mathbb{Q}$, results from an approximation of the swap price leading in general not to the "true" pricing measure. Consequently, any pricing methodology based on approximated averaging can easily be turned to the "correct" risk-neutral measure by an application of our MPDP.

We compare swap prices resulting from geometric averaging with swaps based on approximated averaging in line with with Kemper et al. (2022) and Bjerksund et al. (2010). We find that different averaging techniques lead to a pricing spread that stays untouched by measure changes. In particular, the swap price based on geometric averaging turns out to be smaller than the one resulting from approximated averaging. The spread itself can be characterized by a change of measure based on the MPDP as introduced by Kemper et al. (2022). As the MPDP leads to the true pricing measure, $\widetilde{\mathbb{Q}}$, the spread remediates the approximated swap price and adjusts it downwards to the correct price of the swap contract.

We finally investigate the model under the physical measure as well as the resulting MPDP empirically. To this end, we consider two types of models characterized, on the one hand, by seasonality in the delivery time (see Fanelli and Schmeck (2019)) and, on the other hand, by the Samuelson effect (see Samuelson (1965)). We adapt them to a jump setting, and provide the corresponding discretized swap price models. We fit the discretized models using a two-step estimation procedure. In the first step, we identify jumps and fit their jump size to suitable distributions. We find that the exponential distribution fits the detected jump sizes best. In a second step, we fit the jump free dataset to both types of models. From model selection techniques, we observe that the model of Samuelson type lead to a higher likelihood, while inducing a lower AIC and BIC than the model of Type 1. The absolute goodness of fit, however, confirms that seasonalities in the delivery period can explain the model comparably well. Moreover, we provide empirical evidence for the MPDP of diffusion risk for both types of models. Seasonal delivery dependence causes a MPDP that is constant over trading time and

seasonal in delivery time. In contrast, term-structure dependence induces a decreasing behavior of the MPDP over trading time. Hence, the closer we reach the expiration date, the more pronounced the MPDP, and the larger the pricing spread. Consequently, the MPDP reduces risk caused by approximated averaging especially when the end of the maturity approaches.

In our empirical analysis, the MPDP of jump risk is zero by construction. Moreover, we have assumed the annualized jump intensity to be the same for all swap contracts. Nevertheless, we observe a rather seasonal jump intensity (see Figure 4). It would be very interesting to investigate this phenomenon theoretically and empirically more precisely. This, however, is a question for future research.

To conclude, we expand the MPDP to the jump setting and provide empirical evidence for the MPDP influenced by typical characteristics of the electricity market. We even expect a growing MPDP caused by a rising market share of renewable energy: Varying weather conditions over the seasons of a year will cause stronger seasonal behavior when the share of renewables is growing. Consequently, this increases the importance of the MPDP of diffusion risk, which has to be taken into account to ensure an accurate pricing procedure.

References

Benth, F.E., Benth, J.S., and Koekebakker, S. (2008). Stochastic Modelling of Electricity and Related Markets. Vol. 11. *World Scientific Publishing Company.* (Cited on pages 2, 5, and 10.)

Benth, F.E., Kallsen, J. and Meyer-Brandis, T. (2007). A Non-Gaussian Ornstein-Uhlenbeck Process for Electricity Spot Price Modeling and Derivatives Pricing. *Applied Mathematical Finance* **14**(2), pp. 153-169. (Cited on page 2.)

Benth, F.E., Kiesel, R., and Nazarova, A. (2012). A Critical Empirical Study of Three Electricity Spot Price Models. *Energy Economics* **34**(5), pp. 1589-1616 (Cited on page 19.)

Benth, F.E., Klüppelberg, C., Müller, G., and Vos, L. (2014). Futures Pricing in Electricity Markets Based on Stable CARMA Spot Models. *Energy Economics* **44**, pp. 392-406. (Cited on page 2.)

Benth, F.E. and Koekebakker, S. (2008). Stochastic Modeling of Financial Electricity Contracts. *Energy Economics* **30**(3), pp. 1116-1157. (Cited on page 2.)

Benth, F.E. and Paraschiv, F. (2016). A Structural Model for Electricity Forward Prices. *Working Paper.* (Cited on page 3.)

Benth, F.E., Piccirilli, M., and Vargiolu, T. (2019). Mean-Reverting Additive Energy Forward Curves in a Heath–Jarrow–Morton Framework. *Mathematics and Financial Economics* **13**(4), pp. 543–577. (Cited on pages 2, 3, 4, 5, 10, 12, 13, 34, and 35.)

Bjerksund, P., Rasmussen, H., and Stensland, G. (2010). Valuation and Risk Management in the Norwegian Electricity Market. In: Bjørndal, E., Bjørndal, M., Pardalos, P. M., and Rönnqvist, M. (Editors) *Energy, Natural Resources and Environmental Economics*, pp. 167-185. (Cited on pages 2, 5, 6, and 28.)

Borovkova, S. and Permana, F.J. (2006). Modelling Electricity Prices by the Potential Jump-diffusion. In: Shiryaev, A.N., Grossinho, M.R., Oliveira, P.E., Esquível, M.L. (Editors), *Stochastic Finance. Springer* pp. 239-263. (Cited on pages 17 and 23.)

Borovkova, S. and Schmeck, M.D. (2017). Electricity Price Modeling with Stochastic Time Change. *Energy Economics* **63**, pp. 51-65. (Cited on pages 17, 19, and 23.)

Burger, M., Klar, B., Müller, A., and Schindlmayr, G. (2004). A Spot Market Model for Pricing Derivatives in Electricity Markets. *Quantitative Finance* **4**(1), pp. 109-122. (Cited on page 2.)

Clewlow, L. and Strickland, C. ((1999)). Valuing Energy Options in a One Factor Model fitted to Forward Prices. *SSRN* **160608**. (Cited on page 2.)

Cont, R. and Tankov, P. (2004). Financial Modelling with Jump Processes. *Chapman and Hall/CRC*. (Cited on page 36.)

Crosby, J. and Frau, C. (2022). Jumps in Commodity Prices: New Approaches for Pricing Plain Vanilla Options. *Energy Economics* **114**(106302). (Cited on page 23.)

Cuchiero, C., Persio, L.D., Guida, F., and Svaluto-Ferro, S. (2022). Measure-valued Processes for Energy Markets. *arXiv:2210.09331v1*. (Cited on page 2.)

Dereich, S., Neuenkirch, A., and Szpruch, L. (2012). An Euler-type method for the strong approximation of the Cox–Ingersoll–Ross process. *The Royal Society* **468**, pp. 1105-1115. (Cited on pages 34 and 36.)

Fanelli, V. and Schmeck, M.D. (2019). On the Seasonality in the Implied Volatility of Electricity Options. *Quantitative Finance* **19**(8), pp. 1321-1337. (Cited on pages 3, 15, and 28.)

Goffe, W.L., Ferrier, G.D., and Rogers, J. (1994). Global Optimization of Statistical Functions with Simulated Annealing. *Journal of Econometrics* **60**(1-2), pp. 65-99. (Cited on page 20.)

Gray, R.J. and Pitts, S.M. (2012). Risk Modelling in General Insurance: From Principles to Practice. *Cambridge University Press*. (Cited on pages 16 and 17.)

Heath, D., Jarrow, R., and Morton, A. (1990). Bond Pricing and the Term Structure of Interest Rates: A New Methodology for Contingent Claims Valuation. *Econometrica* **60**(1), pp. 77-105. (Cited on page 2.)

Heston, S.L. (1993). A Closed-Form Solution for Options with Stochastic Volatility with Applications to Bond and Currency Options. *The Review of Financial Studies* **6**(2), pp. 327-343. (Cited on page 34.)

Hinderks, W.J., Korn, R., and Wagner, A. (2020). A Structural Heath–Jarrow–Morton Framework for consistent Intraday Spot and Futures Electricity Prices. *Quantitative Finance* **20**(3), pp. 347-357. (Cited on pages 2 and 23.)

Jaeck, E. and Lautier, D. (2016). Volatility in Electricity Derivative Markets: The Samuelson Effect Revisited. *Energy Economics* **59**, pp. 300-313. (Cited on page 3.)

Johannes, M. and Polson, N. (2010). MCMC Methods for Continuous-time Financial Econometrics. In: *Handbook of Financial Econometrics: Applications*, pp. 1-72. (Cited on page 18.)

Karatzas, I. and Shreve, S.E. (1991). Brownian Motion and Stochastic Calculus. *Springer*; 2nd edition. (Cited on page 34.)

Kemna, A.G.Z. and Vorst, A.C.F. (1990). A Pricing Method for Options based on Average Asset Values. *Journal of Banking and Finance* **14**(1), pp. 113-129. (Cited on page 6.)

Kemper, A., Schmeck, M.D., and Kh.Balci, A. (2022). The Market Price of Risk for Delivery Periods: Pricing Swaps and Options in Electricity Markets. *Energy Economics* **113**(106221). (Cited on pages 1, 2, 3, 4, 5, 6, 7, 9, 15, 17, 18, 27, 28, and 34.)

Kiesel, R., Schindlmayr, G., and Börger, R.H. (2009). A Two-Factor Model for the Electricity Forward Market. *Quantitative Finance* **9**(3), 279-287. (Cited on page 3.)

Kleisinger-Yu, X., Komaric, V., Larsson, M., and Regez, M. (2020). A Multifactor Polynomial Framework for Long-Term Electricity Forwards with Delivery Period. *SIAM Journal on Financial Mathematics* **11**(3), pp. 928-957. (Cited on pages 2 and 3.)

Koekebakker, S. and Ollmar, F. (2005). Forward Curve Dynamics in the Nordic Electricity Market. *Managerial Finance* **31**(6), pp. 73-94. (Cited on pages 2 and 3.)

Latini, L., Piccirilli, M., and Vargiolu, T. (2019). Mean-reverting No-arbitrage Additive Models for Forward Curves in Energy Markets. *Energy Economics* **79**, pp. 157-170. (Cited on pages 2, 3, and 12.)

Lépingle, D. and Mémin, J. (1978). Sur l'intégrabilité Uniforme des Martingales Exponentielles. *Zeitschrift für Wahrscheinlichkeitstheorie und verwandte Gebiete* **42**(3), pp. 175–203. (Cited on page 35.)

Lucia, J.J. and Schwartz, E. (2002). Electricity Prices and Power Derivatives: Evidence from the Nordic Power Exchange. *Review of Derivatives Research* **5**, pp. 5–50. (Cited on page 2.)

Merton, R. (1976). Option Pricing when Underlying Stock Returns are Discontinuous. *Journal of Financial Economics* **3**(1-2), pp. 125-144. (Cited on pages 1, 2, 18, and 23.)

Øksendal, B., Sulem, A. (2007). Applied Stochastic Control of Jump Diffusions. *Springer*. (Cited on pages 6, 7, 8, 11, 12, 13, 14, 32, 33, 35, and 37.)

Papapantoleon, A. (2008). An Introduction to Lévy Processes with Applications in Finance. *arXiv:0804.0482*. (Cited on page 4.)

Protter, P.E. (2005). Stochastic Differential Equations. In: Stochastic Integration and Differential Equations. Stochastic Modelling and Applied Probability, Vol. 21, *Springer*. (Cited on pages 6, 8, 11, 12, 32, and 33.)

Samuelson, P.A. (1965). Proof that Properly Anticipated Prices Fluctuate Randomly. *Industrial Management Review* **6**(2), pp. 41–49. (Cited on pages 3 and 28.)

Schneider, L. and Tavin, B. (2018). From the Samuelson Volatility Effect to a Samuelson Correlation Effect: An Analysis of Crude Oil Calendar Spread Options. *Journal of Banking and Finance* **95**, pp. 185–202. (Cited on pages 3, 16, 20, and 27.)

Shreve, S.E. (2004). Stochastic Calculus for Finance II. Continuous-Time Models. *Springer Finance Series*. (Cited on page 10.)

Zucchini, W., MacDonald, I.L., and Langrock, R. (2021). Hidden Markov Models for Time Series: An Introduction Using R. *Chapman and Hall* Second Edition. (Cited on page 27.)

Appendix

A Technical Requirements

Assumption 1. *For the model (2.1), we make the following assumptions to apply Itô's formula (see Øksendal and Sulem (2007), cf. Theorem 1.16):*

(*i*) *For* $\mathcal{A} := \{(t,\tau) \in [0,\tau_2]^2 \colon t \leq \tau\}$ *the functions* $\sigma \colon \mathcal{A} \to \mathbb{R}^+$ *and* $\eta \colon \mathcal{A} \to \mathbb{R}$ *are adapted such that the integrals exist, meaning that* $\mathbb{Q}[\int_0^t \sigma^2(s,\tau) + \int_{\mathbb{R}} |(e^{\eta(s,\tau)z} - 1)|\ell^{\mathbb{Q}}(dz)ds < \infty] = 1$ *for all* $0 \leq t \leq \tau$.

In order to ensure existence and uniqueness of solutions to Equation (2.6) (see Øksendal and Sulem (2007), cf. Theorem 1.19), we further assume:

(*ii*) *(At most linear growth) There exists a constant* $C_1 < \infty$ *such that*

$$|\sigma(t,\tau)x|^2 + \int_{\mathbb{R}} |(e^{\eta(t,\tau)z} - 1)x|^2 \ell^{\mathbb{Q}}(dz) \leq C_1(1 + |x|^2) \,, \quad \forall x \in \mathbb{R} \,. \tag{A.1}$$

(*iii*) *(Lipschitz continuity) There exists a constant* $C_2 < \infty$ *such that*

$$|\sigma(t,\tau)x - \sigma(t,\tau)y|^2 + \int_{\mathbb{R}} |(e^{\eta(t,\tau)z} - 1)x - (e^{\eta(t,\tau)z} - 1)y|^2 \ell^{\mathbb{Q}}(dz) \leq C_2(|x-y|^2) \,, \quad \forall x,y \in \mathbb{R} \,. \tag{A.2}$$

Hence, by Øksendal and Sulem (2007) (cf. Theorem 1.19), it follows that $\mathbb{E}_{\mathbb{Q}}[|f(t,\tau)|^2] < \infty$ *for all* $t \in [0,\tau]$. *By the Itô-Lévy Isometry (see Øksendal and Sulem (2007), cf. Theorem 1.17) part (iii) implies that*

$$\mathbb{E}_{\mathbb{Q}}[f^2(t,\tau)] = \mathbb{E}_{\mathbb{Q}}\left[\int_0^t \sigma^2(v,\tau)f^2(v,\tau) + f^2(v,\tau)\int_{\mathbb{R}}(e^{\eta(v,\tau)z} - 1)^2 \ell^{\mathbb{Q}}(dz)dv\right] < \infty \,, \tag{A.3}$$

so that the square-integrability conditions are satisfied implying that f *is a true martingale under* $\mathbb{Q}$.

Assumption 2. *For the geometric weightening approach in Equation (2.11), we need to apply the stochastic Fubini Theorem (see Protter (2005), cf. Theorem 65, Chapter IV. 6). Therefore, we assume that*

(*i*) $\sigma(\cdot,\tau)$ *and* $\eta(\cdot,\tau)$ *are* $\mathcal{P} \times \mathcal{B}((\tau_1,\tau_2])$ *measurable, where* $\mathcal{P}$ *is the predictable* σ*-algebra making all adapted, càglàd processes measurable,*

(*ii*) $\mathbb{E}_{\mathbb{Q}}\left[\int_0^{\tau_1}\int_{\tau_1}^{\tau_2} \sigma^2(t,u)w(u,\tau_1,\tau_2)du\ dt\right] < \infty$,

(*iii*) $\mathbb{E}_{\mathbb{Q}}\left[\int_0^{\tau_1}\int_{\tau_1}^{\tau_2} \eta(t,u)w(u,\tau_1,\tau_2)du\ dt\right] < \infty$,

(*iv*) $\mathbb{E}_{\mathbb{Q}}\left[\int_0^{\tau_1}\int_{\mathbb{R}}\int_{\tau_1}^{\tau_2}(e^{\eta(t,u)z} - 1)^2 w(u,\tau_1,\tau_2)du\ \ell^{\mathbb{Q}}(dz)dt\right] < \infty$,

such that the integrals still exist and linear growth and Lipschitz continuity are satisfied (see Assumption 1).

Assumption 3. *To apply Girsanov's Theorem (see Øksendal and Sulem (2007), cf. Theorem 1.35), we assume that* $\Pi_1^{\mathbb{Q}\widetilde{\mathbb{Q}}}$ *and* $\Pi_2^{\mathbb{Q}\widetilde{\mathbb{Q}}}$ *are predictable, satisfying*

(*i*) $\mathbb{E}_{\mathbb{Q}}[\int_0^{\tau_1} \Pi_1^{\mathbb{Q}\widetilde{\mathbb{Q}}}(s,\tau_1,\tau_2)^2 ds] < \infty$, *such that* $Z_1^{\mathbb{Q}\widetilde{\mathbb{Q}}}$ *is a true martingale, and*

(*ii*) $\Pi_2^{\mathbb{Q}\widetilde{\mathbb{Q}}}(t,\tau_1,\tau_2)z \leq 1$ *for all* $t \in [0,\tau_1]$ *and* $\mathbb{E}_{\mathbb{Q}}[\int_0^{\tau_1} \ln(1 - \Pi_2^{\mathbb{Q}\widetilde{\mathbb{Q}}}(s,\tau_1,\tau_2)) + \Pi_2^{\mathbb{Q}\widetilde{\mathbb{Q}}}(s,\tau_1,\tau_2)ds] < \infty$, *such that* $Z_2^{\mathbb{Q}\widetilde{\mathbb{Q}}}$ *is a true martingale.*

Assumption 4. *For the model in Equation (3.1), we make the following assumptions to apply Itô's formula (see Øksendal and Sulem (2007), cf. Theorem 1.16):*

(*i*) *The functions* $\mu\colon \mathcal{A} \to \mathbb{R}$, $\kappa\colon [0,\tau_1] \to \mathbb{R}^+$, $\sigma\colon \mathcal{A} \to \mathbb{R}^+$, *and* $\eta\colon \mathcal{A} \to \mathbb{R}$ *are adapted such that the integrals exist, meaning that for all* $0 \le t \le \tau$, *we have* $\mathbb{P}[\int_0^t \mu^2(v,\tau) + \kappa^2(v) + \sigma^2(v,\tau) + \eta^2(v,\tau) \int_{\mathbb{R}} z^2 \ell^{\mathbb{P}}(dz)dv < \infty] = 1$.

In order to ensure existence and uniqueness of solutions to Equation (3.3) (see Øksendal and Sulem (2007), Theorem 1.19), we further assume:

(*ii*) *(At most linear growth) There exists a constant* $C_1 < \infty$ *such that* $\forall x \in \mathbb{R}$:

$$|\mu(t,\tau)|^2 + |\kappa(t)x|^2 + |\sigma(t,\tau)|^2 + |\eta(t,\tau)|^2 \int_{\mathbb{R}} |z|^2 \ell^{\mathbb{P}}(dz) \le C_1(1+|x|^2)\,. \tag{A.4}$$

(*iii*) *(Lipschitz continuity) There exists a constant* $C_2 < \infty$ *such that*

$$\kappa^2(t)|x-y|^2 + \le C_2(|x-y|^2)\,, \quad \forall x, y \in \mathbb{R}\,. \tag{A.5}$$

Assumption 5. *For the model in Equation (3.1), we make the following assumptions to apply Itô's formula (see Øksendal and Sulem (2007), cf. Theorem 1.16):*

(*i*) $\mathbb{P}[\int_0^t \int_{\mathbb{R}} e^{\eta(v,\tau)z} \ell^{\mathbb{P}}(dz)dv < \infty] = 1$ *holds for all* $0 \le t \le \tau$.

In order to ensure existence and uniqueness of solutions to Equation (3.3) (see Øksendal and Sulem (2007), Theorem 1.19), we further assume that

(*ii*) $\int_{\mathbb{R}} e^{\eta(t,\tau)z} \ell^{\mathbb{P}}(dz)$ *exists and is bounded for all* $(t,\tau) \in \mathcal{A}$, *such that the linear growth condition and Lipschitz continuity are satisfied.*

Assumption 6. *For the geometric weightening approach in Equation (2.11) applied in Section 3, we apply the stochastic Fubini Theorem (see Protter (2005), cf. Theorem 65, Chapter IV. 6). Therefore, we assume that*

(*i*) $\kappa, \mu, \sigma, \eta$ *are* $\mathcal{P} \times \mathcal{B}((\tau_1,\tau_2])$ *measurable, where* $\mathcal{P}$ *is the predictable* σ*-algebra making all adapted, càglàd processes measurable,*

(*ii*) $\mathbb{E}_{\mathbb{P}}\left[\int_0^{\tau_1} \int_{\tau_1}^{\tau_2} \mu(t,u) w(u,\tau_1,\tau_2) du\ dt\right] < \infty$,

(*iii*) $\mathbb{E}_{\mathbb{P}}\left[\int_0^{\tau_1} \int_{\tau_1}^{\tau_2} \sigma^2(t,u) w(u,\tau_1,\tau_2) du\ dt\right] < \infty$,

(*iv*) $\mathbb{E}_{\mathbb{P}}\left[\int_0^{\tau_1} \int_{\mathbb{R}} \int_{\tau_1}^{\tau_2} (e^{\eta(t,u)z} - 1)^2 w(u,\tau_1,\tau_2) du\ \ell^{\mathbb{P}}(dz) dt\right] < \infty$,

(*v*) $\mathbb{E}_{\mathbb{P}}\left[\int_0^{\tau_1} \int_{\tau_1}^{\tau_2} \eta(t,u) w(u,\tau_1,\tau_2) du\ dt\right] < \infty$.

Assumption 7. *To prove that* $Z^{\mathbb{P}\tilde{\mathbb{Q}}}$ *is a true martingale, we assume that* $\kappa, \mu, \sigma, \eta$ *are deterministic and that*

(*i*) $\Pi_2^{\mathbb{P}\tilde{\mathbb{Q}}}(t,\tau_1,\tau_2)z < 1$ *for* $\ell^{\mathbb{P}}$*-a.e.* $z \in \mathbb{R}$ *and each* $t \in [0,\tau_1]$,

(*ii*) $\ell^{\mathbb{P}}$ *has fourth moment, that is* $\int_{\mathbb{R}} z^4 \ell^{\mathbb{P}}(dz) < \infty$,

(*iii*) $\int_0^{\tau_1} \int_{\tau_1}^{\tau_2} w(u,\tau_1,\tau_2)\mu^2(t,u) du\ dt < \infty$,

(*iv*) $\int_0^{\tau_1} \int_{\tau_1}^{\tau_2} w(u,\tau_1,\tau_2)\eta^2(t,u) du\ dt < \infty$,

(*v*) $\int_0^{\tau_1} \int_{\tau_1}^{\tau_2} w(u,\tau_1,\tau_2)\sigma^4(t,u) du\ dt < \infty$,

(*vi*) $\int_0^{\tau_1} \kappa^2(t) dt < \infty$.

B Proof of Proposition 3.2

Inspired by Benth et al. (2019), we prove that $\mathbb{E}_{\mathbb{P}}[Z^{\mathbb{P}\widetilde{\mathbb{Q}}}(\tau_1,\tau_1,\tau_2)] = 1$ and expand their Theorem 3.5 to a geometric setting with stochastic volatility in order to address settings as in Kemper et al. (2022). For the scope of the proof, we consider the swap price F in Equation (3.7) characterized by stochastic volatility of the form

$$\sigma(t,\tau)\sqrt{\nu(t)}\,, \tag{B.1}$$

where $\sigma(t,\tau)$ is deterministic and ν is the stochastic volatility that is modeled as a Cox-Ingersoll-Ross process evolving as

$$d\nu(t) = \kappa_\nu\left(\theta_\nu - \nu(t)\right)dt + \sigma_\nu\sqrt{\nu(t)}dB_t^{\mathbb{P}}\,, \tag{B.2}$$

for $\nu(0) = \nu_0 > 0$, where $B^{\mathbb{P}}$ and $\widetilde{J}^{\mathbb{P}}$ are independent of each other and $B^{\mathbb{P}}$ and $W^{\mathbb{P}}$ are correlated. In particular, we assume a correlation structure $d\langle W^{\mathbb{P}}, B^{\mathbb{P}}\rangle_t = \rho dt$ where $\rho \in (-1,1)$ such that we can rewrite $B^{\mathbb{P}} = \rho W^{\mathbb{P}} + \sqrt{1-\rho^2}\bar{B}^{\mathbb{P}}$ for $\bar{B}^{\mathbb{P}} \perp\!\!\!\perp W^{\mathbb{P}}$. Moreover, we assume that $\kappa_\nu, \theta_\nu, \sigma_\nu > 0$ satisfy the extended Feller condition, i.e., $\sigma_\nu^2 < \kappa_\nu\theta_\nu$, to ensure that $\mathbb{E}_{\mathbb{P}}[\nu^{-2}(t)]$ is bounded on the entire trading time $t \in [0,\tau_1]$ (see Dereich et al. (2012), cf. Chapter 3). Note, that the extended Feller implies the classical Feller condition (see Karatzas and Shreve (1991), cf. Chapter 5) ensuring that the volatility stays positive.

We proceed in the following steps:

1. Derivation of a new risk-neutral measure $\widetilde{\mathbb{Q}}^n$ through a stopping time $\hat{\tau}_n$.
2. Proof that $\mathbb{E}_{\widetilde{\mathbb{Q}}}[Z^{\mathbb{P}\widetilde{\mathbb{Q}}}(\tau_1,\tau_1,\tau_2)]$ is lower boundend, i.e.,

$$\mathbb{E}_{\widetilde{\mathbb{Q}}}\left[Z^{\mathbb{P}\widetilde{\mathbb{Q}}}(\tau_1,\tau_1,\tau_2)\right] \geq 1 - \frac{1}{n}\mathbb{E}_{\widetilde{\mathbb{Q}}^n}\left[\sup_s \widetilde{Y}(s,\tau_1,\tau_2)\right] - \frac{1}{n}\mathbb{E}_{\widetilde{\mathbb{Q}}^n}\left[\sup_s \nu^{-1}(s)\right] - \frac{1}{n}\mathbb{E}_{\widetilde{\mathbb{Q}}^n}\left[\sup_s \nu(s)\right]\,.$$

3. Proof that there exist upper boundaries for $\mathbb{E}_{\widetilde{\mathbb{Q}}^n}[\sup_s \widetilde{Y}(s,\tau_1,\tau_2)]$, $\mathbb{E}_{\widetilde{\mathbb{Q}}^n}[\sup_s \nu^{-1}(s)]$, and $\mathbb{E}_{\widetilde{\mathbb{Q}}^n}[\sup_s \nu(s)]$, that are independent of n.

1. Derivation of $\widetilde{\mathbb{Q}}^n$. Similar to Benth et al. (2019), we set $g(z) := (1+z)\log(1+z) - z$ and define the predictable compensator of $\frac{1}{2}\langle H^c, H^c\rangle + \sum_{t\leq\cdot} g(\Delta H(t))$ by

$$C(t,\tau_1,\tau_2) := \frac{1}{2}\int_0^t \pi_1^{\mathbb{P}\widetilde{\mathbb{Q}}}(s,\tau_1,\tau_2)^2 + \pi_\nu^{\mathbb{P}\widetilde{\mathbb{Q}}}(s,\tau_1,\tau_2)^2 ds + \int_0^t\int_{\mathbb{R}} g(\pi_2^{\mathbb{P}\widetilde{\mathbb{Q}}}(s,\tau_1,\tau_2)z)\ell^{\mathbb{P}}(dz)ds\,,$$

where H from Equation (3.17) now embraces stochastic volatility such that

$$H(t,\tau_1,\tau_2) := \int_0^t \pi_1^{\mathbb{P}\widetilde{\mathbb{Q}}}(s,\tau_1,\tau_2)dW_s^{\mathbb{P}} + \int_0^t\int_{\mathbb{R}} \pi_2^{\mathbb{P}\widetilde{\mathbb{Q}}}(s,\tau_1,\tau_2)z\widetilde{N}^{\mathbb{P}}(ds,dz) + \int_0^t \pi_\nu^{\mathbb{P}\widetilde{\mathbb{Q}}}(s,\tau_1,\tau_2)d\bar{B}_s^{\mathbb{P}}\,.$$

Note that this stochastic volatility setting covers a three-dimensional market price of risk $\pi := (\pi_1,\pi_2,\pi_\nu)$ for all independent random parts $W^{\mathbb{P}}, \widetilde{J}^{\mathbb{P}}, \bar{B}^{\mathbb{P}}$. As we are in an incomplete setting, we choose the market price of volatility risk, π_ν, such that the market price of risk admits the same structure as in the Heston model, i.e., $\rho\pi_1^{\mathbb{P}\widetilde{\mathbb{Q}}} + \sqrt{1-\rho^2}\pi_\nu^{\mathbb{P}\widetilde{\mathbb{Q}}} = \frac{\delta_\nu}{\sigma_\nu}\sqrt{\nu(t)}$ (see Heston (1993)). Now let us define a sequence of stopping times

$$\hat{\tau}_n := \inf\left\{t\in[0,\tau_1] : |\widetilde{Y}(t,\tau_1,\tau_2)| \geq n,\ \text{or}\ |\nu^{-1}(t)| \geq n,\ \text{or}\ |\nu(t)| \geq n\right\}\,, \tag{B.3}$$

and observe that for every $n \in \mathbb{N}$, the stopped process $C(t \wedge \hat{\tau}_n, \tau_1, \tau_2)$ is bounded. Hence, by Lépingle and Mémin (1978) (cf. Theorem III.1), we know that $Z^{\mathbb{P}\widetilde{\mathbb{Q}}}(t \wedge \hat{\tau}_n, \tau_1, \tau_2)$ is a uniformly integrable martingale such that we can define the probability measure $\widetilde{\mathbb{Q}}^n$ by

$$\frac{d\widetilde{\mathbb{Q}}^n}{d\mathbb{P}} := Z^{\mathbb{P}\widetilde{\mathbb{Q}}}(\tau_1 \wedge \hat{\tau}_n, \tau_1, \tau_2) \,. \tag{B.4}$$

2. Proof of lower boundary of $\mathbb{E}_{\mathbb{P}}[Z^{\mathbb{P}\widetilde{\mathbb{Q}}}(\tau_1)]$. First, $Z^{\mathbb{P}\widetilde{\mathbb{Q}}}$ is a positive local martingale by the assumption that $\pi_2^{\mathbb{P}\widetilde{\mathbb{Q}}}(t, \tau_1, \tau_2) \geq -1$ for all $t \in [0, \tau_1]$. Hence, it is a supermartingale, so that we know the upper boundary for $\tau_1 \geq 0$:

$$\mathbb{E}_{\mathbb{P}}[Z^{\mathbb{P}\widetilde{\mathbb{Q}}}(\tau_1, \tau_1, \tau_2)] \leq \mathbb{E}_{\mathbb{P}}[Z^{\mathbb{P}\widetilde{\mathbb{Q}}}(0, \tau_1, \tau_2)] = 1 \,.$$

Next, we consider the lower boundary, following Benth et al. (2019):

$$\mathbb{E}_{\mathbb{P}}[Z^{\mathbb{P}\widetilde{\mathbb{Q}}}(\tau_1, \tau_1, \tau_2)] \geq \mathbb{E}_{\mathbb{P}}[Z^{\mathbb{P}\widetilde{\mathbb{Q}}}(\tau_1, \tau_1, \tau_2)\mathbb{1}_{\hat{\tau}_n > \tau_1}] = \mathbb{E}_{\mathbb{P}}[Z^{\mathbb{P}\widetilde{\mathbb{Q}}}(\tau_1 \wedge \hat{\tau}_n, \tau_1, \tau_2)\mathbb{1}_{\hat{\tau}_n > \tau_1}] = \widetilde{\mathbb{Q}}^n[\hat{\tau}_n > \tau_1] \,,$$

where the last equality follows from the change of measure defined in Step 1 (see Equation (B.4)). By definition of the stopping time $\hat{\tau}_n$ (see Equation (B.3)), we deduce

$$\begin{aligned}
\mathbb{E}_{\mathbb{P}}[Z^{\mathbb{P}\widetilde{\mathbb{Q}}}(\tau_1, \tau_1, \tau_2)] \geq & 1 - \widetilde{\mathbb{Q}}^n[\hat{\tau}_n \leq \tau_1] \\
\geq & 1 - \left(\widetilde{\mathbb{Q}}^n \left[\sup_{s \in [0, \tau_1]} \widetilde{Y}(s, \tau_1, \tau_2) \geq n \right] + \widetilde{\mathbb{Q}}^n \left[\sup_{s \in [0, \tau_1]} \nu^{-1}(s) \geq n \right] + \widetilde{\mathbb{Q}}^n \left[\sup_{s \in [0, \tau_1]} \nu(s) \geq n \right] \right) \\
\geq & 1 - \frac{1}{n} \left(\mathbb{E}_{\widetilde{\mathbb{Q}}^n} \left[\sup_{s \in [0, \tau_1]} \widetilde{Y}(s, \tau_1, \tau_2) \right] + \mathbb{E}_{\widetilde{\mathbb{Q}}^n} \left[\sup_{s \in [0, \tau_1]} \nu^{-1}(s) \right] + \mathbb{E}_{\widetilde{\mathbb{Q}}^n} \left[\sup_{s \in [0, \tau_1]} \nu(s) \right] \right) \,,
\end{aligned}$$

where the last inequality follows from Markov's inequality. If we show that the expectations on the right hand side have upper boundaries that are independent of $n \in \mathbb{N}$, then $\mathbb{E}_{\mathbb{P}}[Z^{\mathbb{P}\widetilde{\mathbb{Q}}}(\tau_1, \tau_1, \tau_2)] = 1$, which is addressed in the third step.

3. Proof of upper boundaries. In order to identify upper boundaries under the measure $\widetilde{\mathbb{Q}}^n$ defined in Equation (B.4), we need to derive the dynamics of $\widetilde{Y}$, ν^{-1}, and ν under $\widetilde{\mathbb{Q}}^n$. We apply Girsanov's theorem (see Øksendal and Sulem (2007), cf. Theorem 1.35) to Equations (3.8) and (B.2), where

$$\begin{aligned}
W_t^{\widetilde{\mathbb{Q}}^n} &= W_t^{\mathbb{P}} + \int_0^t \Pi_1^{\mathbb{P}\widetilde{\mathbb{Q}}}(s, \tau_1, \tau_2)\mathbb{1}_{[0, \hat{\tau}_n]}(s) ds \,, \\
B_t^{\widetilde{\mathbb{Q}}^n} &= B_t^{\mathbb{P}} + \int_0^t \frac{\delta_\nu}{\sigma_\nu} \sqrt{\nu(s)} \mathbb{1}_{[0, \hat{\tau}_n]}(s) ds \,,
\end{aligned}$$

are correlated standard Brownian motions under $\widetilde{\mathbb{Q}}^n$ and

$$\widetilde{N}^{\widetilde{\mathbb{Q}}^n}(dt, dz) = \widetilde{N}^{\mathbb{P}}(dt, dz) + \Pi_2^{\mathbb{P}\widetilde{\mathbb{Q}}}(t, \tau_1, \tau_2)\mathbb{1}_{[0, \hat{\tau}_n]}(t)\ell^{\mathbb{P}}(dz)dt \,,$$

is the $\widetilde{\mathbb{Q}}^n$-compensated Poisson random measure. Moreover, by Ito's formula, we find

$$d\nu^{-1}(t) = \nu^{-1}(t) \left(\kappa_\nu + \delta_\nu \mathbb{1}_{[0, \hat{\tau}_n]}(t) - \nu^{-1}(t)(\kappa_\nu \theta_\nu - \sigma_\nu^2) \right) dt - \sigma_\nu \nu^{-\frac{3}{2}}(t) dB_t^{\widetilde{\mathbb{Q}}^n} \,.$$

Hence, we can show

$$
\begin{aligned}
&\mathbb{E}_{\widetilde{\mathbb{Q}}^n}\left[\sup_{s\in[0,\tau_1]}|\nu^{-1}(s)|\right] \\
&\overset{(\star)}{\leq} \frac{1}{\nu_0} + \mathbb{E}_{\widetilde{\mathbb{Q}}^n}\left[\sup_{s\in[0,\tau_1]}\int_0^s \nu^{-1}(t)\left(\kappa_\nu + \delta_\nu \mathbb{1}_{[0,\hat{\tau}_n]}(t) - \nu^{-1}(t)(\kappa_\nu\theta_\nu - \sigma_\nu^2)\right)dt\right] + \mathbb{E}_{\widetilde{\mathbb{Q}}^n}\left[\sup_{s\in[0,\tau_1]}\int_0^s \sigma_\nu \nu^{-\frac{3}{2}}(t) dB_t^{\widetilde{\mathbb{Q}}^n}\right] \\
&\overset{(\star\star)}{\leq} \frac{1}{\nu_0} + (\kappa + |\delta_\nu|)\mathbb{E}_{\widetilde{\mathbb{Q}}^n}\left[\int_0^{\tau_1}\nu^{-1}(t)dt\right] + (\kappa_\nu\theta_\nu - \sigma_\nu^2)\mathbb{E}_{\widetilde{\mathbb{Q}}^n}\left[\int_0^{\tau_1}\nu^{-2}(t)dt\right] + \sigma_\nu n^{-\frac{3}{2}}\mathbb{E}_{\widetilde{\mathbb{Q}}^n}\left[\sup_{s\in[0,\tau_1]}\int_0^s dB_t^{\widetilde{\mathbb{Q}}^n}\right] \\
&\overset{(\star\star\star)}{=} \frac{1}{\nu_0} + (\kappa + |\delta_\nu|)\int_0^{\tau_1}\mathbb{E}_{\widetilde{\mathbb{Q}}^n}\left[\nu^{-1}(t)\right]dt + (\kappa_\nu\theta_\nu - \sigma_\nu^2)\int_0^{\tau_1}\mathbb{E}_{\widetilde{\mathbb{Q}}^n}\left[\nu^{-2}(t)\right]dt\,.
\end{aligned}
$$

Inequality $(\star)$ follows from the integral representation of ν^{-1} and the triangle inequality. Inequality $(\star\star)$ results from the fact, that the extended Feller condition is satisfied (i.e., $\sigma_\nu^2 < \kappa_\nu\theta_\nu$) and that $\nu^{-1} \leq n$ under $\widetilde{\mathbb{Q}}^n$. Since both processes ν^{-1} and ν^{-2} are positive, the supremum disappears in the first two cases and the upper boundary is used. Equality $(\star\star\star)$ is reached by stochastic Fubini to the first two integrals and the last term disappears. From Dereich et al. (2012) (cf. Chapter 3), we know that the expectations of the inverse and the inverse quadratic stochastic volatility, $\mathbb{E}_{\widetilde{\mathbb{Q}}^n}\left[\nu^{-1}(t)\right]$ and $\mathbb{E}_{\widetilde{\mathbb{Q}}^n}\left[\nu^{-2}(t)\right]$, can be characterized explicitly and are bounded independently of n, as long as the extended Feller condition $\sigma_\nu^2 < \kappa_\nu\theta_\nu$ is satisfied. Hence, $\mathbb{E}_{\widetilde{\mathbb{Q}}^n}\left[\sup_{s\in[0,\tau_1]}|\nu^{-1}(s)|\right] \leq c_1 \perp\!\!\!\perp n$.

Moreover, we can show that $|\nu|^2$ is uniformly integrable:

$$
\begin{aligned}
&\mathbb{E}_{\widetilde{\mathbb{Q}}^n}\left[\sup_{s\in[0,\tau_1]}|\nu(s)|^2\right] = \mathbb{E}_{\widetilde{\mathbb{Q}}^n}\left[\sup_{s\in[0,\tau_1]}\left(\nu_0 + \int_0^s \kappa_\nu\theta_\nu - (\kappa_\nu + \delta_\nu\mathbb{1}_{[0,\hat{\tau}_n]}(t))\nu(t)dt + \int_0^s \sigma_\nu\sqrt{\nu(t)}dB^{\widetilde{\mathbb{Q}}^n}(t)\right)^2\right] \\
&\overset{(\star)}{\leq} 4\left(v_0^2 + \mathbb{E}_{\widetilde{\mathbb{Q}}^n}\left[\sup_{s\in[0,\tau_1]}\left(\int_0^s \kappa_\nu\theta_\nu dt\right)^2 + \sup_{s\in[0,\tau_1]}\left(\int_0^s (\kappa_\nu + \delta_\nu\mathbb{1}_{[0,\hat{\tau}_n]}(t))\nu(t)dt\right)^2 + \sup_{s\in[0,\tau_1]}\left(\int_0^s \sigma_\nu\sqrt{\nu(t)}dB_t^{\widetilde{\mathbb{Q}}^n}\right)^2\right]\right) \\
&\overset{(\star\star)}{\leq} 4\left(v_0^2 + 4\mathbb{E}_{\widetilde{\mathbb{Q}}^n}\left[\left(\int_0^{\tau_1}\kappa_\nu\theta_\nu dt\right)^2\right] + 4\mathbb{E}_{\widetilde{\mathbb{Q}}^n}\left[\left(\int_0^{\tau_1}(\kappa_\nu + \delta_\nu\mathbb{1}_{[0,\hat{\tau}_n]}(t))\nu(t)dt\right)^2\right] + 4\mathbb{E}_{\widetilde{\mathbb{Q}}^n}\left[\left(\int_0^{\tau_1}\sigma_\nu\sqrt{\nu(t)}dB_t^{\widetilde{\mathbb{Q}}^n}\right)^2\right]\right) \\
&\overset{(\star\star\star)}{\leq} 4\left(v_0^2 + 4\tau_1\int_0^{\tau_1}\kappa_\nu^2\theta_\nu^2 dt + 4\tau_1(\kappa_\nu + |\delta_\nu|)^2\int_0^{\tau_1}\mathbb{E}_{\widetilde{\mathbb{Q}}^n}\left[\sup_{s\in[0,t]}\nu^2(s)\right]dt + 4\sigma_\nu^2\mathbb{E}_{\widetilde{\mathbb{Q}}^n}\left[\int_0^{\tau_1}\nu(t)dt\right]\,,\right)
\end{aligned}
$$

where the first equality represents the integral version of ν. Inequality $(\star)$ results from the Cauchy-Schwartz inequality to the sum and an application of the triangle inequality. We apply Doob's inequality to all expectations in Inequality $(\star\star)$. In Inequality $(\star\star\star)$, we apply the Cauchy-Schwartz inequality to the first and second integral and apply Ito's isometry to the last summand. We finish with the stochastic Fubini to the second integral while making the integrand even bigger. Note that for the last summand, we have $\mathbb{E}_{\widetilde{\mathbb{Q}}^n}\left[\int_0^{\tau_1}\nu(t)dt\right] \leq \tilde{c}_\nu \perp\!\!\!\perp n$ since we can find explicit expressions in Cont and Tankov (2004) (cf. Chapter 15). Setting $c_\nu := 4v_0^2 + 16\tau_1^2\kappa_\nu^2\theta_\nu^2 + 16\sigma_\nu^2\tilde{c}_\nu$, then, by Gronwall, we receive $\mathbb{E}_{\widetilde{\mathbb{Q}}^n}\left[\sup_{s\in[0,\tau_1]}|\nu(s)|^2\right] \leq c_\nu e^{16(\kappa_\nu + |\delta_\nu|)^2\tau_1^2} =: c_2 \perp\!\!\!\perp n$.

Next, we show that $|\widetilde{Y}|^2$ is uniformly integrable:

$$
\begin{aligned}
&\mathbb{E}_{\widetilde{\mathbb{Q}}^n}\left[\sup_{s\in[0,\tau_1]}|\widetilde{Y}(s,\tau_1,\tau_2)|^2\right] \\
&= \mathbb{E}_{\widetilde{\mathbb{Q}}^n}\Bigg[\sup_{s\in[0,\tau_1]}\left(\widetilde{Y}(0,\tau_1,\tau_2) + \int_0^s \left(1 - \mathbb{1}_{[0,\hat{\tau}_n]}(t)\right)\left(\mathbb{E}[\mu(t,U)] - \kappa(t)\widetilde{Y}(t,\tau_1,\tau_2)\right)dt - \int_0^s \frac{1}{2}\mathbb{E}[\sigma(t,U)]^2\nu(t)\mathbb{1}_{[0,\hat{\tau}_n]}(t)dt\right. \\
&\quad + \int_0^s \mathbb{E}[\sigma(t,U)]\sqrt{\nu(t)}dW_t^{\widetilde{\mathbb{Q}}^n} + \int_0^s \mathbb{E}[\eta(t,U)]d\widetilde{J}_t^{\widetilde{\mathbb{Q}}^n} \\
&\quad \left.- \int_0^s \mathbb{E}[\eta(t,U)]\left(1 - \frac{\mathbb{E}[\eta(t,U)]\int_{\mathbb{R}} z\ell^{\mathbb{P}}(dz)}{\int_{\mathbb{R}} e^{\mathbb{E}[\eta(t,U)]z} - 1\ell^{\mathbb{P}}(dz)}\right)\mathbb{1}_{[0,\hat{\tau}_n]}(t)\int_{\mathbb{R}} z\ell^{\mathbb{P}}(dz)dt\right)^2\Bigg]
\end{aligned}
$$

$$
\begin{aligned}
&\overset{(\star)}{\leq} 7\Bigg(\widetilde{Y}^2(0,\tau_1,\tau_2) + \mathbb{E}_{\widetilde{\mathbb{Q}}^n}\left[\sup_{s\in[0,\tau_1]}\left(\int_0^s \left(1-\mathbb{1}_{[0,\hat{\tau}_n]}(t)\right)\mathbb{E}[\mu(t,U)]dt\right)^2\right] \\
&\quad + \mathbb{E}_{\widetilde{\mathbb{Q}}^n}\left[\sup_{s\in[0,\tau_1]}\left(\int_0^s \frac{1}{2}\mathbb{E}[\sigma(t,U)]^2\nu(t)\mathbb{1}_{[0,\hat{\tau}_n]}(t)dt\right)^2\right] + \mathbb{E}_{\widetilde{\mathbb{Q}}^n}\left[\sup_{s\in[0,\tau_1]}\left(\int_0^s \left(1-\mathbb{1}_{[0,\hat{\tau}_n]}(t)\right)\kappa(t)\widetilde{Y}(t,\tau_1,\tau_2)dt\right)^2\right] \\
&\quad + \mathbb{E}_{\widetilde{\mathbb{Q}}^n}\left[\sup_{s\in[0,\tau_1]}\left(\int_0^s \mathbb{E}[\sigma(t,U)]\sqrt{\nu(t)}dW_t^{\widetilde{\mathbb{Q}}^n}\right)^2\right] + \mathbb{E}_{\widetilde{\mathbb{Q}}^n}\left[\sup_{s\in[0,\tau_1]}\left(\int_0^s \mathbb{E}[\eta(t,U)]d\widetilde{J}_t^{\widetilde{\mathbb{Q}}^n}\right)^2\right] \\
&\quad + \mathbb{E}_{\widetilde{\mathbb{Q}}^n}\left[\sup_{s\in[0,\tau_1]}\left(\int_0^s \mathbb{E}[\eta(t,U)]\left(1-\frac{\mathbb{E}[\eta(t,U)]\int_{\mathbb{R}} z\ell^{\mathbb{P}}(dz)}{\int_{\mathbb{R}} e^{\mathbb{E}[\eta(t,U)]z}-1\ell^{\mathbb{P}}(dz)}\right)\mathbb{1}_{[0,\hat{\tau}_n]}(t)\int_{\mathbb{R}} z\ell^{\mathbb{P}}(dz)dt\right)^2\right]\Bigg) \\
&\overset{(\star\star)}{\leq} 7\Bigg(\widetilde{Y}^2(0,\tau_1,\tau_2) + 4\mathbb{E}_{\widetilde{\mathbb{Q}}^n}\left[\left(\int_0^{\tau_1} \left(1-\mathbb{1}_{[0,\hat{\tau}_n]}(t)\right)\mathbb{E}[\mu(t,U)]dt\right)^2\right] \\
&\quad + 4\mathbb{E}_{\widetilde{\mathbb{Q}}^n}\left[\left(\int_0^{\tau_1} \frac{1}{2}\mathbb{E}[\sigma(t,U)]^2\nu(t)\mathbb{1}_{[0,\hat{\tau}_n]}(t)dt\right)^2\right] + 4\mathbb{E}_{\widetilde{\mathbb{Q}}^n}\left[\left(\int_0^{\tau_1} \left(1-\mathbb{1}_{[0,\hat{\tau}_n]}(t)\right)\kappa(t)\widetilde{Y}(t,\tau_1,\tau_2)dt\right)^2\right] \\
&\quad + 4\mathbb{E}_{\widetilde{\mathbb{Q}}^n}\left[\left(\int_0^{\tau_1} \mathbb{E}[\sigma(t,U)]\sqrt{\nu(t)}dW_t^{\widetilde{\mathbb{Q}}^n}\right)^2\right] + 4\mathbb{E}_{\widetilde{\mathbb{Q}}^n}\left[\left(\int_0^{\tau_1} \mathbb{E}[\eta(t,U)]d\widetilde{J}_t^{\widetilde{\mathbb{Q}}^n}\right)^2\right] \\
&\quad + 4\mathbb{E}_{\widetilde{\mathbb{Q}}^n}\left[\left(\int_0^{\tau_1} \mathbb{E}[\eta(t,U)]\left(1-\frac{\mathbb{E}[\eta(t,U)]\int_{\mathbb{R}} z\ell^{\mathbb{P}}(dz)}{\int_{\mathbb{R}} e^{\mathbb{E}[\eta(t,U)]z}-1\ell^{\mathbb{P}}(dz)}\right)\mathbb{1}_{[0,\hat{\tau}_n]}(t)\int_{\mathbb{R}} z\ell^{\mathbb{P}}(dz)dt\right)^2\right]\Bigg) \\
&\overset{(\star\star\star)}{\leq} 7\Bigg(\widetilde{Y}^2(0,\tau_1,\tau_2) + 4\tau_1\int_0^{\tau_1}\mathbb{E}[\mu(t,U)]^2dt \\
&\quad + 4\int_0^{\tau_1}\mathbb{E}[\sigma(t,U)]^4dt\;\mathbb{E}_{\widetilde{\mathbb{Q}}^n}\left[\int_0^{\tau_1}\nu^2(t)dt\right] + 4\int_0^{\tau_1}\kappa^2(t)dt\;\mathbb{E}_{\widetilde{\mathbb{Q}}^n}\left[\int_0^{\tau_1}\widetilde{Y}^2(t,\tau_1,\tau_2)dt\right] \\
&\quad + 4\mathbb{E}_{\widetilde{\mathbb{Q}}^n}\left[\left(\int_0^{\tau_1} \mathbb{E}[\sigma(t,U)]\sqrt{\nu(t)}dW_t^{\widetilde{\mathbb{Q}}^n}\right)^2\right] + 4\mathbb{E}_{\widetilde{\mathbb{Q}}^n}\left[\left(\int_0^{\tau_1} \mathbb{E}[\eta(t,U)]d\widetilde{J}_t^{\widetilde{\mathbb{Q}}^n}\right)^2\right] \\
&\quad + 4\int_0^{\tau_1}\mathbb{E}[\eta(t,U)]^2dt\mathbb{E}_{\widetilde{\mathbb{Q}}^n}\left[\int_0^{\tau_1}\left(1-\mathbb{E}[\eta(t,U)]^2\frac{\left(\int_{\mathbb{R}} z\ell^{\mathbb{P}}(dz)\right)^2}{\left(\int_{\mathbb{R}} e^{\mathbb{E}[\eta(t,U)]z}-1\ell^{\mathbb{P}}(dz)\right)^2}\right)\left(\int_{\mathbb{R}} z\ell^{\mathbb{P}}(dz)\right)^2 dt\right]\Bigg) \\
&\leq 7\Bigg(\widetilde{Y}^2(0,\tau_1,\tau_2) + 4\tau_1\int_0^{\tau_1}\mathbb{E}[\mu(t,U)]^2dt + 4c_2\tau_1\int_0^{\tau_1}\mathbb{E}[\sigma(t,U)]^4dt \\
&\quad + 4\int_0^{\tau_1}\kappa^2(t)dt\;\mathbb{E}_{\widetilde{\mathbb{Q}}^n}\left[\int_0^{\tau_1}\sup_{s\in[0,t]}\widetilde{Y}^2(s,\tau_1,\tau_2)dt\right] + 4\sqrt{\int_0^{\tau_1}\mathbb{E}[\sigma(t,U)]^4dt}\sqrt{\tau_1 c_2} + 4\int_0^{\tau_1}\mathbb{E}[\eta(t,U)]^2\int_{\mathbb{R}} z^2\ell^{\widetilde{\mathbb{Q}}^n}(dz)dt \\
&\quad + 4\int_0^{\tau_1}\mathbb{E}[\eta(t,U)]^2dt\int_0^{\tau_1}\left(\left(\int_{\mathbb{R}} z\ell^{\mathbb{P}}(dz)\right)^2 + \mathbb{E}[\eta(t,U)]^2\frac{\left(\int_{\mathbb{R}} z\ell^{\mathbb{P}}(dz)\right)^4}{\left(\int_{\mathbb{R}} e^{\mathbb{E}[\eta(t,U)]z}-1\ell^{\mathbb{P}}(dz)\right)^2}\right)dt\Bigg), \\
&=: c_Y + 28\int_0^{\tau_1}\kappa^2(t)dt\;\mathbb{E}_{\widetilde{\mathbb{Q}}^n}\left[\int_0^{\tau_1}\sup_{s\in[0,t]}\widetilde{Y}^2(s,\tau_1,\tau_2)dt\right].
\end{aligned}
$$

The first equality represents the integral version of $\widetilde{Y}$. Inequality $(\star)$ results from the Cauchy-Schwartz inequality to the sum and an application of the triangle inequality. We apply Doob's inequality to all expectations in Inequality $(\star\star)$. In Inequality $(\star\star\star)$, we apply the Cauchy-Schwartz inequality to the first three integrals. We finish with Itô-Lévy Isometry (see Øksendal and Sulem (2007), cf. Theorem 1.17) to the last summand and an application of the stochastic Fubini theorem to the fourth summand (including $\widetilde{Y}$) while making the integrand even bigger. By the previous considerations, we know that $\mathbb{E}_{\widetilde{\mathbb{Q}}^n}\left[\int_0^{\tau_1}\mathbb{E}[\sigma(t,U)]^2\nu(t)dt\right] \leq \sqrt{\int_0^{\tau_1}\mathbb{E}[\sigma(t,U)]^4dt}\mathbb{E}_{\widetilde{\mathbb{Q}}^n}\left[\sqrt{\int_0^{\tau_1}\nu^2(t)dt}\right] \leq \sqrt{\int_0^{\tau_1}\mathbb{E}[\sigma(t,U)]^4dt}\sqrt{\tau_1 c_2}$ is bounded independently of n and that $\int_0^{\tau_1}\mathbb{E}[\sigma(t,U)]^4dt\;\mathbb{E}_{\widetilde{\mathbb{Q}}^n}\left[\int_0^{\tau_1}\nu^2(t)dt\right] \leq c_2\tau_1\int_0^{\tau_1}\mathbb{E}[\sigma(t,U)]^4dt$ is independent of n. By the choice of c_Y, an application of Gronwall's inequality yields $\mathbb{E}_{\mathbb{P}^n}\left[\sup_{s\in[0,\tau_1]}|\widetilde{Y}(s,\tau_1,\tau_2)|^2\right] \leq c_Y e^{28\int_0^{\tau_1}\kappa^2(t)dt} =: c_3 \perp\!\!\!\perp n$, such that we have shown, that $Z^{\mathbb{P}\widetilde{\mathbb{Q}}}$ is indeed a true martingale.

C Further Plots on the Description of the Data in Section 4.4

C.1 Histogram of Logarithmic Returns

(a) January

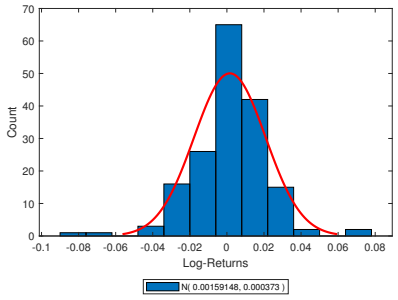

(b) February

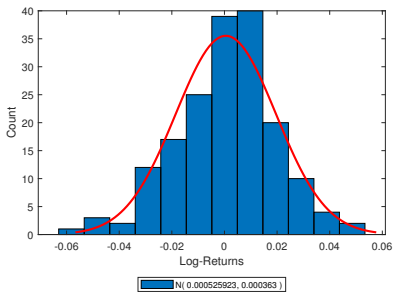

(c) March

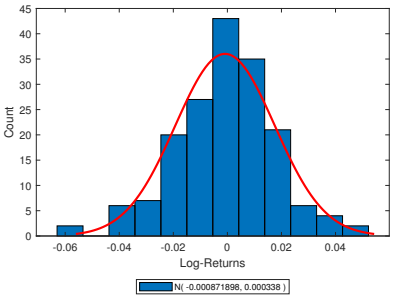

(d) April

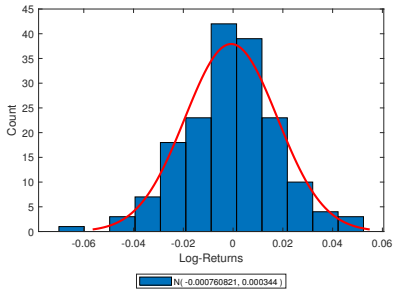

(e) May

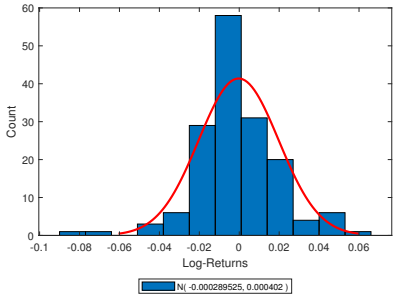

(f) June

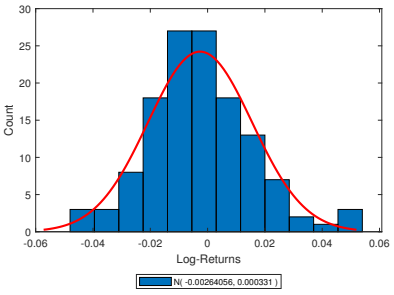

(g) July

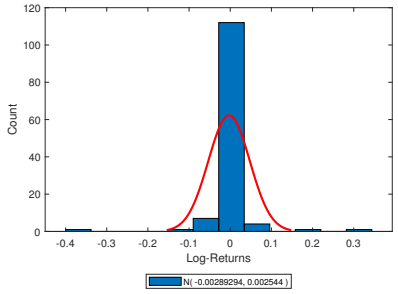

(h) August

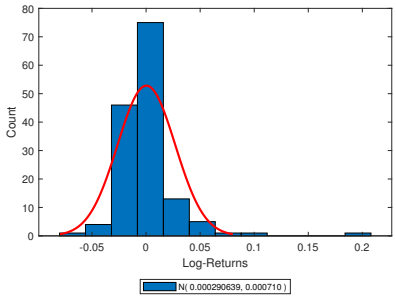

(i) September

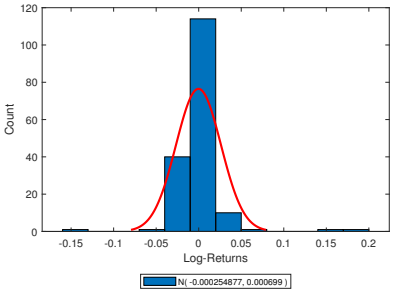

(j) October

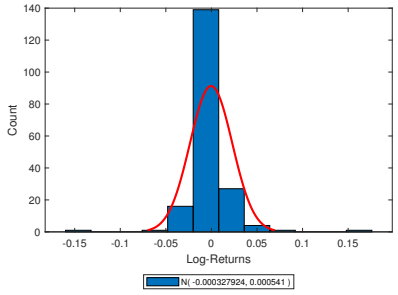

(k) November

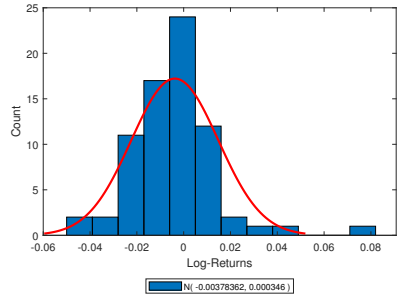

(l) December

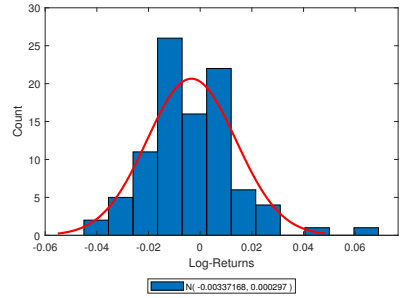

C.2 Logarithmic Returns per Contract

(a) January

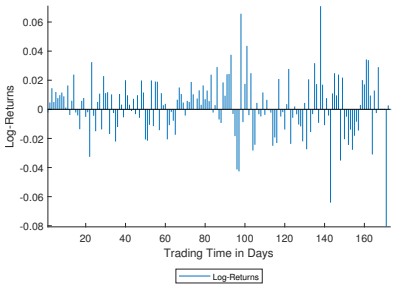

(b) February

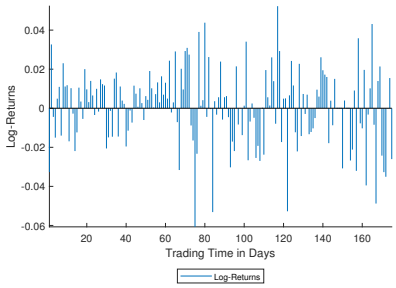

(c) March

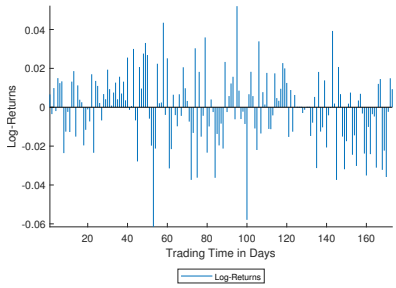

(d) April

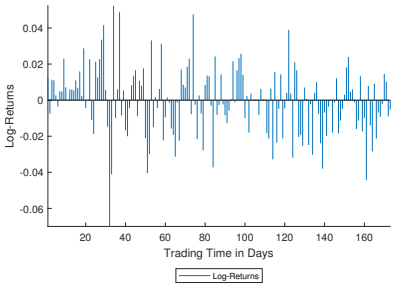

(e) May

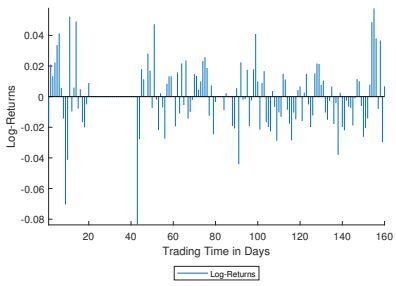

(f) June

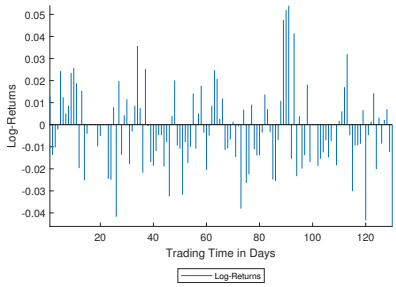

(g) July

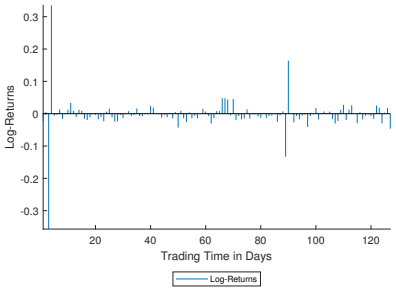

(h) August

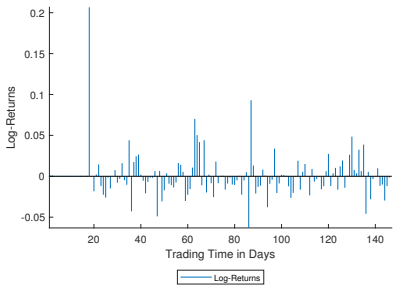

(i) September

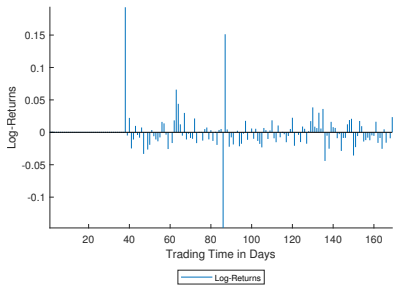

(j) October

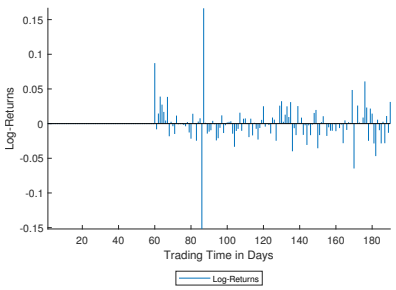

(k) November

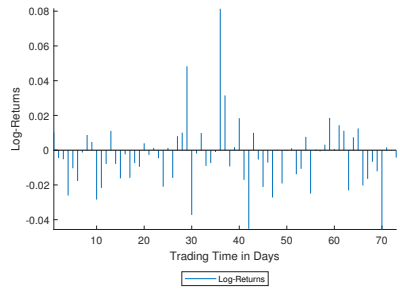

(l) December

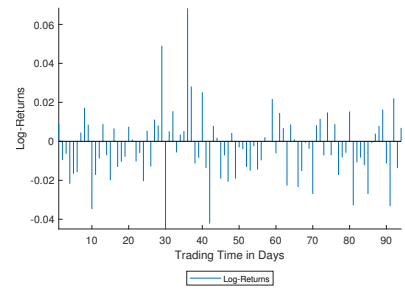

D Further Plots on Step I in Section 4.5

D.1 Jump Identification Procedure per Contract

(a) January

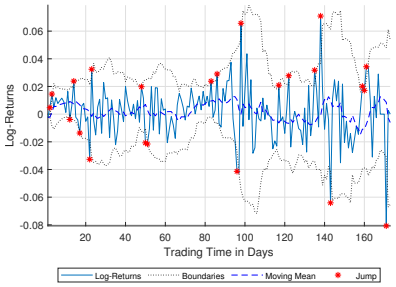

(b) February

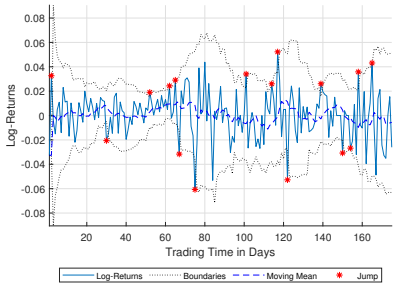

(c) March

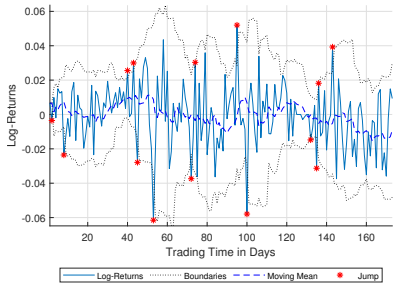

(d) April

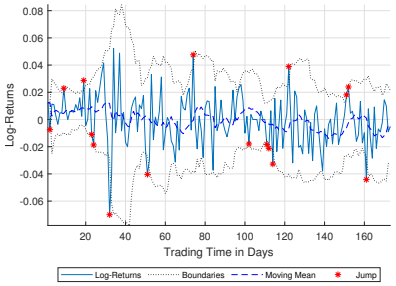

(e) May

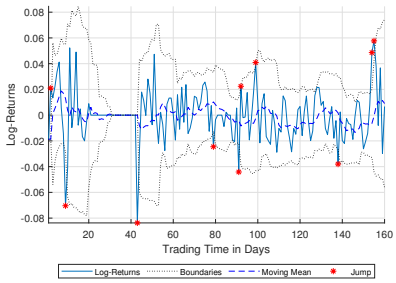

(f) June

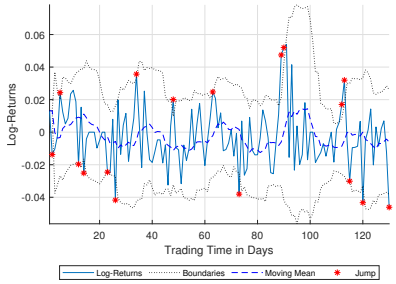

(g) July

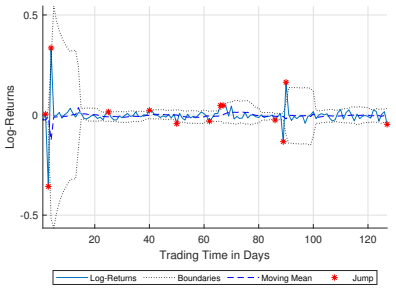

(h) August

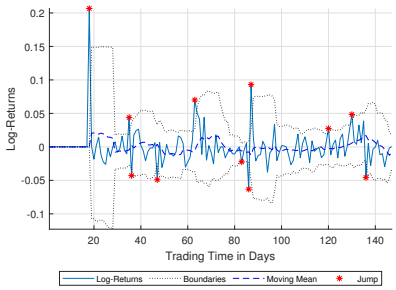

(i) September

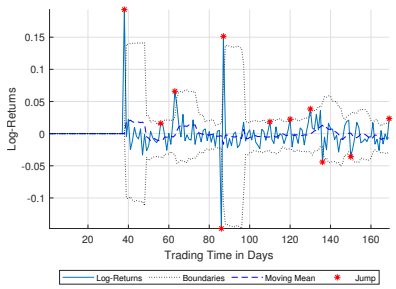

(j) October

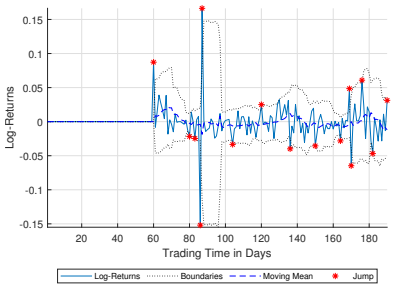

(k) November

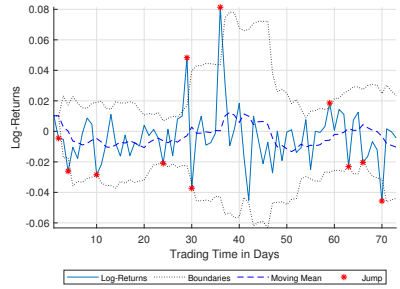

(l) December

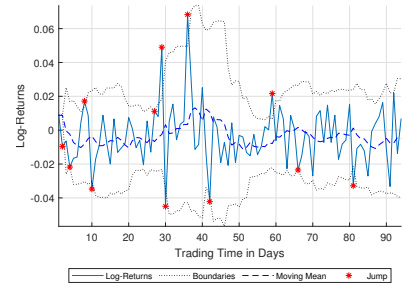

D.2 Identified Jumps per Contract

(a) January

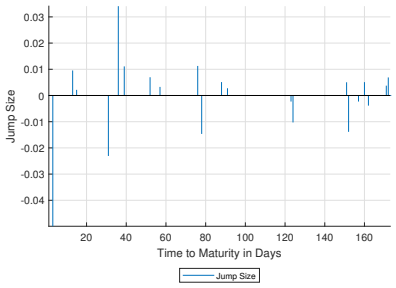

(b) February

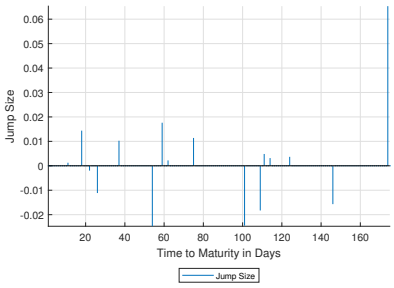

(c) March

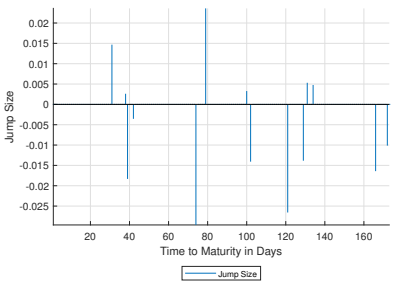

(d) April

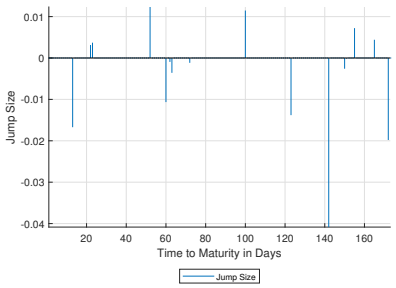

(e) May

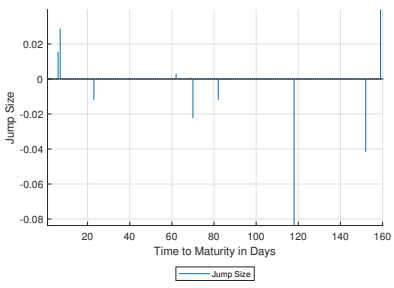

(f) June

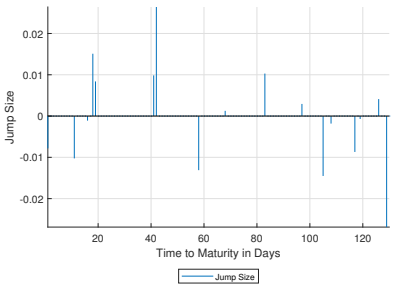

(g) July

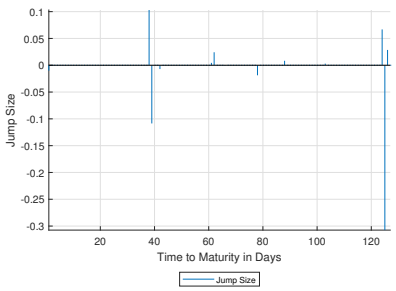

(h) August

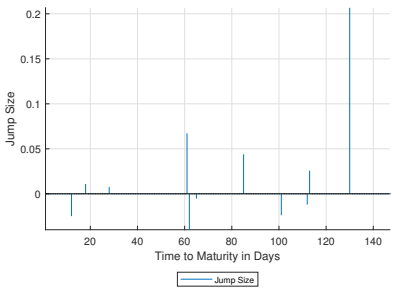

(i) September

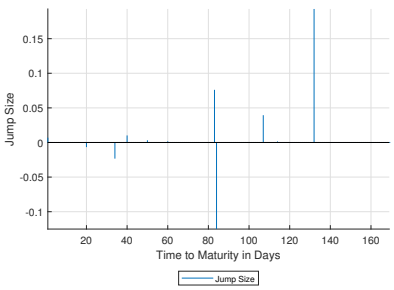

(j) October

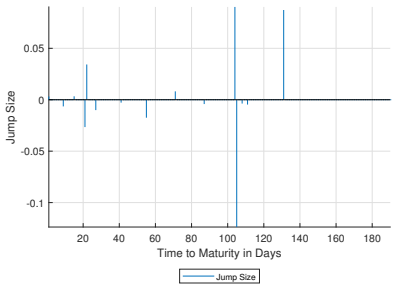

(k) November

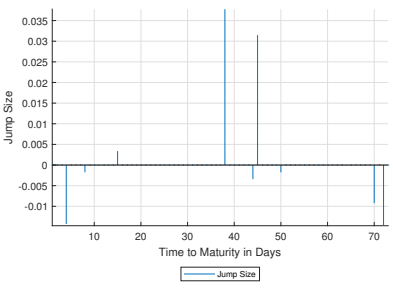

(l) December

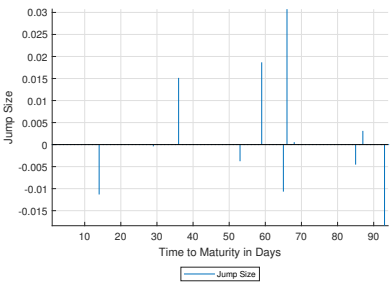

E Simulation of Logarithmic Returns with Exponential Jump Sizes

E.1 Simulation of Logarithmic Returns per Contract – Type 1

(a) January

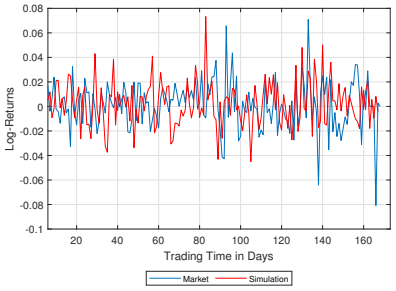

(b) February

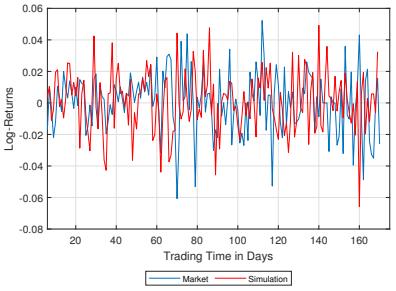

(c) March

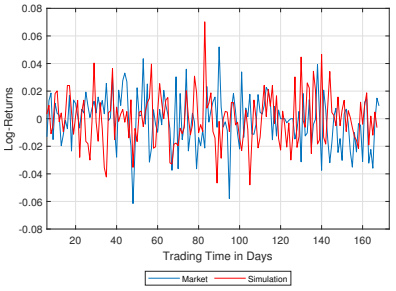

(d) April

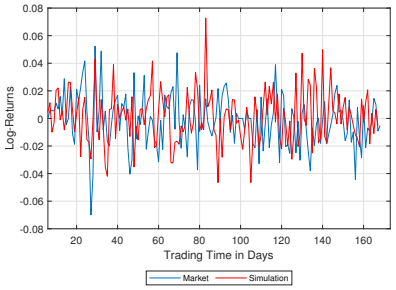

(e) May

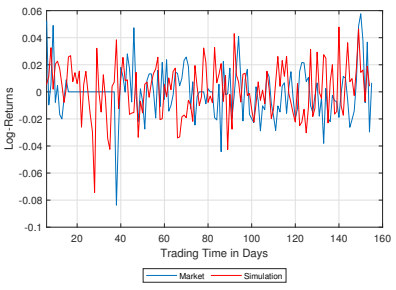

(f) June

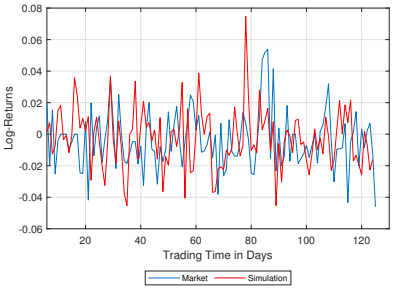

(g) July

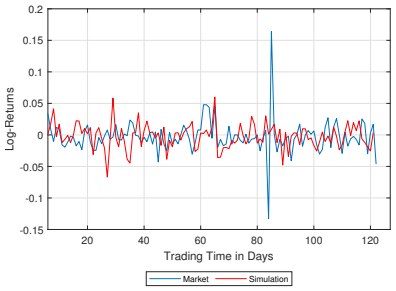

(h) August

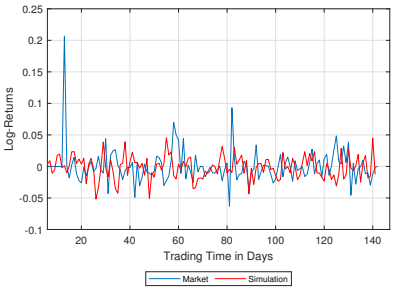

(i) September

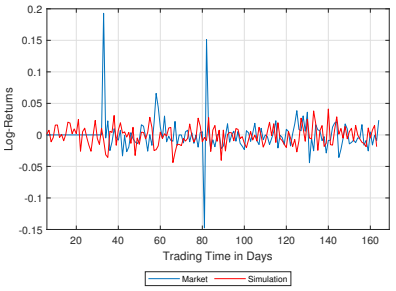

(j) October

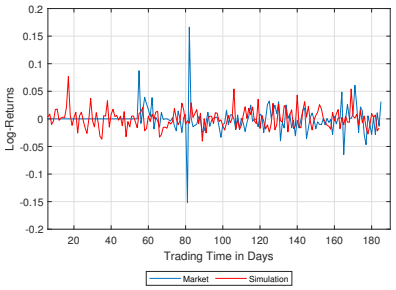

(k) November

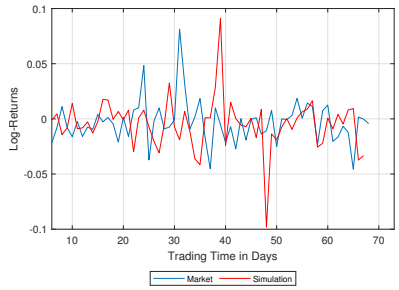

(l) December

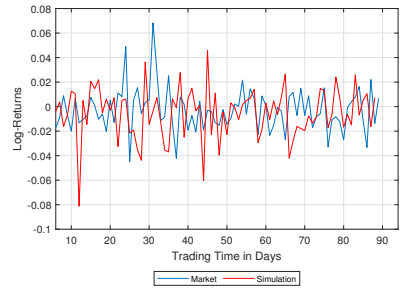

E.2 Simulation of Logarithmic Returns per Contract – Type 2

(a) January

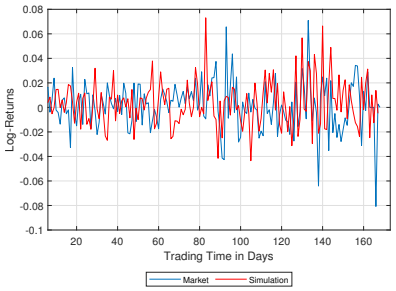

(b) February

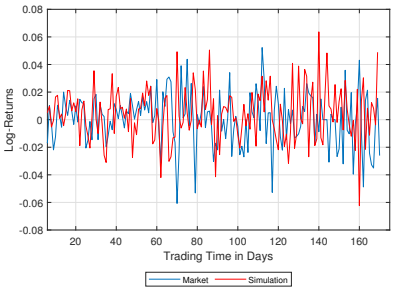

(c) March

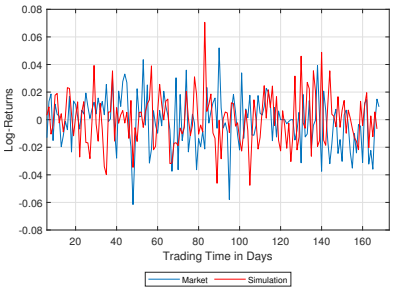

(d) April

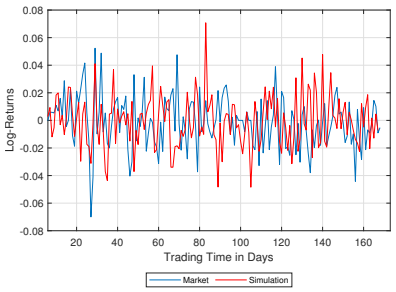

(e) May

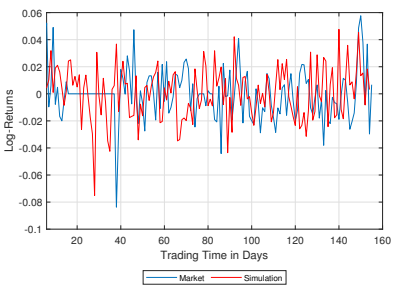

(f) June

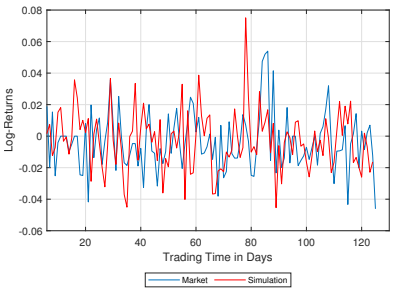

(g) July

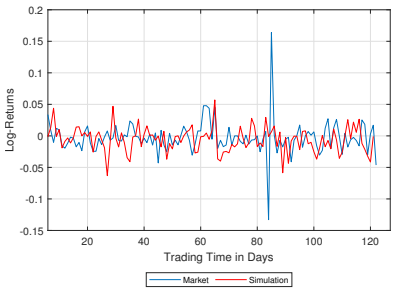

(h) August

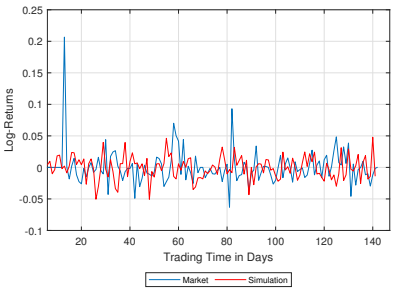

(i) September

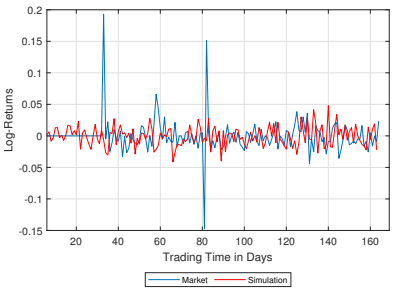

(j) October

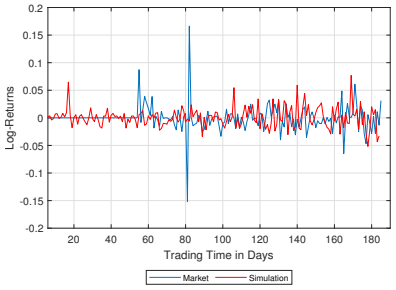

(k) November

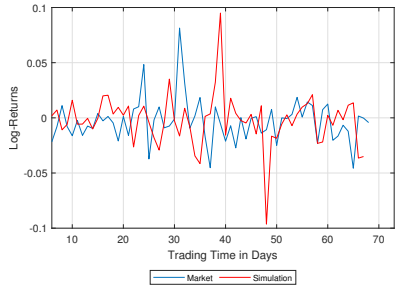

(l) December